International Institute for
Applied Systems Analysis
Schlossplatz 1
A-2361 Laxenburg, Austria

Tel: +43 2236 807 342
Fax: +43 2236 71313
E-mail: publications@iiasa.ac.at
Web: www.iiasa.ac.at

Interim Report IR-02-004

Assessment of Impact of Russian Nuclear Fleet Operations on Russian Far Eastern Coastal Regions

Alexander Mahura *mahura@inep.ksc.ru*

Approved by

Frank L. Parker
Project Leader
Radiation Safety of the Biosphere

January 22, 2002

Abstract

The main purpose of this study is evaluation of the atmospheric transport of pollutants from the Vladivostok and Kamchatka nuclear risk sites (NRSs) - nuclear submarines and radioactive storage facilities - located at the Russian Far East. The evaluation is given from the probabilistic point of view. The main question is: What is the probability for radionuclide atmospheric transport to the neighboring countries in the case of an accident at the nuclear risk sites in the Russian Far East?

To answer this question, we applied two research tools. The first tool is the isentropic atmospheric trajectory model to calculate trajectories originating at two NRSs. The second tool is the statistical analyses - exploratory, cluster, and probability field analyses - to explore the structure of the calculated trajectory data sets seasonally, monthly, and year-to-year. The selected regions of potential impact due to atmospheric transport – Japan, China, North and South Koreas, State of Alaska, and Aleutian Chain Islands. Additionally, we discussed possible approaches to investigate impacts of the radionuclide removal processes during atmospheric transport.

The main findings of this study are:

1) For both NRSs:

- The westerly flow is dominant throughout the year in the boundary layer (more than 60% of the time). At altitudes of the free troposphere, the probability of transport from the west increases up to 85% of the time.
- The relatively rapid westerly flow toward the North America reaches maximum occurrence during fall-winter (8-11% of the time) and during winter-spring (12-13% of the time) for the Kamchatka and Vladivostok NRSs, respectively.

2) For the Vladivostok NRS:

- The North China and North Japan regions are at the highest risk of possible impact in comparison with other regions. The lower (and upper) bounds of the Vladivostok NRS's possible impact are about of 32 (54) and 35 (87)% for the North China and North Japan regions, respectively.
- On average, atmospheric transport to these regions could occur in 0.5 and 1.6 days, respectively. The fast transport events (i.e. in less than 1 day) could represent major concerns for the Japanese and North Korean regions, but these are not common for the US territories.
- Except for the US territories, the boundary layer transport reaches all considered regions more than half of time.

3) For the Kamchatka NRS:

- The US territories are at the highest risk compared to the rest of the regions. The lower (and upper) bounds of the Kamchatka NRS's possible impact are 30 (54) and 13.4 (32.1)% for the Aleutian Chain Islands and State of Alaska, respectively.
- On average, atmospheric transport to these regions could occur in 3.0 and 5.1 days, respectively.
- The free troposphere transport dominates in the Chinese and North Korean regions, but boundary layer transport dominates in other considered regions.

We believe that results of the study are applicable for the emergency response and preparedness measures in the cases of the accidental releases at NRSs. Several directions for applicability of results in the studies of the consequences for population and environment, risk and vulnerability analysis, social and economical aspects resulting from the accidental releases at the nuclear risk sites as well as recommendations for the future studies are discussed.

Acknowledgments

The author is grateful to Drs. Frank Parker (Vanderbilt University, Nashville, TN, USA), Vladimir Novikov (International Institute for Applied Systems Analysis, IIASA, Laxenburg, Austria), and Keith Compton (IIASA) for the scientific leadership on the FARCES study, constructive discussions, and valuable comments.

The author would like to thank Drs. Alexander Baklanov (Danish Meteorological Institute, Copenhagen, Denmark), John Merrill (University of Rhode Island, Graduate School of Oceanography, Narragansett, RI, USA), and Robert Andres (University of North Dakota, Space Studies Department, Grand Forks, ND, USA) for collaboration and constructive comments.

The computer facilities at the International Institute for Applied Systems Analysis (IIASA), National Center for Atmospheric Research (NCAR, Boulder, CO, USA), and Vanderbilt University (Nashville, TN, USA) have been used extensively in this study. The meteorological data archives from the NCAR facilities were used as input in the trajectory modeling.

The author is grateful to Drs. Assen Novatchkov, Helmut Klarn, Jaroslav Chovanec, and Serge Medow (Computer Services, IIASA), and Ginger Caldwell (Scientific Computing Division, NCAR) for the collaboration, computer assistance, and advice. Thanks to Drs. William Hamilton (Department of Civil and Environmental Engineering, Vanderbilt University, Nashville, TN, USA) and Ann Clarke (ANC Associates, Inc., Brentwood, TN, USA) for running the cluster analysis at the Vanderbilt University computer facilities. Thanks to the computer consulting services at IIASA and NCAR. Thank you to Ulli Neudeck (IIASA) for taking care of the administrative issues.

The following software products had been used in this study: Matlab, SPSS, SAS, GMT, NCAR Graphics.

Financial sponsors of this study included the International Institute for Applied Systems Analysis and the United States Department of Energy (US DOE). The Swedish National Member Organization (SNMO) and Swedish Research Council for Environment, Agricultural Sciences and Spatial Planning (FORMAS) provided financial support for the Young Summer Scientist Program 2001 scientist.

The views and opinions of the author expressed in this publication do not necessarily reflect or state those of the sponsoring agencies or their institutions.

About the Author

Alexander Mahura is a scientist at the Institute of the Northern Environmental Problems (INEP) of the Kola Science Center, Russian Academy of Sciences (Apatity, Murmansk Region, Russia) in the laboratory of mathematical modeling of environment. During Summer 2001, he had been doing research at the Radiation Safety of the Biosphere Project, Far East Coastal Regions Study.

Contents

List of Figures and Tables

1. INTRODUCTION

1.1. Background

Nuclear power, in comparison to other energy sources, remains a compelling option in the nearest future. To have the public as well as political support it must meet certain requirements. The nuclear industry has always faced a public concern. Eventually, to reduce public concern and opposition some important issues must be considered. First, control measures to regulate radiation should be taken. Second, transparency in the radiation levels reporting should prevail. Third, the possible impact from the nuclear objects with respect to the environment and population should be evaluated.

In the second half of the 20th century, the United States (US) and former Soviet Union (FSU) were the world's largest producers of the nuclear related materials, and now they are experiencing the largest environmental consequences. As a result of the nuclear weapons development, production, and testing, as well as accidents at the various nuclear facilities, the radioactively contaminated locations and sites of the potential radiation risk had been identified in these countries. Since the late 80s, some information about the FSU activities became available and it allowed researchers to gain insight on the seriousness of the radiation pollution problems.

"The Radiation Safety of the Biosphere" (RAD) Project, started several years ago, is focused on the independent evaluation of the currently existing radioactive pollution problems and specifically those of the Russian Federation, and in particular, its emphasis is on the potential trans-boundary aspects. Research activities of the RAD Project are performed through the collaboration and networking between scientists and experts from the different organizations and research centers and institutions of the MinAtom, Russian Academy of Sciences (RAS), Kurchatov Institute and others.

During the beginning of the RAD project, the priority was the gaining of an overview of the FSU radiation legacy with a focus on Russia (*Laverov et al., 1997a; Laverov et al., 1997b; Novikov, 1997; Segerstahl et al., 1997; Egorov et al., 2000;*). Within the frameworks of the RAD project several studies had been performed. Among these were analysis of the Techa River and Lake Karachai, possibly the most radioactively contaminated site at the Earth, pollution due to Mayak (Southern Ural, Russia) activities (*Parker et al., 1999a*). Another study evaluated radiological impacts of radionuclide releases into the surface waters from two Siberian nuclear complexes: the Mining and Chemical Combine in Zheleznogorsk (Krasnoyarsk-26) and the Chemical Combine in Seversk (Tomsk-7) (*Waters et al., 1999; Parker et al., 1999b*). It has been found that contamination is still present in the Tom` and Yenisey Rivers, and it can be traced all the way to the Arctic Ocean. The detailed analysis of the results of the radioactive wastes injections into the deep geological formations at Krasnoyarsk-26, which for a long time raised safety concerns, have been performed by *Parker et al., 1999c; Compton et al., 2000; Parker et al., 2000; Compton et al., 2001a*.

The first attempts to investigate the radioactive pollution problems in the northern territories of Russia, and in particular, for the Russian Northern Fleet (RNF),

had been done by *Nilsen & Bøhmer, 1994; Baklanov et al., 1996; Bergman et al., 1996*). However, information about existing problems of the Russian Pacific Fleet (RPF) is scarce and limited, although recently some data became available (*Danilyan et al., 2000a; Danilyan et al., 2000b*).

Therefore, the RAD Project (starting from Spring 2000) initiated a new study titled: "Assessment of Impact of Russian Nuclear Fleet Operations on Russian **Far E**astern **C**oastal Regions" **S**tudy (**FARECS**). The focus of this study is gathering of the existing information and analyzing problems associated with the Russian Pacific Fleet operations. In 2000, research activities were concentrated on the gathering of available information, evaluating data, and preliminary analyses (*Takano et al., 2001; Romanova, 2001*). In 2001, the focus was on the analysis of possible danger to the environment and population in the neighboring countries due to normal operations and potential accidental situations at the nuclear submarines and storage facilities.

The main purpose of the FARECS study is an attempt to combine atmospheric transport modeling and analysis with the radiological assessment in order to evaluate consequences of an accident at the nuclear risk sites. The main question we are trying to answer in this part of the study is: What is the probability of radionuclide atmospheric transport to adjacent countries in a case of an accident at the nuclear risk sites (NRSs) in the Russian Far East (RFE)? The specific objectives are examination of the atmospheric transport patterns from the selected NRSs, evaluation of the probability of the fast transport (i.e. transport in less than 1 day), and an attempt to select approaches to investigate possible impacts of the radionuclide removal processes during atmospheric transport.

In our study, to answer the above mentioned questions we applied the following research tools. The atmospheric trajectory model was used to calculate trajectories originating over two nuclear risk sites locations in the Russian Far East – Kamchatka and Vladivostok. Several statistical analysis tools such as exploratory, cluster, and probability field analyses were applied to explore the structure of the trajectory data sets. We did it in order to evaluate the general atmospheric transport pathways, airflow patterns, fast transport, and typical transport time fields, as well as characteristics of the atmospheric transport (number trajectories and days throughout the year when air parcels might reach remote geographical regions, predominant atmospheric layers for transport, average and minimum transport times, etc) from NRSs. We also investigated the seasonal, monthly, and year-to-year flow patterns in order to get a better insight into the flow variations.

The current report has the following structure. In the "Introduction" Chapter, we describe existing sources of the radiation risk, geographical background, and general meteorological conditions in the Russian Far East. The "Methodology" Chapter provides information about research tools applied in this study. The detailed evaluation and analysis of the obtained results for the NRSs impact to the remote geographical regions, variations in the common atmospheric pathways, airflow patterns, fast, and typical transports, are summarized in the "Results and Discussion" Chapter, that is followed the "Conclusions", "Recommendations and Future Studies" sections. The seasonal variations of the atmospheric transport pathways, airflow patterns, fast transport, and typical transport time for the Kamchatka and Vladivostok NRSs as well as description of the visualization software tools are combined into several Appendices.

1.2. Nuclear Risk Sites at the Russian Far East

Despite the limited financial support due to economical problems and current significant political changes the Pacific and Northern Fleets are rated as the two most powerful of the four Russian Fleets. Both Fleets include nuclear strategicand general-purpose submarines, and various surface vessels. The Pacific Fleet headquarters is located in Vladivostok, and additional bases are at Petropavlovsk-Kamchatskiy, Magadan, and Sovetskaya Gavan. The Northern Fleet headquarters is located in Severomorsk, and additional bases are Kola, Motovsky, Gremikha, and Ura Guba. To ensure the country's defense and security in the near future, the priorities of navy's development could be nuclear strategic submarines and general-purpose submarines.

The Russian Northern and Pacific Fleets are experiencing problems with upkeep of their nuclear powered vessels, storage of spent nuclear fuel, and radioactive waste as a result of operation of these vessels. In particular, the Kola Peninsula and Severodvinsk area have the highest concentration of nuclear reactors in the world. A comparable number of nuclear reactors is in the Russian Far East.

Around 250 nuclear-powered submarines were built in the former Soviet Union. According to *Egorov et al. 2000*, about 140 nuclear submarines had been taken out of operation by 1995. By 2000, 156 nuclear submarines would be removed from the service. Updated recent data (*Bellona-www, 2001*) shows that so far, Russia has removed 183 nuclear-powered submarines from the Northern and Pacific Fleet service (113 submarines in the Northern Fleet). These submarines are taken out of service for three primary reasons: requirements of the arms reduction treaty (called START-1), aging of the nuclear submarines, and lack of means for proper maintenance and repair (*Nuclear Waste in the Arctic, 1995*). If the strategic arms reduction talks treaty (called START-2) will be finalized, an additional large number of the nuclear submarines would be taken out of the service. Taking into account the reactors at nuclear submarines and nuclear powered surface ships still in service or laid up there are total of 476 naval military reactors (*Baklanov et al., 1996*).

Currently Russia experiences problems with infrastructure and equipment to dismantle nuclear-powered submarines and deal with their spent fuel. Spent fuel is stored in obsolete onshore and floating storage facilities, inside the reactors of laid-up nuclear submarines and in transport containers. Storage and reprocessing sites for the Northern Fleet are situated in the Andreeva Bay, Gremikha, and Severomorsk (Kola Peninsula region) and for the Pacific Fleet in Shkotovo and Chazhma Bay (Primorie and Kamchatka Regions) (*Bradley, 1997*).

The United States Department of Defense (US DOD) has been most active in assisting the Russian Pacific Fleet to remove missiles from the nuclear submarines, but future activities are under discussion. The assistance was carried out through the Co-operative Threat Reduction Program. The United States Department of Energy (USDOE) also refurbished the Shkotovo site and supplied it with the security systems. In 1999, two storage facilities for liquid radioactive waste in Primorskiy Kray were opened. Japan also showed an initiative to increase a co-operation with Russia on the nuclear submarines decommissioning in the Russian Far East. Japan started its nuclear safety assistance to Russia in 1993. It subsidized construction of the mobile floating liquid waste processing facility (located at the Zvezda shipyard, Bolshoy Kamen').

As with all other radiation risk sources, the nuclear submarines and storage facilities for the nuclear fuel represent a radiation hazard for the environment and population. Accidents may take place during refueling and de-fueling of the submarine's nuclear reactors (*Takano et al., 2001*), transportation of the spent nuclear fuel from/to storage facilities, etc. The accident may be caused by a human error, technological problems, natural hazards, terrorist actions, etc. The last well-known accident with a nuclear submarine, which was not followed by the release of radioactive material , took place on 12 August 2000. The Russian nuclear submarine "Kursk" sank in the Barents Sea following two explosions in the missile area in the front portion of the vessel. , This occurred not far from the Kola Peninsula (Russia, Murmansk region). The radiation levels in the vicinity of the submarine have been monitored by the Norwegian Radiation Protection Agency (NRPA) as well as the Murmansk Meteorological Institute (MMI). So far, there are no signs of short-lived isotopes in the surrounding water. Another issue of concern is that the U.S. and Russian nuclear-weapons systems remain on a high alert. and This situation , combined with the aging of the Russian technical systems, increases the risk of an accidental launch of the nuclear weapons (*Forrow et al., 2000*).

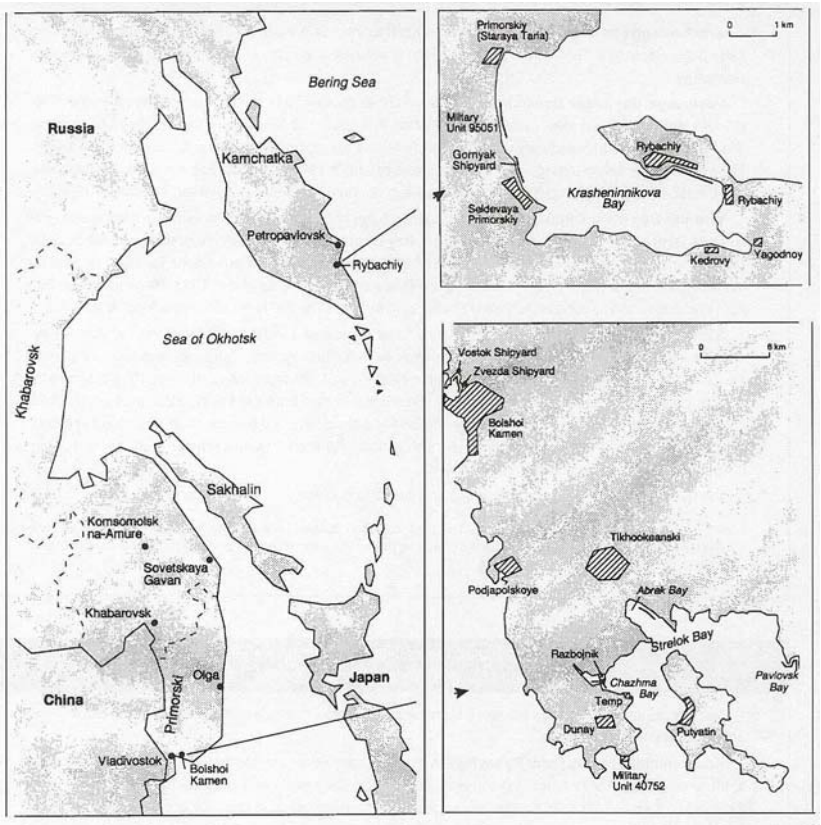

Figure 1.2.1. Nuclear risk sites in the Russian Far East

(map source: Nuclear Wastes in the Arctic, OTA-ENV-632)

This study is focused on the sites of potential nuclear risk in the Vladivostok and Kamchatka regions (Figure 1.2.1) (*Nuclear Wastes in the Arctic, 1995*). In particular, we considered two NRSs. Each of the NRSs consists of the several nuclear hazard sources. First, the Vladivostok nuclear risk site (VNRS) comprises the Zvezda shipyard, ship repair facility in Chazhma Bay, and the waste management facilities. It has geographical coordinates, which we used further in the trajectory modeling, 42°55'N and 132°25'E. Second, the Kamchatka nuclear risk site (KNRS) is represented by the Rybachiy submarine base, Gornyak shipyard, and facilities for the radioactive wastes. Its geographical coordinates are 52°55'N and 158°30'E. We have assigned these coordinates for the purposes of the atmospheric transport modeling. The geographical region of interest for modeling covers a large domain of the North Pacific region. It included Russia, Japan, Korea, China, and USA. In the USA, it is the Aleutian Islands, State of Alaska and territories on the US western shore (States of Washington, Oregon, etc).

Within the framework of the FARECS Study, *Takano et al., 2001* and *Romanova, 2001* considered two reactivity accidents (Chazhma Bay and hypothetical) at the nuclear submarine near the Vladivostok navy base. It has been stated that both accidents took place during refueling and de-fueling of the submarine's nuclear reactors. In their study, the Worldwide version of the SPEEDI code (System for Prediction of Environmental Emergency Dose Information) (*Ishikawa, 1991; Ishikawa & Chino, 1991; Ishikawa, 1994*) was used to simulate long-range atmospheric transport of radionuclides from the accident location and estimate radiological consequences to the neighboring countries. They estimated doses due to inhalation and concentration near the surface. Although they did not obtain high radiological doses in the remote areas, they have mentioned that for the winter typical meteorological conditions, the radionuclide atmospheric transport to Japan might occur in one to several days. Such transport might lead to contamination of a large area of Japan. Due to proximity of China and Korean Peninsula to the accident location, the doses there might be much higher under certain wind conditions.

Although the focus of our study is only the two NRSs, there are other sources of radiation hazards at the Russian Far East. Among other sources – nuclear risk sites - of the radiation risk are the nuclear reactors at the nuclear power plants (NPPs). Since the Chernobyl accident and FSU break up, the nuclear power system in Russia underwent intense scrutiny. The main issue is a requirement that all plants should undergo safety upgrades or be closed. However, economic problems and decrease in the electricity demand led to lack of resources to maintain and upgrade NPPs. At the same time, Russia is extending licenses for its nuclear power plants for further years of service.

Currently, there is only one operable NPP – Bilibino - on the territory of the Russian Far East (Chukotka Autonomous Region, Russia). This plant uses four light-water-cooled, graphite-moderated reactors (LGR) with a net output of 12 MWe each. It was constructed, and then put into commercial operation between 1973-1976. Although, it is the only operable NPP in the area, according to the International Nuclear Safety Center (INSC), there are plans, although postponed at this moment, of the Russian Government to build 2 new NPPs, called the Far East and Primorskaya, at the Russian Far East. It is proposed to construct the Pressurized Water Reactor (PWR) type of

reactors, model VVER-600 of passive safety, and having a net output of 950 MWe each.

Therefore, in the "Recommendation and Future Studies" section of this report we suggested additional approaches and directions for studies of the nuclear risk sources in the Russian Far East as well as in neighboring countries of the North Pacific region.

1.3. Meteorology of the Russian Far East

The Russian Far East occupies a large territory, which is more than a third of the total territory of the Russian Federation. It has borders with China and North Korea, and only short distances separate the Sakhalin Island from Japan, and the Chukotka Peninsula from Alaska. It ranges from the mixed forests and steppes in the southern territories to tundra and arctic deserts in the northern territories. Coniferous forests cover an enormous area, but trees are sparsely distributed and slow growing. The climate in the region varies significantly from north to south, and is influenced by proximity to the seas.

The Primorskiy Kray (where VNRS is situated) stretches along the Japan Sea on the southeastern coast of the Russian Far East. Its area is approximately 161 thousand km^2. Almost two-thirds of the territory is covered by forest. The mildest climate is observed there. Winters are relatively short and cold with an average temperature of -20°C (January). Summers are relatively cloudy, with frequent rain and an average temperature of 25°C (July). In particular, for Vladivostok, during July-September the amount of precipitation is on average above 100 mm per month. The minimum of precipitation is 15.4 mm (January) and maximum is 148.7 mm (August).

The Kamchatka Region (where KNRS is situated) is between the Okhotsk Sea on the west and Pacific Ocean and Bering Sea on the east. Its area is approximately 171 thousand km^2. The central and southern parts of the Kamchatka Peninsula have more than 20 active volcanoes. They are subject to a frequent seismic activity. Surrounded by seas, the Kamchatka Peninsula has a mild climate. Average temperature ranges from –10°C (January) to 14°C (July). In particular, for Petropavlovsk-Kamchatskiy the minimum of precipitation is 50.8 mm (April) and the maximum is 139.2 mm (October).

It is well known that the most immediate danger from an accident is exposure to high levels of radiation. There may be radiation hazard in the surrounding areas both near and far, depending on the type of accident, amounts of radioactivity released, as well as weather conditions. The influence on the environment and population will vary with temporal and spatial conditions.

The meteorological conditions will play a critical role in the estimation of the possible atmospheric transport of any kind of pollution, including radioactive materials from the nuclear risk sites. Among the most important parameters are the wind field characteristics, temperature and humidity fields, precipitation in various forms, etc. Values of these parameters could depend also on the considered scale of the processes such as local-, meso-, regional-, large-, hemispheric-, and global scales.

The complexity of the climate in the North Pacific region derives from the several factors. First, there are significant variations in the radiative effects of the underlying surface. Second, the studied region has unequal distribution of land and

water surfaces, and in particular, for our NRSs the transport mostly took place above the Pacific Ocean and adjacent seas territories. Third, there is well known and studied horizontal transport of the heat toward the northern latitudes from the south. In general, the North Pacific region is considered as a synoptically active region. It is characterized by the relatively fast cyclone development.

The wind patterns exhibit a remarkable uniformity in the southern and eastern parts of the North Pacific region. Trade and westerly winds are well-developed patterns of the global scale and are modified by seasonal fluctuations. Due to the continental influence, the climatic uniformity is much less pronounced in the western and eastern regions at the same latitudinal belt. The western part of the North Pacific has a monsoon signature. The rainy season occurs during summer, when moisturized winds blow toward the land surface from the ocean. During winter, there is a dry season when winds blow from the Asian continent toward the ocean. During May-December, the southeast and eastern areas of Asia are under influence of the tropical cyclones (called typhoons).

Three major centers of atmospheric activity - the Aleutian Low, Siberian High, and Honolulu High - have influence on the transport of air masses within the North Pacific and Arctic regions. All these have decadal time scales. During winter the Russian Far East lies on the boundary of the Arctic front, which separates two air masses with different characteristics: cold and dense Arctic air and the warmer and moister maritime air of the Northern Pacific. In summer, the position of the Arctic front is shifted above the Arctic Circle, and it lies in the seashore areas of the Arctic Ocean (*Shaw, 1988*). The main cyclone and anticyclone pathways are associated with activity of the Aleutian Low, and characterized by the 5-10° latitudinal north-south shift throughout the year. Due to presence of the Arctic front as well as topographical effects, a large numbers of cyclones stagnate upon reaching the area of the Bering Sea.

For most of these territories, there is a large variation in the precipitation pattern. Increased precipitation will favor the washout of pollutants, and hence impact the deposition levels and patterns. Atmospheric circulation over these regions is strongly affected by the Coriolis force. In the far northern regions, the cold air temperatures, limited low-level moisture supply, and high static stability will be characteristic during winter. These conditions limit the intensity of the vertical circulation. During summer-fall, when the background stratification is not excessively strong, intensity of cyclone development over the regions will depend critically on the conditions of the underlying surface (e.g. water surface or land, open or covered by snow or ice). In the southern regions, the cyclones develop over the seashore and continental parts of Asia. During winter, the atmosphere is in a stable state due to cold surface temperature. It is characterized by the large frequency of inversions. However, in spring it became unstable due to radiative heating. The intense transport of the heat and moisture from the low toward northern latitudes triggers the intensity of the cyclone development in the region. At the same time, the climatological differences in the airflow from the Asian continent could be observed between low and middle latitudes. During summer monsoon season, there is warm and humid southeasterly airflow in the region.

As we mentioned, the focus of this study is an analysis of the airflow patterns from the NRSs regions from the probabilistic point of view. We expect that the obtained patterns should be in a good agreement with the general synoptic scale patterns.

2. METHODOLOGY

2.1. Impact Region Specification

As mentioned in Chapter 1, the Vladivostok and Kamchatka nuclear risk sites, located AT132.5°E vs. 43°N and 158.5°E vs. 53°N, respectively, might be subject to possible accidents. *Bergman et al., 1996* and *Takano et al., 2001* mentioned that nuclear submarines and radioactive storage facilities are potential radiation risk sources in the northern regions. Depending on the scenario, an accident at these sites, following by a subsequent radionuclide release, may have a significant impact on the environment and population in the North Pacific region.

In this study, we examined the probabilistic atmospheric transport patterns from the nuclear risk sites near Vladivostok and Petropavlovsk-Kamchatskiy. These patterns, would be useful to estimate the possible radiological impact on different remote geographical regions. For this study, we selected (as shown in Figures 2.1.1 and 2.1.2 Japan, Korea, China, Aleutian Chain Islands, and State of Alaska (US). We named them as the regions of the NRS potential impact.

Japan was divided into three major sub-regions representing northern (140-145°E vs. 38-45°N), central (136-142°E vs. 33-38°N), and southern (130-136°E vs. 30-36°N) territories of Japan. These include the islands and adjacent seashores. In a similar manner, the Korean region consists of two areas, North (124-130°E vs. 38-43°N) and South (125-130°E vs. 34-38°N) Korea. Due to the more complex configuration of the Chinese region, we selected two areas. The first is closely adjacent to the Vladivostok region - the Northern Chinese Territories (120-132°E vs. 43-48°N). The second is the Central Shoreline China (112-124°E vs. 31-43°N).

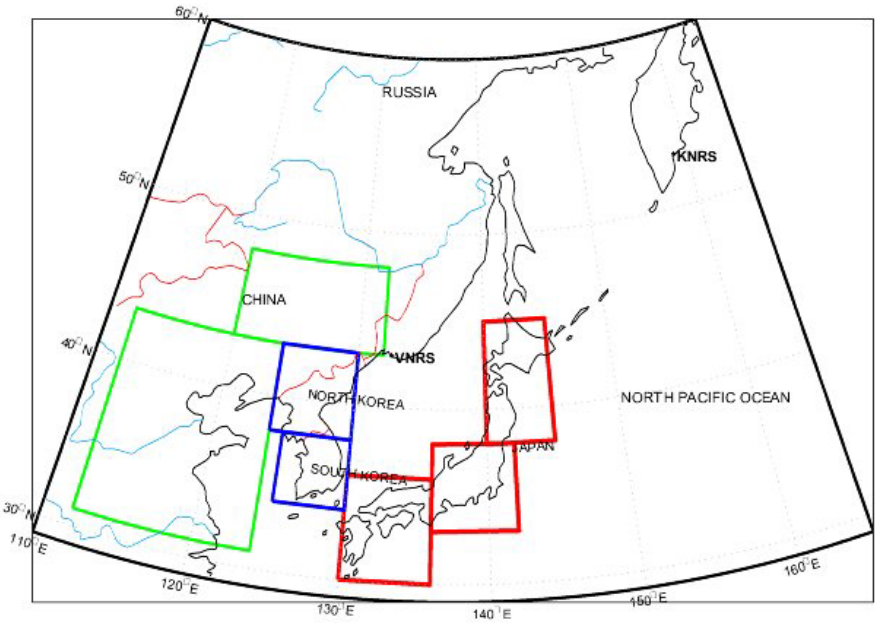

Figure 2.1.1. Geographical impact region in the Western North Pacific region

For the USA, we limited our investigation to only the two northern regions – Aleutian Chain Islands (170E-160°W vs. 50-55°N), and western territories of the State of Alaska (166-150°W vs. 55-72°N). The mainland US territories, in particular, the US western shore territories of the states – Washington, Oregon, etc - were not considered due to 1) on average, longer than 5 days transport time from the NRS locations to these territories, 2) questionable accuracy of trajectory calculations after 5 days, and 3) framework limitations in the current study, and computer resources needed for statistical analysis of the longer series.

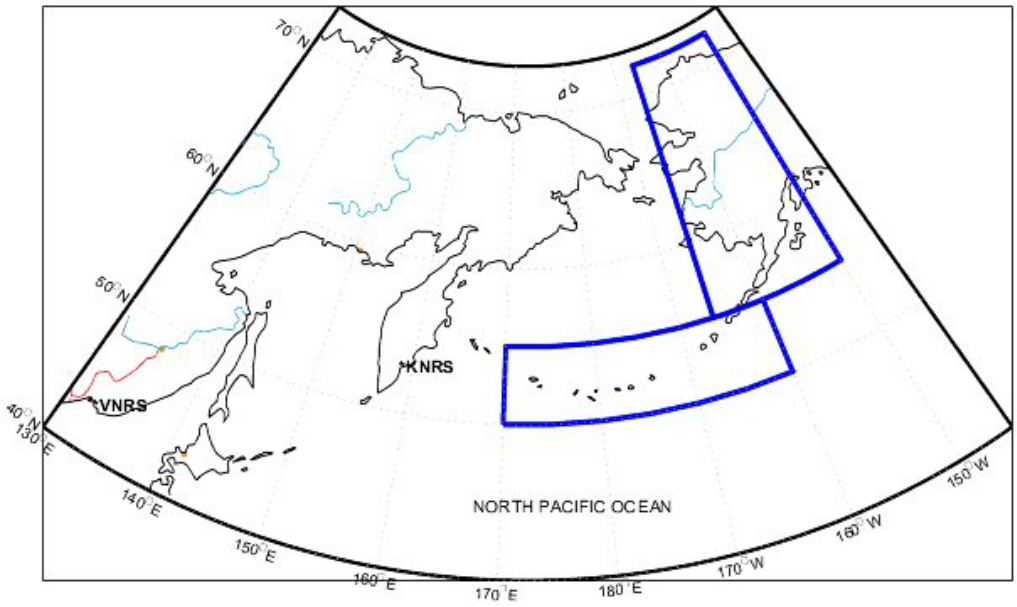

Figure 2.1.2. Geographical impact regions in the Eastern North Pacific region

All boundaries of the selected geographical regions were chosen based on an assumption of the most populated geographical areas and various climatic atmospheric transport regimes. We note that the more precise separation of the geographical regions might be done by application of the GIS technology. That would permit to evaluate more clearly trajectory passages through the selected country.We believe that for the first preliminary evaluation the selection of the latitude vs. longitude box-areas is sufficient.

2.2. NCEP Global Tropospheric Analysis Dataset

Data analysis is basic for atmospheric sciences research. Data might be represented in different forms and at different temporal and spatial scales. They might be obtained from a variety of different sources such as ground meteorological stations, radars, sounding, satellites, airplanes, etc. Models, which rely on intensive usage of the supercomputing resources, can produce gridded arrays for the commonly used basic

variables. Atmospheric models can calculate temperature, humidity, wind components, vertical motions and other variables at different levels.

In our study, as input data, we used such a gridded dataset. Dataset DS082.0 - NCEP Global Tropospheric Analyses (from July 1976 till April 1997) is one of the major gridded analyses available at the National Center for Atmospheric Research (NCAR, Boulder, Colorado). It is a part of the operational and gridded analyses performed at the National Center for Environmental Prediction (NCEP; prior to 1995 known as the National Meteorological Center – NMC).

This dataset has a resolution of 2.5° x 2.5° latitude vs. longitude (145 x 37 grids, ~3 Megabytes (Mb) per day) for both Northern and Southern hemispheres. It consists of the surface, tropospheric, tropopause, and lower stratospheric analyses as well as at the standard levels up to 50 millibars (mb). The main analyzed variables are the following: geopotential height, temperature, u-, v-, and w-components of the wind, relative humidity, sea level pressure, surface pressure and temperature, sea surface temperature, snowfall, precipitable water, potential temperature, vertical motion, tropopause pressure and temperature. Analysis has been done on a daily basis at 00 and 12 UTC terms (Universal Coordinated Time).

The dataset is only available from the NCAR Mass Storage System (MSS). Only users having NCAR computer accounts may download and use. More detail information about DS082.0 dataset could be found at the www-address http://dss.ucar.edu/datasets/ds082.0/ and in publications by *Baker, 1992; Trenberth & Olson, 1988; Randel, 1992*. Starting in April 1997, the NCEP Global Tropospheric Analysis is accumulated in the DS083.0 dataset. A more detailed finer analysis (beginning 15 September 1999) is in the DS083.2 dataset. It has a global coverage too, but with a better - 1° x 1° latitude vs. longitude - resolution (360 x 181 grids, ~80 Mb per day). This analysis is given every 6 hours at the standard UTC terms of 00, 06, 12, and 18 hours. In our study, we did not use this most recent data.

2.3. Isentropic Trajectory Modeling

In general, each computed atmospheric trajectory represents a pathway of an air parcel motion in time and space. We consider trajectories as an estimation of the mean motion of a diffusing cloud of some material. There are a few approaches to model atmospheric trajectories. Two of these approaches are commonly used: 1) isobaric and 2) isentropic (*Danielsen, 1961*). For isobaric trajectories it is assumed that air parcels are moving along the surfaces of the constant pressure. For isentropic trajectories it is assumed that air parcels are moving along the surfaces of the constant potential temperature. In general, of course, modeling of more realistic trajectories –the "fully 3-D trajectories" - is preferable, but it is complex and requires incorporation of a large number of variables and parameters into the simulation increases the computational time as well.

In our study we selected the isentropic approach. Although this type of trajectory model uses the assumption of adiabatically moving air parcels and neglects various physical effects, it is still a useful research tool for evaluating common airflow patterns within meteorological systems on various scales (*Merrill et al., 1985; Harris & Kahl, 1990; Harris & Kahl, 1994; Jaffe et al., 1997a; Mahura et al., 1997a; Jaffe et al.,*

1997b; Mahura et al., 1999 and others). Some uncertainties in these models are related to the interpolation of meteorological data, which might be sparsely measured, applicability of the considered horizontal and vertical scales, and assumptions of vertical transport (*Merrill et al., 1986; Draxler, 1987; Kahl, 1996*). More detail about computation, accuracy, and applications of trajectories is given in an excellent review prepared by *Stohl, 1998.*

We interpolated the original National Center for Environmental Prediction (NCEP) gridded wind fields (from the database DS.082, see Chapter 2.2) to potential temperature (isentropic) surfaces. We choose isentropic assumption in our study because isentropic trajectories are a better representation of the air parcels atmospheric transport in comparison with isobaric trajectories because they are more realistic. Additionally we should note that the quality of trajectory calculation is highly dependent on the original quality of the NCEP's fields (2.5° x 2.5° latitude vs. longitude), and it may not reflect the contribution of the frontal passages and local terrain phenomena. However, the trajectory errors rising during a single calculation might be smoothed in the further analysis due to the large number of trajectories in the multiyear dataset.

An interpolation procedure has been performed for a period of 10 years, 1987-1996. We applied a technique described by *Merrill et al., 1986.* All interpolated 3-D meteorological fields were stored at the Mass Storage System (MSS) at NCAR. Then, we used the wind fields on isentropic surfaces to calculate trajectories in the model domain at various levels within the atmosphere. The model grid domain selected for this study, covering the North Pacific territories with adjacent countries and seas, is located between 2.5°-77°N and 90°E-82.5°W.

All forward isentropic trajectories from the nuclear risk sites regions were computed twice per day (at 00 and 12 UTC, Universal Coordinated Time) at different potential temperature levels. These levels (total 16) ranged from 255°K to 330°K with a steps of 5°K. The National Center for Atmospheric Research (NCAR, Boulder, CO, USA) and International Center for Applied Systems Analysis (IIASA, Laxenburg, Austria) CRAY Ouray and SUN computer resources, respectively, were used to compute more than 467 thousand trajectories for each NRS. Less than two percent of the trajectories were missing because of the absence of archived meteorological data and processing problems.

In this study, instead of calculating only one trajectory for each NRS per UTC term, we used four trajectories for every calculation. The initial points of trajectories are located at each corner of a 1°x 1° of latitude vs. longitude box, where NRS is in the center of the box. Calculation of four trajectories simultaneously allowed us to evaluate a consistency of the wind field in the direction of the atmospheric transport.

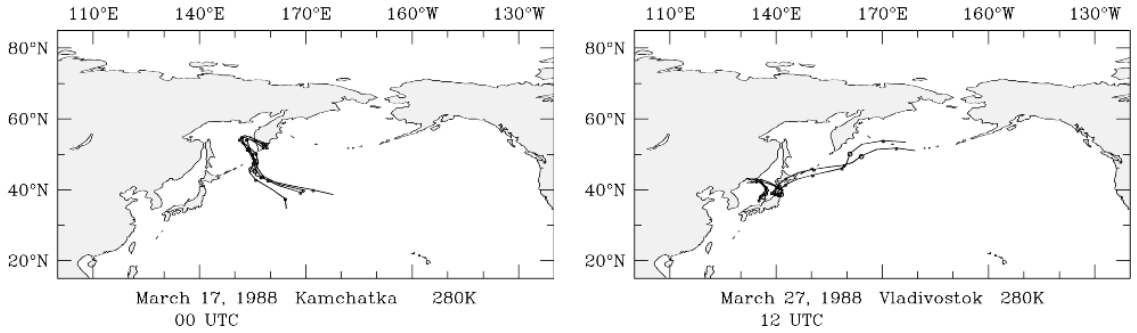

Figure 2.3.1. Examples of trajectories showing consistent air flow for Kamchatka NRS (left) and Vladivostok NRS (right)

Although we analyzed all calculated trajectories, we should note that there are differences in the representation of the general flow along trajectories. The flow is considered to be a reasonably consistent along the transport pathway if all four trajectories had shown a similar direction (reflecting convergence of flow) of transport for one time period (as shown in Figure 2.3.1). Trajectories, showing a strong divergence of flow, are assigned to a category of the "complex trajectories" (as shown in Figure 2.3.2). These trajectories reflect more uncertainties in the air parcel motion. These differences are not so important in evaluation of the general climatological patterns, but they can be significant in, for example, identification of source regions for air pollutants, evaluation of the nature of the specific events with recorded elevated concentration of species, tracking tracers in the atmosphere, and others.

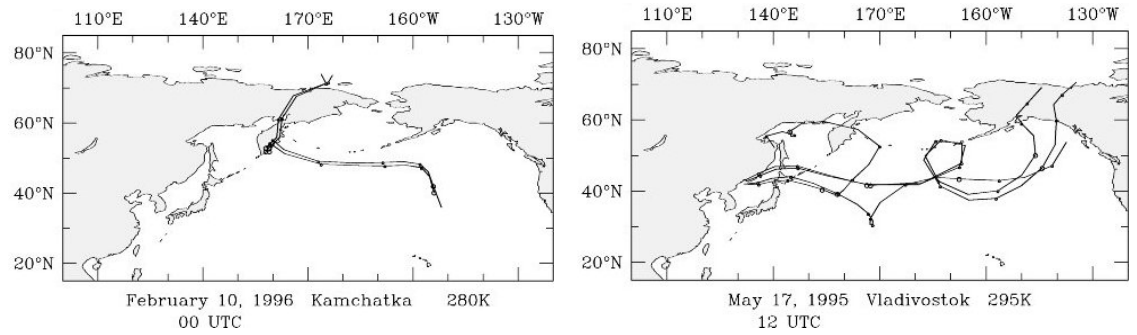

Figure 2.3.2. Examples of trajectories showing divergence of flow (complex trajectories) for Kamchatka NRS (left) and Vladivostok NRS (right)

For example, as shown in Figure 2.3.1 (right), the air parcels that originated over the Vladivostok NRS region at 27 March 1988, 12 UTC passed over the northern areas of Japan during the first days of transport. Then, it followed along the main pathway for the North Pacific cyclone systems toward the Aleutian Chain islands and reached the Aleutian Low. It should be noted that a large portion of cyclones, originating over the continental and shoreline parts of the Russian Far East, Japan, Korea and China, follow this track on the way to the Bering and Chukchi Seas.

For both NRS, which contains the nuclear submarine reactors and radioactive storage facilities, in a case of an accidental release, the most probable release heights would be within the surface layer of atmosphere i.e. within the first hundred meters above the ground. Therefore, as the next step, from all isentropic trajectories we selected only those trajectories originating within this layer. So, for each site, we extracted approximately 29 thousand trajectories (from original more than 467 thousand trajectories). All chosen trajectories for further statistical analysis have duration of 5 days. We decided to use this limitation in duration of trajectories because of 1) quality and accuracy of trajectory calculations after 5 days drops significantly, 2) observing development frames of the synoptic scales systems in the North Pacific region, as well as 3) relative proximity of the analyzed NRS impact geographical regions from the sites of interest.

Finally, to study altitudinal variations in the flow patterns (in particular, within the boundary layer and free troposphere), we also considered trajectories that originated over the NRS regions at the top of the boundary layer (i.e. we assumed - near 1.5 km above sea level (asl)).

2.4. Trajectory Cluster Analysis

In general, the cluster analysis is a variety of multivariate statistical analysis techniques, which could be used to explore the existing structure within data sets (*Romesburg, 1984*). The specific purpose of this analysis is to divide a data set into groups (or clusters) of similar variables (or cases). *Miller (1981)* initiated application of the cluster analysis on trajectories. It was used to analyze the general atmospheric transport pathways at the Mauna Loa Observatory (Hawaii) over the North Pacific Ocean. The important output of the study was evaluation of the airflow climatology, in particular, over long time periods. Later, cluster analysis techniques on trajectories were used extensively by various researchers in different scientific fields.

In general, output of cluster analysis on trajectories can provide insights on the tracers transport, common atmospheric flow patterns for the sites of interest, identification of the source regions for atmospheric pollutants, and etc. Some of these studies with respect to atmospheric pollutants were conducted by *Moody (1986), Moody & Galloway (1988), Harris & Kahl (1990), Harris (1992), Harris & Kahl (1994), Moody et al. (1994); Dorling & Davies (1995)* and others. Further, application of cluster analysis with respect to the nuclear risk sites, and in particular, for the nuclear power plants located in the Murmansk and Chukotka regions of Russia, have been performed by *Jaffe et al. (1997a), Mahura et al. (1997a), Mahura et al. (1997b), Baklanov et al. (1999), Mahura et al. (1999), Saltbones et al. (2000), Baklanov et al. (2001).*

In this study, we used the same cluster analysis technique that was applied in *Jaffe et al. (1997a), Jaffe et al. (1998a), Mahura et al. (1999),* and *Baklanov et al. (2001).* The SAS/STAT software package (developed by SAS Institute Inc., http://www.sas.com/) has tools for many types of statistical analysis techniques including various cluster analysis procedures. In our study, we used the FASTCLUS procedure, which performs a disjoint cluster analysis on a basis of the Euclidean distances computed from one or more quantitative variables. All available observations are divided into clusters in such a manner that every observation belongs to, at least, one

cluster. In the case of separate analyses for different number of clusters, we run the FASTCLUS procedure once for each calculation. This procedure is intended for use with large data sets, up to 100000 observations, which is very helpful in our study due to large number of trajectories. It is also possible to print brief summaries of all clusters it finds for further detailed analysis and visualization. We requested output data sets containing the designated cluster membership variables for more extensive examination

In the FARECS study, we used cluster analysis to divide calculated trajectories into groups, which represent the major airflow transport regimes. The following criteria were used: latitude and longitude values at each time interval of 12 hours. These represent both direction and velocity of air parcel motion. Similarity among trajectories in each cluster is maximized considering the full length of each 5-day forward trajectory. Within each cluster, individual trajectories can be averaged to obtain the mean cluster trajectory (or transport pathway). Thus, the original large data set of trajectories can be reduced to a small number of mean cluster plots. And further, these plots then could be interpreted, based on common synoptic conditions and features.

Using cluster analysis techniques, we summarized the airflow climatology for both NRSs regions – Vladivostok and Kamchatka. We performed the analyses on a seasonally, yearly, and for the entire period of 1987-1996 basis. Details on clustering and discussion of the results are presented in the Section of the "Results and Discussion" Chapter as well as in Appendix A.

2.5. Probability Field Analysis

Probabilistic analysis is one of the ways to estimate the likelihood of occurrence of one or more phenomena or events. As we mentioned, in this study we calculated a large number of trajectories that passed over various geographical regions. Each calculated trajectory contained information about longitude, latitude, altitude, pressure, temperature, relative humidity, and other variables at each 12 hours interval. The probability fields for these characteristics, either individual or combined, can be represented by a superposition of probabilities for the air parcels reaching each grid region in the chosen domain or on the geographical map. The most interest for the further analysis would be the following probabilistic fields: a) airflow patterns, b) precipitation factor, and c) fast transport.

The first type of the fields shows the common features in the atmospheric transport patterns, i.e. it may provide a general insight on the possible main direction of the radioactive cloud's transport as well as the probability that it will reach or pass any geographical area. The result of this analysis is an appropriate test to support or disprove results of the cluster analysis. This is because the atmospheric transport pathways, (or mean trajectory clusters), show only common direction of an airflow from the site. However, information between these pathways (or clusters) is missing.

The second type of probabilistic field describes the possibility for removal processes from the contaminated air mass while air parcels pass over the particular geographical area. Such an analysis was used in *INTAS, 2000*. In our study, due to time constraints, we did not evaluate such fields, but discussion of the possibility of the

radionuclide removal during atmospheric transport is included in the "Results and Discussion" Chapter of this report.

The third type of probabilistic field indicates the probability of the fast movement of air parcels during the first day of transport. It is important information, especially, for estimation of the radionuclides impact such as iodine and cesium isotopes. These fast transport fields show, which territories may be reached after the first day, and which areas are at the most danger due to faster transport probability.

In our study, probabilistic fields were constructed two types of the fields – airflow and fast transport fields. To construct these fields we used latitude, longitude, altitude, and time step values for each 5 and 1 day's trajectory. At the first step, a new rectangular grid domain was created with a resolution of 2.5° x 2.5° latitude vs. longitude grid cells. The NRS is located at the center of domain on the intersection between grid lines. All intersections of trajectories with each grid cell were counted. Among all grid cells, the cell where the absolute maximum of intersections took place was identified as an "absolute maximum cell" (AMC). Because all trajectories start near the NRS region, to account for contribution into the flow at the larger distances from the site, we extended the area of maximum to adjacent cells to the AMC. We compared the number of intersections in cells adjacent to AMC and assigned additional cells, which had less than 10% of difference between cells. Therefore, this new "area of maximums", if isolines are drawn, will represent area of the highest probability of the possible impact (AHPPI) from NRS. Assuming the value of 100% for this area, the rest could be re-calculated as percentage of the area at the highest probability of the possible impact. An illustration of the probability field for the Vladivostok NRS fast transport patterns is shown in Figure 2.5.1. This figure shows that during January, if an accidental release should take place at the Vladivostok NRS, the northern territories of Japan would be at the higher risk of possible NRS impact in comparison with central and southern territories.

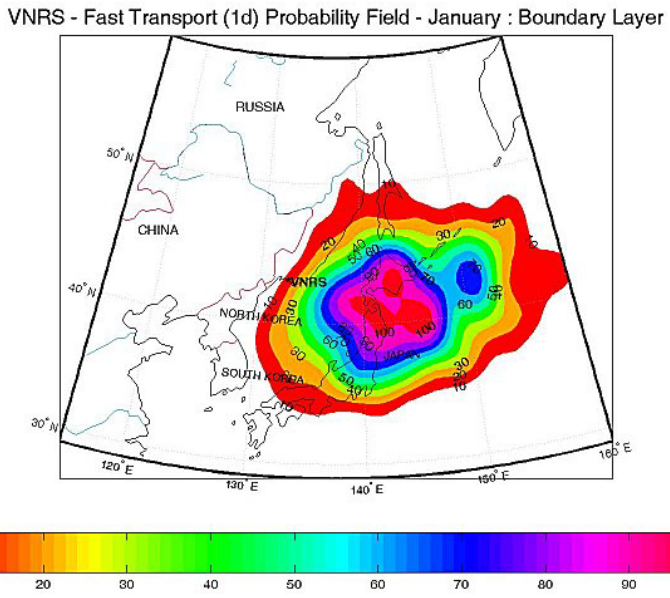

Figure 2.5.1. Vladivostok NRS fast transport probability field during January

In our study, probability fields reflect existing variations in the flow patterns for trajectories originating within the boundary layer. The analysis was done for the period of 1987-1996, by year, season, and month. Results of the probability field analysis are presented in the Section of the "Results and Discussion" Chapter as well as in Appendixes B and C. For this study, we also developed a visualization package using Matlab software (developed by MathWorks Inc., http://www.mathworks.com) to represent in an interactive regime monthly, seasonally, and 1987-1996 airflow and fast transport probability fields for the Vladivostok and Kamchatka NRS. Details are described in Appendix E - "Software Visualization Tools".

2.6. Typical Transport Time Analysis

In the emergency response systems for nuclear accidents, the estimation of the radionuclide transport time to a particular territory, region, county, city, and etc is one of the important input parameters in the decision-making process. It is possible to extract such information from calculated trajectories and construct typical transport time fields. Such fields may show how long it will take to reach a particular geographical area from the nuclear risk site location, and what areas are at the highest risk during the first days after an accidental release.

At the first step, we created a new polar grid domain with the risk site in the center. We divided the entire region into 36 sectors, where each sector represents 10 degrees. Along each sector line, we divided distance by 2 degrees starting at the NRS location. For our study, we selected 70 degrees along each sector line. It is approximately 7.1 thousand km in distance along the latitude, if we assume that for the middle latitudes 1 degree is equal to 110 km. Therefore, we created a grid domain containing of 1260 grid cells.

In the same way as in the probability field analysis, we counted number of intersections in each grid cell of the domain. To perform this operation, we initially transformed all trajectory end points for one time interval (for example, 2 days) expressed by the latitude vs. longitude into the angle and distance (or radius) from the NRS location. Then, for this time interval of 2 days, we compared number of intersections in cells along each sector line to find an absolute maximum cell (AMC). It should be noted that sometimes more than one maximum could be identified along the sector line. Because our concern is a possibility of the fastest transport to the remote territory, we selected the first AMC, which is the closest to NRS. After AMCs had been identified for all 36 sectors, the locations of sectors' centers from the polar grid domain were converted back into geographical coordinates of latitude vs. longitude. Finally, an isoline for the typical transport time of 2 days had been drawn through these new geographical coordinates as shown, for example, in Figure 2.6.1. Applying a similar procedure, we are able to construct isolines for other terms such as 0.5,1, 1.5 and etc days of transport.

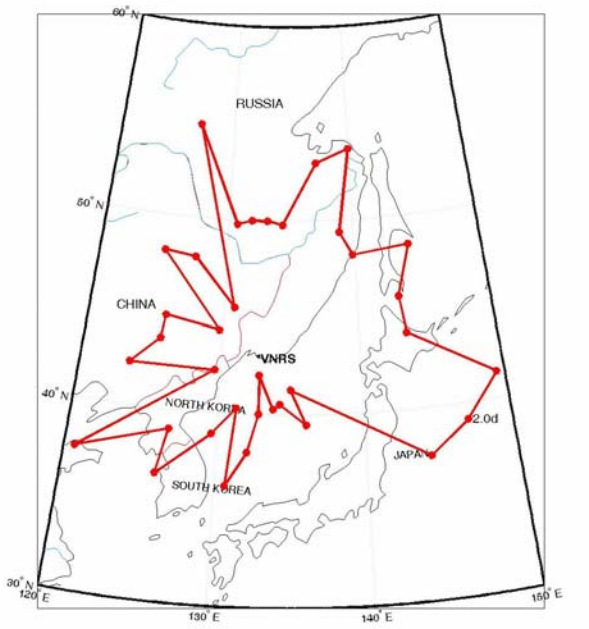

Figure 2.6.1. Typical transport time field at 2 days (case: Vladivostok NRS, spring)

A pitfall in the interpretation of such analytic results is the fact that the airflow pattern is not usually symmetrically distributed around the site of interest. Generally speaking, it should propagate toward the main direction of the large-scale flow pattern. After a few days of transport air parcels definitely will leave the area surrounding the nuclear risk site. Therefore, the constructed typical transport time fields in the direction of the lower probability of atmospheric transport will not reflect a realistic figure. That is illustrated by the data shown in Table 2.6.1.

As shown in the table, for term (in days) in each sector ranging from 0 to 360 degrees, there are a number of trajectory intersections in AMC (#), percentage of trajectories contribution into the 360 degrees belt (%), and test of obtained data significance (SS) to plot final isoline. If the distribution is symmetrical, we will have approximately 2.78% (100% / 36 sectors = 2.78% in each sector) of each sector's contribution in the entire belt. Assuming now 2.78% as 100% of plausible contribution, we can recalculate the threshold (or separation) values for 75, 50, and 25%, which are 2.08, 1.39, and 0.69%, respectively. For further analysis (or construction of the typical transport time isolines), we use only those AMCs, which are above 1.39% in the total contribution from individual sectors. For example, as shown in the table, in the sector between 50-60 degrees the number of trajectories accounted in the AMC is equal to 190 for term of 2 days. These trajectories contribute into the 360 degrees belt almost 6% of the total, and this contribution is higher than for the symmetrical distribution case (2.78%).

Sector	#	%	SS	Sector	#	%	SS
0-10	34	1.1	*	180-190	35	1.1	*
10-20	55	1.7	>50	190-200	30	1.0	*
20-30	80	2.5	>75	200-210	33	1.1	*
30-40	109	3.5	**OK**	210-220	21	0.7	-
40-50	136	4.3	**OK**	220-230	14	0.4	-
50-60	190	6.0	**OK**	230-240	13	0.4	-
60-70	282	8.9	**OK**	240-250	7	0.2	-
70-80	337	10.7	**OK**	250-260	13	0.4	-
80-90	408	12.9	**OK**	260-270	16	0.5	-
90-100	460	14.6	**OK**	270-280	12	0.4	-
100-110	274	8.7	**OK**	280-290	12	0.4	-
110-120	156	4.9	**OK**	290-300	13	0.4	-
120-130	90	2.9	**OK**	300-310	16	0.5	-
130-140	38	1.2	*	310-320	22	0.7	*
140-150	35	1.1	*	320-330	20	0.6	-
150-160	36	1.1	*	330-340	25	0.8	*
160-170	33	1.1	*	340-350	39	1.2	*
170-180	19	0.6	-	350-360	43	1.4	*

Table 2.6.1. Evaluation of contribution of absolute maximum cells in the construction of the typical transport time field at 2 days (case: Vladivostok NRS, spring)

To resolve differences in contribution issue the AMC data represented in the table with higher (threshold is higher than 1.39%) and lower (threshold is lower than 1.39%) percentage of occurrence were marked differently (“OK” - 100% and more of the AMC contribution into the 360 degrees belt; “>75” – 75-100%; “>50” - 50-75%, ”*” - 25-50%, ”-“ - <25%). Although we understand that the second type of isolines is based on lower number of data points, this still might reflect useful information for a case where an accident did happen and atmospheric transport took place in a low probability sector. In our study, analysis for each site was performed for the period of 1987-1996 and by seasons. The results of this analysis are summarized in the Section of the “Results and Discussion” Chapter as well as in Appendix D.

3. RESULTS AND DISCUSSION

3.1. Nuclear Risk Sites Possible Impact

In the FARECS study we analyzed all forward trajectories that originated over the Kamchatka and Vladivostok NRSs locations to investigate the likelihood that the nuclear risk sites would impact on several distant geographical regions. We assumed that any isentropic trajectory, which crosses into the boundaries of the chosen geographical region, might bring air parcels containing radionuclides. Therefore, only trajectories crossing boundaries of these regions were used in the further analysis. To analyze the probability of the NRSs' impact, we estimated the following parameters.

First, we estimated the number and percentage of trajectories reaching the boundaries of the chosen geographical regions. Second, we evaluated the number and percentage of days that at least one trajectory had reached the region. Third, we calculated the average transport time of air parcels to reach these regions. Fourth, we analyzed the probability of transport within different atmospheric layers. Fifth, we investigated the likelihood of very rapid (fast) transport of air parcels, i.e. transport in one day or less. We performed such evaluation over the 10 year study period (1987-1996), by individual year, season, and month to investigate possible temporal and spatial variations in the airflow patterns from the NRSs' regions. A summary of the transport from the Kamchatka and Vladivostok NRSs to the chosen geographical regions is shown in Table 3.1.1. Monthly variations in the average transport time (in days) and number of trajectories reaching regions during 1987-1996 are shown in Figures 3.1.1 and 3.1.2 for both NRSs.

To estimate the probability of impact, the number of trajectories reaching the region and the number of days this took were calculated. If one or more trajectories crossed a region during the day (00 and 12 UTC), we assume that this day is a day of impact in that region. This approach yields two values to estimate the probability of impact that air in the VNRS region will be transported to geographical region. If one considers all the forward trajectories starting at the Vladivostok NRS, then, for example (as shown in Table 3.1.1.), 31.9% of these reach the North Japan region. If instead one considers the percentage of days when one or more trajectories reach the same region, then an annual average value of 53.5% is obtained. Since there are 8 forward trajectories from VNRS calculated per day (4 each at 00 and 12 UTC), then on average, 3-4 (7249/1919=3.8) trajectories will reach this geographical region, if any do on that day. To some extent, the understanding of the probability of impact is related to the duration of any release that may occur. The percentage of all trajectories represents the probability that air from the Vladivostok NRS region is transported to the North Japan region at any given moment. However, if an accident release was to occur for 24 hours, then the 53.5% value is probably more appropriate to consider. Therefore, the 53.5 and 31.9% values represent upper and lower bounds to the probability of impact.

Taking into account that the thickness of the boundary layer for a neutral stratification of the atmosphere is close to 850 hPa (≈1.5 km), the trajectories were divided into two categories. First, there are trajectories that transport air within the boundary layer. Second, there are trajectories that transport air in the free troposphere.

The higher concentrations of radionuclides are more likely at the surface in the cases of the boundary layer transport,. For the Kamchatka NRS (see Table 3.1.1), the boundary layer transport dominates in the South Japan region and it occurs in 69.2% of the cases. The lowest probabilities of such transport are 7.2, 9.8, and 6.7% of the time for the North Korea, North China, and Seashore China regions. For the Vladivostok NRS, the boundary layer transport also prevails in the South Japan region (87.1% of the cases) as well as in the South Korea region (72.6%). The highest probabilities of the free troposphere transport are for the US territories. Although the boundary layer transport may occur in any time of the year, there are times of the year when it is more frequent. We reflected this in Table 3.1.1 as the higher occurrence of the boundary transport.

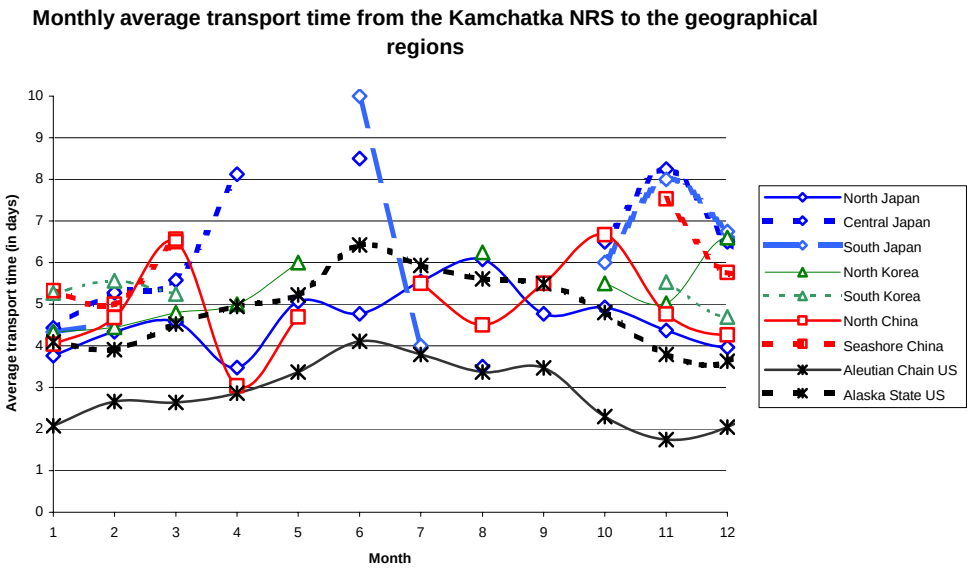

Figure 3.1.1A. Monthly variations in the average transport time (in days) from the Kamchatka NRS to geographical regions based on the forward trajectories during 1987-1996

The cases of the fast transport (1 day or less), as shown in Table 3.1.1, account on average between 0-24.1% (KNRS) and 0-62.8% (VNRS) of the cases from the total number of trajectories that crossed into the regions. In particular, it depends on the NRS's proximity to a particular geographical region. For example, 4555 trajectories reached the North Japan region in a day or less from the total of 7249 trajectories that reached the same region during 1987-1996. These 4555 trajectories represent 62.8% of the 7249 trajectories (as 100%). For the Kamchatka NRS, we did not identify any fast transport events to the Korean, Chinese, and Central and South Japan regions. The highest possibility of such events – 24.1% of the time - is for the Aleutian Chain Islands. For the Vladivostok NRS, we did not observe any fast transport events to either US territory, but they are common in all other geographical regions. Their occurrence depends on the proximity of the nuclear risk site to the region.

The monthly variations of the average transport time from NRSs to the geographical regions (shown in Figures 3.1.1A and 3.1.1B) are obvious. In general, it depends on the seasonal change in the wind speed. During winter, the speed is higher compared with the summer period. Therefore, the travel time increases in summer and decreases in winter. The yearly averages and standard deviations for the transport time are shown in Table 3.1.1. For the Kamchatka NRS, the average transport time is the shortest to reach the Aleutian Chain Islands and it is equal to approximately 3 days. For all other regions, it varies from 4.3 to 6.3 days. For the Vladivostok NRS,

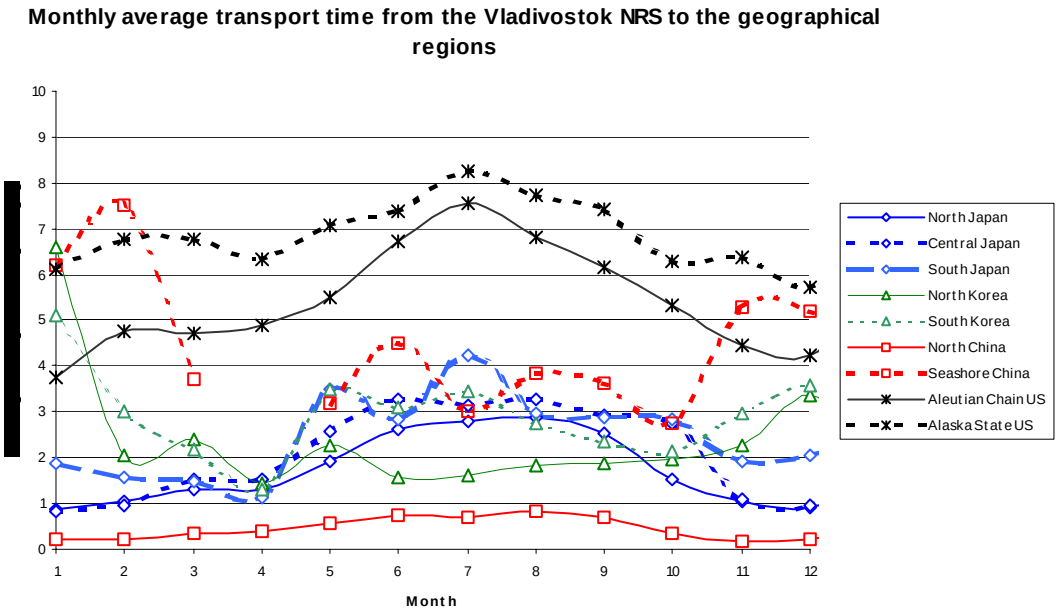

Figure 3.1.1B. Monthly variations in the average transport time (in days) from the Vladivostok NRS to geographical regions based on the forward trajectories during 1987-1996

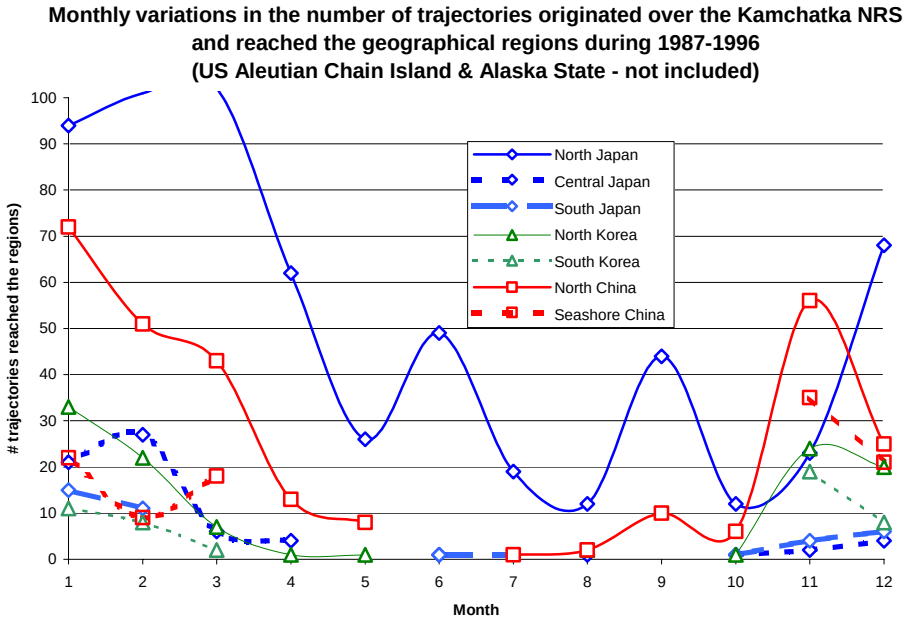

Figure 3.1.2A1. Monthly variations in the number of trajectories originating over the Kamchatka NRS at lower altitudes within the boundary layer and reaching the geographical regions during 1987-1996

the average transport time is the shortest – 0.5 days - for the North China region (it is due to proximity of the geographical region to NRS), and the longest – 7 days – for the Alaska State region. For all other regions, it varies from 1.6 to 5.7 days.

The monthly variations of the higher occurrence of transport for trajectories reaching the geographical regions during 1987-1996 are shown in Figures 3.1.2 and summarized in Table 3.1.1. The atmospheric transport from the Kamchatka NRS to the Japanese regions occurs more often during winter season, although it continues in the spring in the North and Central Japan regions. This transport dominates during November-February in the Korean regions, and during November-March in the Chinese regions. For the US territories, transport in summer is more common, although for the Aleutian Chain Islands the period continues from April to November. For the Vladivostok NRS, atmospheric transport toward the US territories is more frequent during August-October (Figure 3.1.2B), although a peculiarity is the high probability of transport in May too. The transport occurs most frequently during winter-spring for the North and Central Japan regions, although in the South Japan, Korean, and North China regions it takes place during the spring-fall months.

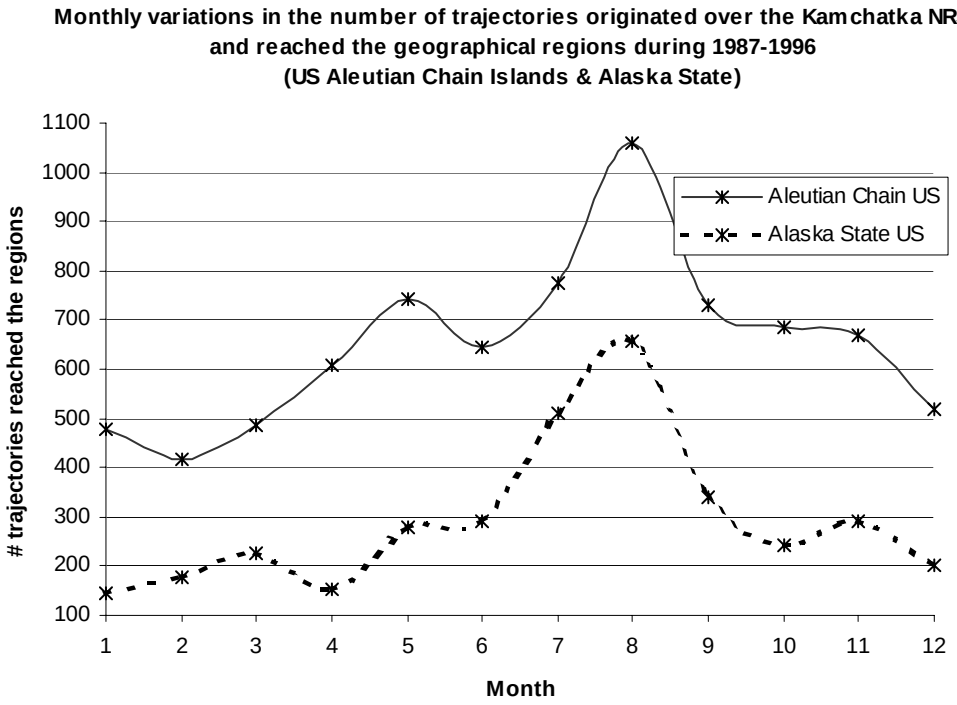

Figure 3.1.2A2. Monthly variations in the number of trajectories originated over the Kamchatka NRS at lower altitudes within the boundary layer and reached the US regions during 1987-1996

Finally, we should mention several findings from the analysis of the NRSs possible impact to the studied geographical regions.

For the Vladivostok NRS, the North China and North Japan regions are at higher risk of possible impact than the other regions. It is mainly due to their proximity to NRS. For the Korean regions, it is lower due to peculiarities in the general airflow patterns of westerly origin. The lower and (upper) bounds of the probability of impact are 31.9 (53.5)% and 34.7 (86.9)% for the North China and North Japan regions, respectively. On average, atmospheric transport to these regions could occur in 0.5 and 1.6 days, respectively. The fast transport events are not common for the US territories, but these events could represent the major concerns for the Japanese and North Korea regions. The boundary layer transport is common for all regions for more than half of the time, except for the US regions.

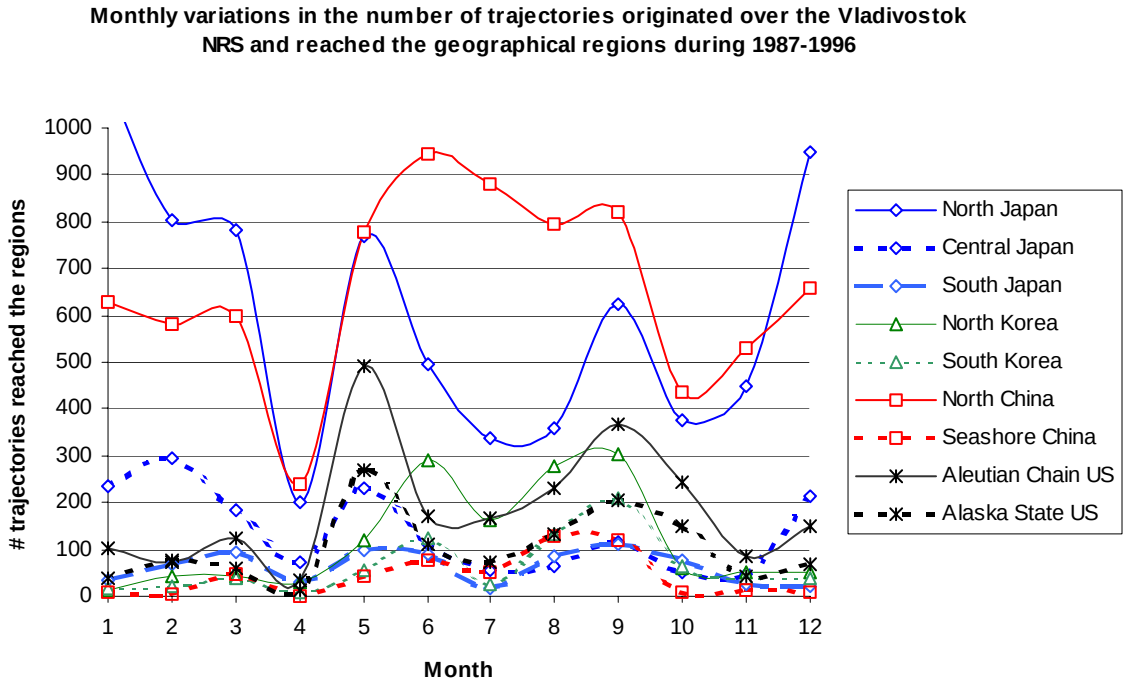

Figure 3.1.2B. Monthly variations in the number of trajectories originating over the Vladivostok NRS at lower altitudes within the boundary layer and reaching the geographical regions during 1987-1996

For the Kamchatka NRS, the US territories are at the highest risk compared to the other regions. The lower and (upper) bounds of the probability of impact are 29.9 (53.8)% and 13.4 (32.1)% for the Aleutian Chain Islands and State of Alaska, respectively. On average, atmospheric transport to these regions could occur in 3.0 and 5.1 days, respectively. For all other regions, the bounds of the probability of impact are only around a few percent with the exception of the North Japan region (8%). In the same way, the fast transport events are also observed only in these – North Japan, Aleutian Chain Islands, and State of Alaska geographical regions. The boundary layer transport dominates in most of the studied regions, but the free troposphere transport dominates in the Chinese and North Korea regions.

3.2. Atmospheric Transport Pathways

In this study, we evaluated the transport patterns from the NRSs regions. We found that the average transport times to the chosen geographical regions (as shown in Table 3.1.1) vary from half a day to 7 days, depending on the NRS considered. Because of uncertainties in the trajectory calculations after 5 days, we decided to use in the cluster analysis only forward trajectories with the duration of 5 days. Figures 3.2.1 and 3.2.2 show the atmospheric transport pathways from the KNRS and VNRS regions using trajectories during 1987-1996, which had an origin within the atmospheric boundary layer. The mean trajectory for each cluster is given with points indicating 12-hour intervals. Two numbers were used for each cluster: first - identifier of a cluster;

second - percentage of trajectories within a cluster. The seasonal summary for atmospheric transport pathways from both NRSs is shown in Table 3.2.1.

Season	Kamchatka NRS			Vladivostok NRS		
	Transport to (in %)			Transport to (in %)		
	West	**North**	**East**	**West**	**North**	**East**
Spring	23		87	7	17	76
Summer	26		74		18	82
Fall	15	17	68		32	68
Winter	37		63	10	14	76

Table 3.2.1. Seasonal summary for atmospheric transport pathways from the Kamchatka and Vladivostok NRSs

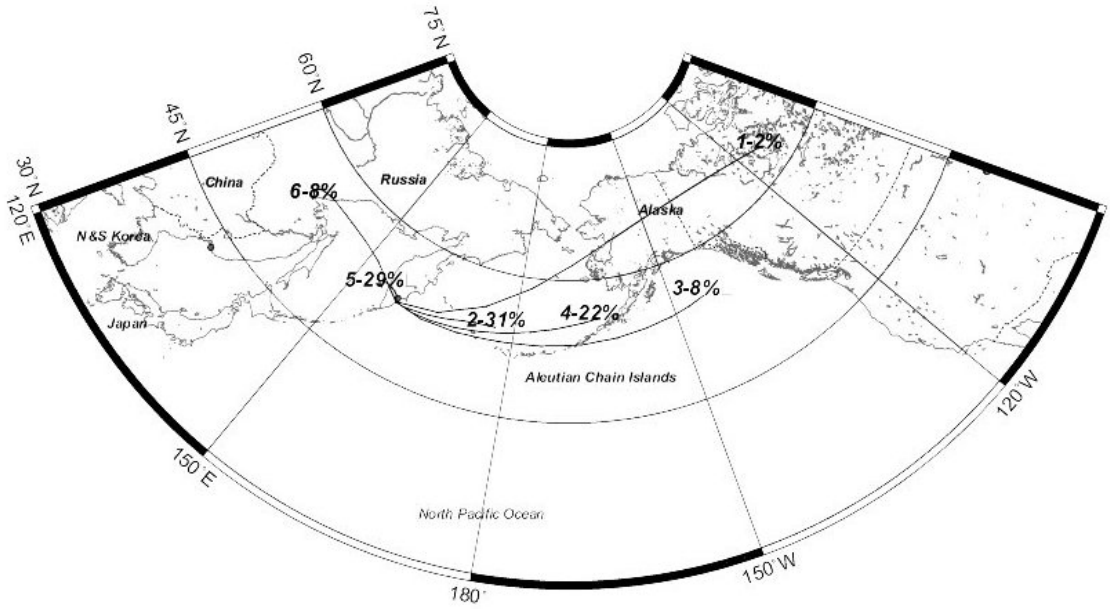

Figure 3.2.1. Atmospheric transport pathways (cluster mean trajectories) from the Kamchatka NRS region based on the forward trajectories during 1987-1996

In our study, six clusters were identified for the trajectories originating over the Kamchatka NRS region within the boundary layer (Figure 3.2.1). Four of them (#1, 2, 3 and 4 with 2, 31, 8 and 22% of occurrence, respectively) show westerly flow. These were observed about 63% of the time. Cluster #1 was used to show the possibility of the relatively rapid westerly flow toward the State of Alaska and Canadian territories.

Cluster #6 (8%) shows easterly flow toward the continent both within the boundary layer and free troposphere. Cluster #5, which occur 29% of the time, is also transport to the west but it is significantly slower compared with cluster #6. Throughout the year, westerly flow is predominant for the Kamchatka NRS (see Table 3.2.1). Transport from the west varies from 63% (in winter) to 87% (in spring) of the time. Transport from the east occurs from 15% (in fall) to 37% (in winter) of the cases. Transport with the northward component is only during fall and it is equal to 17% of the cases.

A similar number of clusters – six – were identified for the trajectories originating within the boundary layer over the Vladivostok NRS region (Figure 3.2.2). Four of them (#1, 3, 5 and 6 with 32, 3, 11 and 21% of occurrence, respectively) show westerly flow too. These were observed about 67% of the time. Among these clusters, cluster #3 represents the possibility of the relatively rapid westerly flow toward the North America territories. Cluster #4 (22%) shows easterly flow. Cluster #2, which occur 11% of the time, is transport with the northward component of the flow through the Okhotsk Sea. Throughout the year, the westerly flow is also dominant for the Vladivostok NRS (see Table 3.2.1). Transport from the west varies from 68% (in fall) to 82% (in summer) of the time. Transport from the east occurs only during winter-spring and varies from 7% (in spring) to 10% (in winter) of the cases. Transport with the northward component is a peculiarity of the Vladivostok NRS. It is reflected in each season throughout the year and varies from 14% (in winter) to 32% (in fall) of the time.

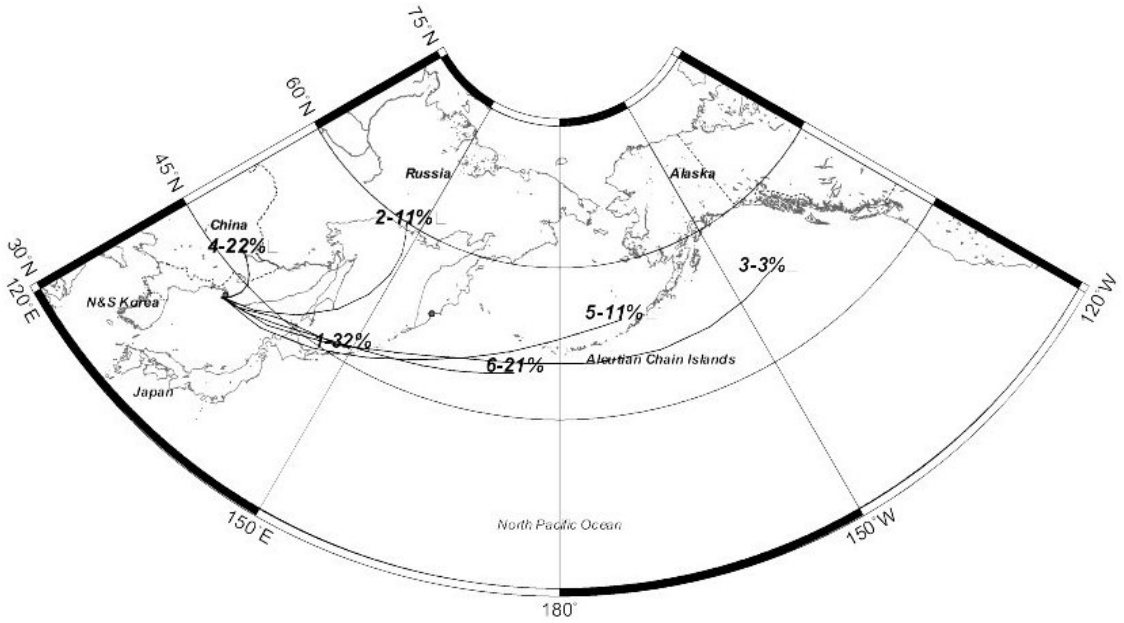

Figure 3.2.2. Atmospheric transport pathways (cluster mean trajectories) from the Vladivostok NRS region based on the forward trajectories during 1987-1996

We found that for both NRSs the westerly flow is dominant throughout the year, and occurs more than 60% of the time. The relatively rapid westerly flow toward the North America continent can reach the maximum occurrence during fall-winter (8-11% of the time) and during winter-spring (12-13% of the time) for the Kamchatka and Vladivostok NRSs, respectively. At the higher altitudes - 1.5 and 3 km asl (i.e. within

the free troposphere) the probability of transport from the west increases up to 85% of the time. Detailed seasonal variations in the mean transport pathways from the Kamchatka and Vladivostok NRSs within the boundary layer are shown in Appendix A.

3.3. Airflow and Fast Transport Probability Fields within the Boundary Layer

To test and compare the results of clustering we calculated the airflow probability field using all forward trajectories that originated over the Kamchatka and Vladivostok NRSs regions during 1987-1996. Such probability fields show geographical variations in the airflow patterns from the chosen sites. In a climatological sense, the path of airflow from the chosen site could be represented by a superposition of the probability of air parcels reaching each grid region on a geographical map. The regions with higher occurrence of trajectory passages are areas where the probability of the possible NRSs impact will be higher.

Figure 3.3.1 and 3.3.2 show the airflow probability fields for the Kamchatka and Vladivostok NRSs constructed using all the 1987-1996 trajectories. Each probabilistic field is presented using isolines, given with an interval of 5%, on the background of the geographical maps. The areas of the higher probability, which are located close to the NRSs regions, indicate that trajectories have spent more time in this geographical area. Because all trajectories start near the site, the cumulative probability is 100% there. Thus, the field was altered using the similar correction factor as *Poirot & Wishinski, 1986* and *Merrill, 1994*. This factor takes into account the contribution of flow at greater distances. The airflow probability fields also show that westerly flows are predominant for the Kamchatka and Vladivostok NRSs regions. It is in agreement with the results of the trajectories' cluster analysis.

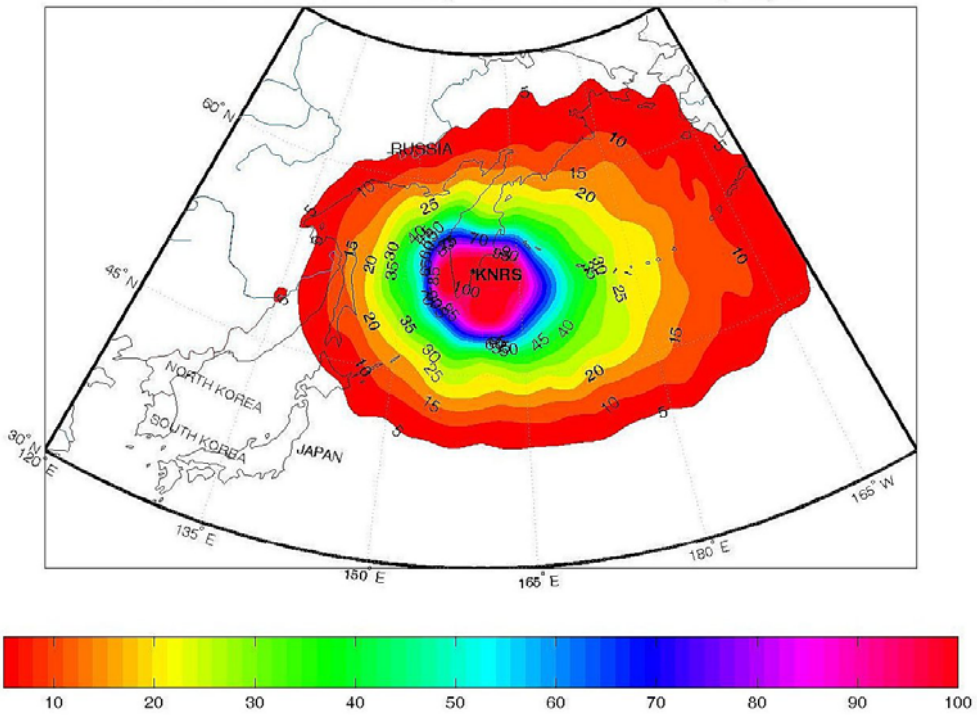

Figure 3.3.1. Airflow probability field within the boundary layer for the trajectories, originated over the Kamchatka NRS region during 1987-1996 (isolines are shown every 5%)

For the Kamchatka NRS, the airflow is concentrated along the major tracks of the high and lower pressure systems. These systems are always under the influence of the Aleutian Low and Siberian High activities. During fall, the airflow reaches the North America continent. During May-November the possibility for the air masses to pass over the North Japan region is the lowest. November is a time when air masses have ability to reach the Arctic shore territories, and it is a time for the Arctic front to move northward at the Russian Far East. During August, the airflow could pass over parts of the State of Alaska.

For the Vladivostok NRS, the similar dominance of the westerly flow could be identified. During summer, the northward component of the airflow became evident. At the end of the spring, it passes over the northern parts of the continental areas of the Russian Far East. During August-November, the airflow could reach the northern areas of the Okhotsk Sea and seashore of the Magadan Region. In September, the airflow pattern could be observed in the Seashore China region reaching the lower 30°N latitudes. Detailed seasonal airflow probability fields within the boundary layer for both sites are shown in Appendix B.

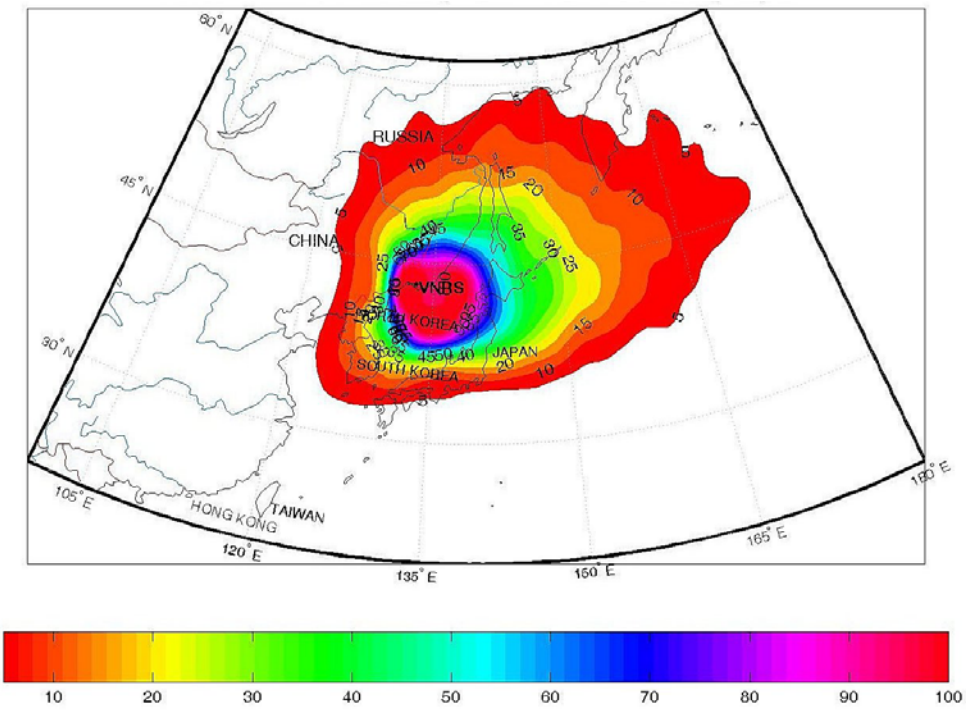

Figure 3.3.2. Airflow probability field within the boundary layer for the trajectories, originated over the Vladivostok NRS region during 1987-1996 (isolines are shown every 5%)

Although atmospheric transport from the radiation risk site or region to another geographical area might occur at any time, the fast transport is the greatest concern. It is an especially valid and important issue for the measures of the emergency response and preparedness. To study the contribution of the fast transport we evaluated all available trajectories during the first day of their transport, i.e. all trajectories were routinely terminated after 1 day of transport. In a similar way, as for the airflow probability, we constructed the fast transport probability fields. All these fields show the probability of air transport from the NRSs during the first day with respect to the area of the maximum possible impact from the NRSs marked as 100 (Figure 3.3.3 and 3.3.4). The analysis has been done for the entire period and each year, as well as by season and month. We analyzed the lowest altitude of trajectories, i.e. trajectories starting below 0.5 km asl. This is due to the major importance of the boundary layer transport, especially for the relatively short-lived radionuclides and during the first several hours after an accident.

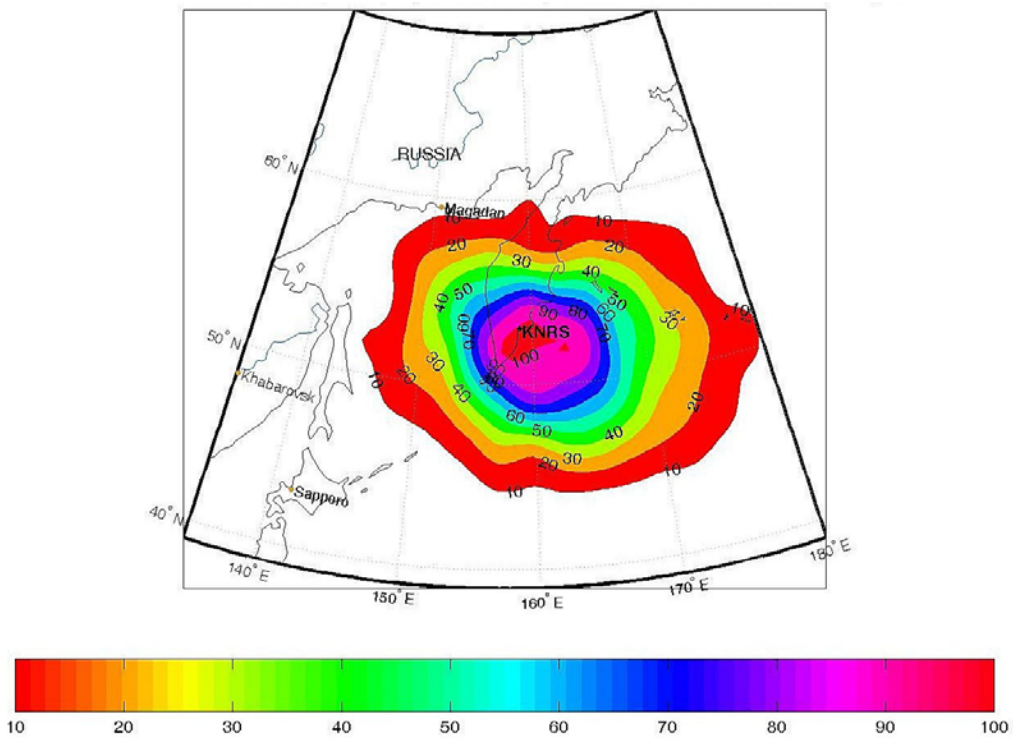

Figure 3.3.3. Fast transport probability field within the boundary layer for the trajectories, originated over the Kamchatka NRS region during 1987-1996 (isolines are shown every 10%)

Our analysis of the fast transport probability fields showed that the westerly flow is dominant for both NRSs. It is also in agreement with the results of the cluster analysis of trajectories.

For the Kamchatka NRS, the area of the highest probability of the possible impact (AHPPI) from the NRS is located to the southeast from the site, except during summer. During winter, there is a possibility of the fast transport toward the Sakhalin Island. During fall and spring, it could reach the Magadan Region territories. In summer due to lower wind speeds, it is concentrated around the NRS region. During December-April, the fast transport field reflects possibility of reaching the Sakhalin Island and Magadan Region territories. During September-October, it almost reaches the Magadan city adjacent territories. In November, there is a possibility to reach the Primorskiy Kray. The AHPPI is located to the east and south of the NRS during November-December. In October, it is to the north, and during February-March – to the west of the site. Starting in May, the total area of the AHPPI, which is under influence of the fast transport pattern, decreases, but in August, it will start again to increase.

For the Vladivostok NRS, the AHPPI is also to the east and south of the site. Although during winter it is located far from NRS, during summer it is around the site. During fall, AHPPI is over the Japan Sea territories. During December-April, it is above the North and Central Japan regions. In May, which might be considered as a transition period, there are two AHPPI – above the Japan Sea and to the north of VNRS in the Russian Far East. During June-August and October-November, the AHPPI is situated above the Japan Sea. In September, the southward component prevails. During September-November, there is a possibility to reach rapidly the North and South Korean

regions. Appendix D shows seasonal variations in the fast transport pattern for both NRSs. The monthly variations of the airflow and fast transport patterns for both sites are stored at the RAD FARECS CD. They could be displayed using developed MATLAB-oriented software (see details in Appendix D).

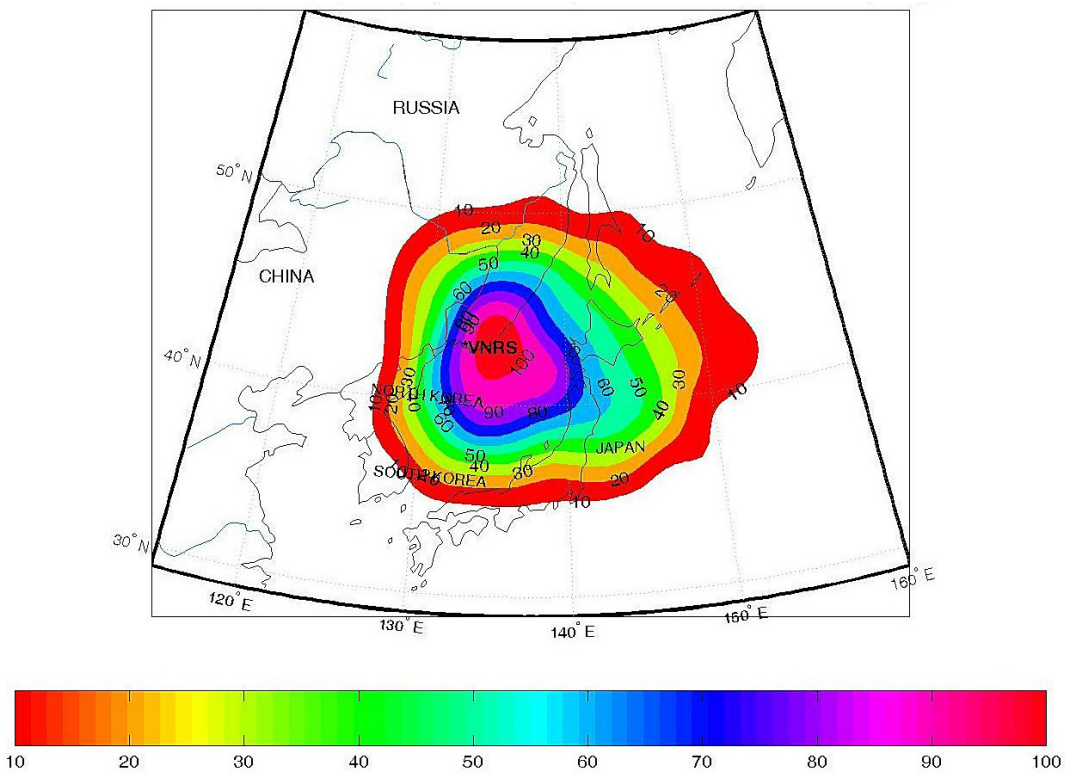

Figure 3.3.4. Fast transport probability field within the boundary layer for the trajectories, originated over the Vladivostok NRS region during 1987-1996 (isolines are shown every 10%)

3.4. Typical Transport Time Fields

Typical transport time fields are shown in Figures 3.4.1 and 3.4.2 for the Kamchatka and Vladivostok NRSs, respectively. Isolines of 0.5, 1, 1.5, 2, and 2.5 days of transport were constructed using 36 points (i.e. for each sector of 10º of total 360º there is one point). Due to time constraints, we created fields for only 1987-1996 period. All summarized data for seasons are tabulated in Appendix D and RAD FARECS CD. Therefore, if required, the typical transport time fields could be constructed independently.

As shown in Figure 3.4.1 the typical transport time from the Vladivostok NRS to reach the northern seashore areas of Japan is 1 day. Further, during 1-2 days the air parcels will pass over the Northern Japan. Typical transport time to reach the Koreas is about 2 days. We should note that the pattern of these fields depends strongly on the dominance of the westerly flows. Therefore, it is stretched toward the main tracks of the cyclones traveling to the Bering Sea and Gulf of Alaska. For the Kamchatka NRS (Figure 3.4.2), only the territories of the Kamchatka Region and islands in the adjacent seas, in particular, the Komandor Islands (Russia) and the far western islands of the Aleutian Chain Islands (USA) can be reached during the first 2.5 days

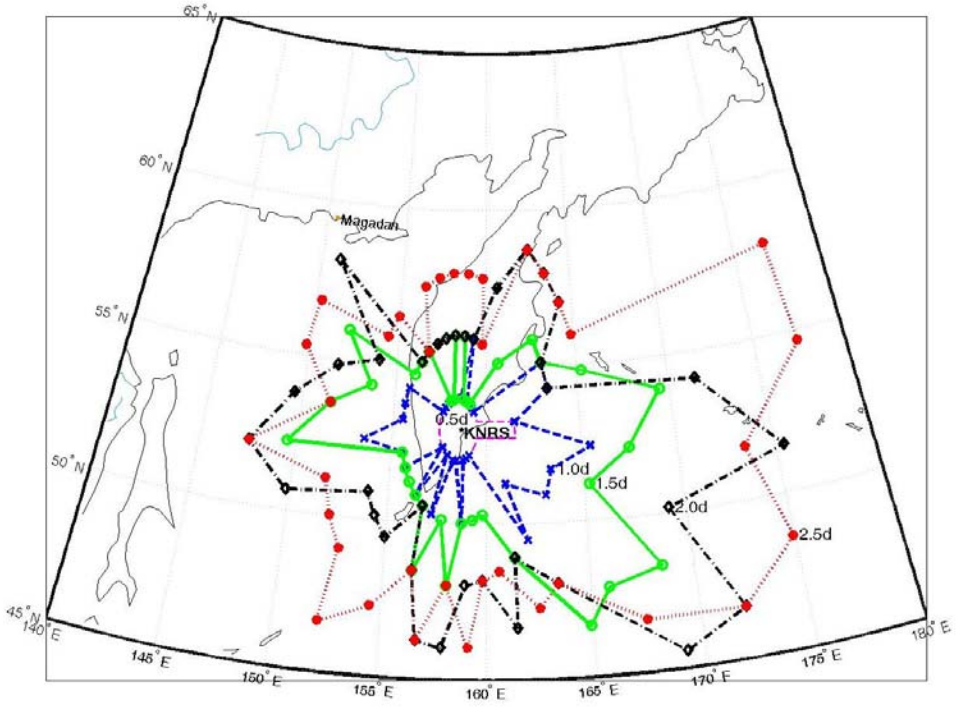

Figure 3.4.1. Typical transport time field from the Kamchatka NRS

The typical transport time fields are useful information in the emergency preparedness and response because these fields show: 1) How far the air parcels might travel from the NRS location during X-days of transport, and 2) What time it could take for an air parcel to reach the particular geographical area of concern.

An additional difficulty in construction of these fields also depends on how many data points we use to construct the fields. At the first approximation, we have only 36 for each temporal isoline. Near the site, due to short distances, we did not expect any difficulties. Far from the site, all original data points are relatively distant from each other along the isolines, i.e. there is a large gap between data points. The "smoothing" interpolation procedure will require additional intermediate points in the 10° sectors. To resolve this issue we suggest, in the future studies, to perform

calculation for the larger number of sectors; for example, 72 (5° in each sector) or finer resolution. It will allow one to construct the typical transport time fields more exactly.

Although we have data for seasons (tabulated in Tables of Appendix D) and 1987-1996 (shown in Figures 3.4.1 and 3.4.2), we would recommend consider month-to-month variability for better interpretation of the typical transport times to geographical territories.

In the FARECS study, due to time constraints, we did not analyze the probabilistic fields for the precipitation factor, although in the next section of this report we discuss approaches that could be used to evaluate the radionuclide transport, dispersion, and removal.

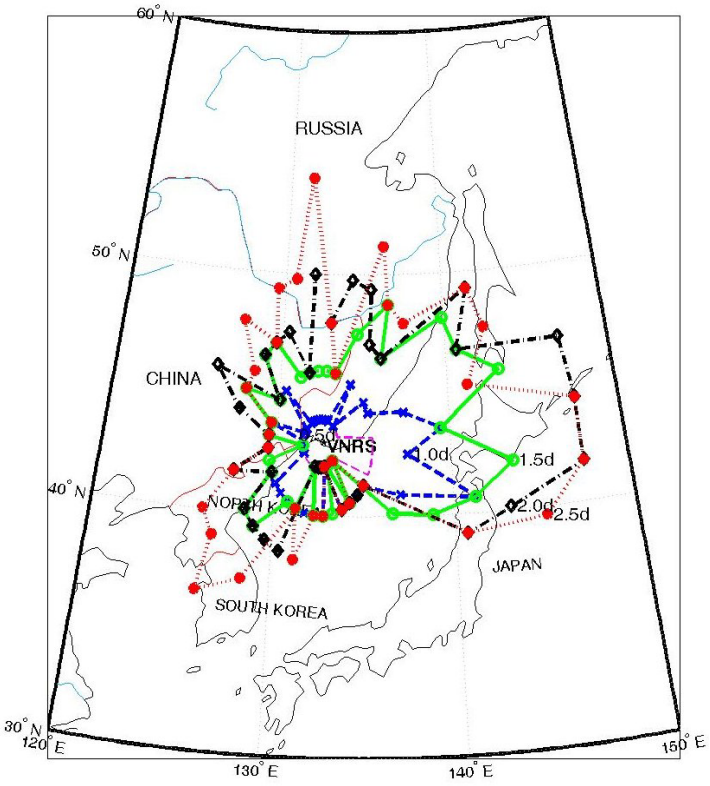

Figure 3.4.2. Typical transport time field from the Vladivostok NRS

3.5. Approaches to Evaluate Radionuclide Transport, Dispersion, and Removal

During the transport of any kind of pollutants, including radionuclides, within the atmosphere many different processes may influence the distribution of substances. In general, the temporal change of the radionuclide concentration during atmospheric transport will depend on the following factors. The dispersion, in all directions, due to horizontal advection by a wind velocity vector and turbulent diffusion processes are the most important factors. All radionuclides during transport are subject to dry deposition

of gaseous and particulate nuclides from the atmosphere by vegetation, biological, or mechanical processes and wet removal by precipitation, rainout, and snow. Other factors are radioactive decay and resuspension (i.e. lifting of already deposited material again back into the atmosphere), which is a secondary source of contamination and mostly appropriate on a local scale. Although contribution of all factors are important, there is always a possibility to ignore some of them depending on the scale of analysis and each term's contribution to a particular problem.

Wet deposition is the term of most concern. It is highly temporally and spatially dependent. It plays important role in the estimation of the radionuclide surface deposition. Deposition of radionuclides at the surface due to washout might produce a cellular figure as was recorded after the Chernobyl accident. Among several tens of radionuclides there are only a few of main interest - $^{137, 134}$Cs, $^{131, 133}$I, $^{89, 90}$Sr, ^{132}Te, ^{140}Ba, ^{103}Ru, and $^{238, 239}$Pu. In particular, iodine and cesium are isotopes of the major concern after the nuclear accidents, and especially during the first days.

In our study, due to time constraints, we did not analyze the possible contribution of the removal processes during atmospheric transport from the NRSs locations. There are several approaches how we might investigate this topic.

The first approach is based on the evaluation of the precipitation climatology for the particular geographical area. Such climatological maps (on a multiyear and seasonal basis for the large scale domains) might be obtained from the meteorological weather services. These maps would reflect the accumulated precipitation measured near the surface for each interval of time. It may be used for identification of the large size areas having common precipitation patterns. In particular, on such maps these areas are connected with the major centers of synoptic activity, for example, Aleutian Low. However, air parcels might travel within different atmospheric layers during their transport from the NRS region. For example, an air parcel could travel in the free troposphere and there may be no precipitation in this layer. However, the area is marked as precipitable on the climatological map and that will raise a misleading concern.

Therefore, the second approach is based on the evaluation of the probabilistic fields for the "precipitation factor" (*Mahura et al., 1999; INTAS, 2000*). Relative humidity "plays a role" of the precipitation factor. As we mentioned in the Second Chapter of this report, at each time interval of 12 hours for each forward trajectory we can calculate additional parameters including relative humidity. It is one of the factors, which will determine the possibility of radionuclide removal during transport. Increasing relative humidity in the atmosphere is one of the signals of the water vapor's increasing presence, and it may, in the presence of the cloud condensation nuclear (CCN), lead to formation of cloud cover. After clouds develop and form, under certain conditions there is a possibility of precipitation, and hence, radionuclide removal. Construction of the relative humidity fields is similar to the first steps in the probability field analysis. In this case we calculate an average value of the relative humidity in each grid cell. Both the precipitation and relative humidity fields have a cellular figure in comparison with the airflow pattern. A pitfall in this analysis is the fact that all relative humidity values are directly related to the existing flow pattern. So, each field is valid only with respect to a particular NRS. Nevertheless, it is a more realistic pattern of the

possible removal during transport than calculating rainfall climatological maps used in the first approach, because it includes processes above the surface.

The limitation always is how we might resolve precipitation processes during air parcels transport. To resolve them we would need a finer meteorological data resolution. The third approach is based on the direct evaluation of the wet deposition factor fields at the surface (*DMI-NARP, 2001*). It is also required to have multiyear output fields for comparison. For these purposes, we might run a transport model for a multiyear period and include one of the parameters of interest. Both the National Center for Environmental Prediction (NCEP, USA, North America) and European Center Medium Weather Forecast (ECMWF, Reiding, Great Britain, Europe) analyses, have resolution of more than 1 degree. Although HIRLAM model (at Danish Meteorological Institute, DMI) data might provide 3-D meteorological fields with a resolution of 0.15º x 0.15º latitude vs. longitude grids, there is still an issue of the computational resources usage.

If we assume either a unit puff release or continuous release every 12 hours at NRS, and run a model of atmospheric transport, dispersion, and removal of the radioactive material, we might produce a field for the wet deposition accumulated during a multiyear period. From one side, we might estimate what would be accumulated deposition field if a continuous release took place. From another side, we might identify the geographical areas, presumably of the cellular nature. These areas are territories where greatest removal of radionuclides is possible during transport from the site. It should be noted that such fields are also (as in the second approach) valid with respect to the particular site of interest.

Additionally, useful information might be obtained if we have the averaged climatological airflow patterns for the regional or local scale. We can evaluate seasonal and monthly average wet deposition factor fields applying averages for wind characteristics, precipitation, temperature, relative humidity, etc. For this case, the averaged 3-D meteorological fields are simulated, and then they are used in the transport model to calculate such characteristics as the air concentration, surface deposition, and doses. Specific cases for both unit and hypothetical, such as maximum projected accident (MPA), releases might be considered. Additional cases of the unfavorable meteorological conditions might be evaluated too (*INTAS, 2000; OCB, 2000*). Produced characteristic monthly or seasonal fields of the air concentration, deposition, and various doses could be used in the decision-making process at the first stages of the NRS accidents.

4. CONCLUSIONS

The main purpose of the FARECS study was to evaluate the atmospheric transport of pollutants from the Vladivostok and Kamchatka NRSs from the probabilistic point of view. The main question was: What is the probability to neighboring countries of radionuclide atmospheric transport in the case of an accident at the nuclear risk sites in the Russian Far East?

To answer this question, we applied the following research tools. The atmospheric isentropic trajectory model had been used to calculate trajectories that originated at two nuclear risk sites locations in the Russian Far East – Kamchatka and Vladivostok. The statistical analysis tools - exploratory, cluster, and probability field analyses - have been applied to explore the structure of the trajectory data sets. We evaluated the common atmospheric transport pathways from NRSs, airflow patterns, fast transport (i.e. transport in less than 1 day), and typical transport time, as well as characteristics of the atmospheric transport to the selected regions of interest – Japan, China, North and South Korea, State of Alaska, and Aleutian Chain Islands. We also investigated the seasonal, monthly, and year-to-year flow patterns in order to get better insight into the airflow variations. Further studies on the possible impacts of the radionuclide removal processes during atmospheric transport are suggested.

The main findings of this study are:

I. We found that for both NRSs, the westerly flow is dominant within the boundary layer throughout the year, and occurs more than 60% of the time. At the higher altitudes - 1.5 and 3 km asl (i.e. within the free troposphere), the probability of transport from the west increases up to 85% of the time. The relatively rapid westerly flow toward the North America continent reaches maximum occurrence during fall-winter (8-11% of the time) and during winter-spring (12-13% of the time) for the Kamchatka and Vladivostok NRSs, respectively.

II. For the Vladivostok NRS, the North China and North Japan regions are at the highest risk of possible impact. It is mainly due to their proximity to VNRS. It is lower for the Korean regions due to peculiarities in the general airflow patterns of westerly origin. The lower (and upper) bounds of the VNRS's possible impact are about 32 (54) and 35 (87)% for the North China and North Japan regions, respectively. On average, atmospheric transport to these regions could occur in 0.5 and 1.6 days, respectively. The fast transport events are not common for the US territories, but they could represent major concerns for the Japanese and North Korean regions. Except for the US territories, the boundary layer transport reaches all regions more than half of time,

III. For the Kamchatka NRS, the US territories are at the highest risk compared to the rest of the regions. The lower (and upper) bounds of the KNRS's possible

impact are 30 (54) and 13 (32)% for the Aleutian Chain Islands and State of Alaska, respectively. On average, atmospheric transport to these regions could occur in 3.0 and 5.1 days, respectively. For all other regions, the bounds of possible impact are only a few percent with the exception of the North Japan region (8%). In the same way, the fast transport events are observed only in these three – Aleutian Chain Islands, State of Alaska, and Northern Japan geographical regions. The boundary layer transport dominates in most of the considered regions, but free troposphere transport dominates in the Chinese and North Korean regions.

IV. The typical transport time from the Vladivostok NRS to reach the northern seashore areas of Japan is 1 day. Further, during 1-2 days the air parcels will pass over the Northern Japan. Typical transport time to reach the Koreas is about 2 days. For the Kamchatka NRS, only the territories of the Kamchatka Region and islands in the adjacent seas - Komandor Islands (Russia) and the far western islands of the Aleutian Chain Islands (USA) - can be reached during the first 2.5 days

We believe that results of the FARECS study are applicable for the emergency response and preparedness measures in the cases of the accidental releases at the nuclear risk sites. They should be included in the decision-making processes and required provision plans to accidents for the countries surrounding NRSs. We believe, that our study methodology – trajectory modeling and a variety of the statistical analysis tools – is also a useful approach to estimating the possible impact from any other sources. There could be chemical, biological or other sources of the pollution that represent risk to population and environment.

5. RECOMMENDATIONS AND FUTURE STUDIES

Several concluding remarks and recommendations are made to clarify the applicability and importance of the FARECS's study results.

These results are initial steps to estimate probabilities of the atmospheric transport from the nuclear risk sites locations situated at the Russian Far East. In the event of an accidental release they can be used as a preliminary estimation of the likelihood and direction of the atmospheric transport, evaluation of the minimum and average transport times, and identification of the predominant atmospheric layer during transport reaching the borders of counties, countries, and remote geographical regions.

Emergency response plans to possible radionuclide releases from the nuclear risk sites could be improved by analyses of the fast transport, airflow patterns, and average transport time fields. These are input to better understanding of seriousness of possible radionuclide releases from the nuclear risk sites. The FARECS's study output is valuable input data for the studies of the social and economical consequences for population and environment of the neighboring countries, and especially, on a regional scale due to impact of accidents at the nuclear risk sites. These are important data for the studies of the multidisciplinary risk and vulnerability analysis, and probabilistic assessment of the radionuclide meso-, regional-, and long-range transport. Additionally, these results could be used for testing of higher resolution models.

Therefore, we recommend further studies on the following issues:

I. Analysis of the probabilistic patterns of atmospheric transport from the Vladivostok and Kamchatka NRSs raises concerns for the possible fast transport as well as radionuclide deposition in the neighboring countries such as Japan, Korea, China, and USA. Although a specific case study had been performed by *Romanova et al., 2001* and *Takano et al., 2001* for one of the months during winter, an additional extended study would be required to evaluate possible air concentration, surface deposition and doses with respect to different geographical regions and countries under other seasonal conditions. A simple scoping approach to evaluate these characteristics at remote distances from the nuclear risk site location was suggested by *Compton, 2001b.* For a more advanced study, these characteristics might be evaluated on a monthly and seasonal basis using obtained probabilistic fields. An evaluation of these characteristics would provide insight on the level and probability of the risk for the population in the North Pacific region.

II. Another interesting aspect would be an evaluation of the impact from the nuclear weapons-related facilities and nuclear fuel reprocessing facilities located in the northern regions of China and Japan, respectively. A similar approach but more detailed analysis might be taken as in the FARECS study. This analysis could include both the probabilistic approach for the atmospheric transport patterns

and evaluation of the air concentration, surface deposition, and doses for the neighboring countries due to possible accidental releases.

III. There is large number of the radiation risk sources located in the countries of the North Pacific region. All of these sources represent risks of different magnitudes, and their "possible danger" is highly dependent on many factors. In general, the simplest approach is to know the source term as one of the main factors. But it seems reasonable to ask: What is the range of each radiation risk source with respect to another as well as due to other various factors? At the first step, an evaluation of the probabilities' matrix for the transport pathways in different environments, fast transport, and removal processes might give an answer on this question. For comprehensive evaluation, the additional factors such as probabilities of the accidental releases, prevailing scenarios, accumulated activities, types of radioactive material, and etc should be considered. Such analysis might rank the risk sources in the order of their potential danger with respect to population and environment. This allows the policy and decision makers to make an informed decision – which sources should be considered as the first priority of study, and what measures should be taken if an accidental release will occur. Of course, for an accident, the detailed examination of the conditions at the site, the accident scenario and prevailing atmospheric conditions must be taken into account.

IV. As we mentioned in the Introduction, there are plans of the Russian Government to build new NPPs - Far East and Primorskaya - on the Russian Far East. According to *Bergman et al., 1996* and *Baklanov et al., 1996* the nuclear power plants in comparison with the nuclear submarines could be objects of the highest potential risk because of their much higher inventory of radioactive material. Hence, an evaluation of the possible impact of these proposed facilities to the neighboring countries in a case of an accidental release would be important. The detailed information about the current status of the planned NPPs could be obtained from the Russian MinAtom International Nuclear Safety Center, RMINSC (http://www.insc.ru/) as well as International Nuclear Safety Center, INSC (http://www.insc.anl.gov/).

5. REFERENCES

Baker, Wayman, ed. (**1992)**: Research Highlights of the NMC Development Division: 1989-1991; NOAA, 469 pp.

Baklanov A., R. Bergman, B. Segerstahl, L. Thaning (**1996**): Assessment of Risk of Airborne Radioactive Contamination from Nuclear Units in North-West Russia. IIASA Research Report, XP-96-043

Baklanov A., A.Mahura, D.Jaffe, R.Andres, L.Thaning & R.Bergman (**1999**): Atmospheric Transport Patterns and Possible Consequences for the European North after a Nuclear Accident. Proceedings of the Fourth International Conference on Environmental Radioactivity in the Arctic, Edinburgh, Scotland, 20-23 September 1999, pp. 81-84

Baklanov A., A.Mahura, R.Andres, D.Jaffe, L.Thaning, R.Bergman (**2001**): Atmospheric Transport Patterns and Estimation of Consequences after the Nuclear Accident at the Russian North-West. In Press, Journal of Environmental Radioactivity.

Bergman R., A. Baklanov, B. Segerstahl (**1996**): Integrated Regional Risk Assessment: The Case of Radioactive Contamination on the Kola Peninsula. IIASA Research Report, XP-96-044

Bradley D.J. (1997): Behind the Nuclear Curtain: Radioactive Waste Management in the Former Soviet Union. Battelle Press, ed. Payson, 716 pp.

Compton K.L., V. Novikov, F. Parker (**2000**): Deep Well Injection of Liquid Radioactive Waste at Krasnoyarsk-26. IIASA Research Report, RR-00-001

Compton K.L., V. Novikov, F. Parker (**2001a**): Deep Well Injection of Liquid Radioactive Waste at Krasnoyarsk-26: Analysis of Hypothetical Scenarios. Volume II. IIASA Research Report, RR-01-001

Compton K.L. (**2001b**): Evaluation of Deposition and Dose from in Neighbouring Countries from a Severe Nuclear Accident in the Russian Far East. IIASA Interim Report.

Danielsen E. (1961): Trajectories: isobaric, isentropic and actual. Journal of Meteorology, Vol 18, pp.479-486

Danilyan V.A., VL.Vysotskii, A.A.Maksimov (**2000a**): Radioecological Conditions on the Territory of Coastal Service Bases in the Far-Eastern region. Atomic Energy, Vol 89, #2, pp. 673-679

Danilyan V.A., VL.Vysotskii, A.A.Maksimov, Y.V.Sivintsev (**2000b**): Effect of the Utilization of Nuclear-Powered Submarines on the Radioecological Conditions in the Far-East Region. Atomic Energy, Vol 89, #6, pp. 982-1003

DMI-NARP (**2001**): On-going Project Atmospheric Transport Pathways, Vulnerability and Possible Accidental Consequences from the Nuclear Risk Sites in the European Arctic of the NARP: Nordic Arctic Research Programme vs. Danish Meteorological Institute. Leader: Dr. Alexander Baklanov, alb@dmi.dk.

Dorling, S.R. and Davies, T.D. (**1995**): Extending Cluster Analysis -- Synoptic Meteorology Links to Characterize Chemical Climates at Six Northwest European Monitoring Stations. Atmospheric Environment, Vol 29, Iss 2, p 45-167

Draxler, R. (**1987**). Sensitivity of the trajectory model to the spatial and temporal resolution of the meteorological data during CAPTEX. Journal of Climatology and Applied Meteorology, 26, pp. 1577-1588.

Egorov N., V. Novikov, F. Parker, V.K. Popov (eds) (**2000**): The Radiation Legacy of the Soviet Nuclear Complex. Earthscan Publications Ltd., 236 pp.

Forrow L.; Blair B.G.; Helfand I.; Lewis G.; Postol T.; Sidel V.; Levy B.S.; Abrams H.; Cassel C. (**1998**): Accidental nuclear war - A post-Cold War assessment

New England Journal of Medicine, Vol. 338, Iss 18, pp.1326-1331

Harris, J. M. & Kahl, J. D. (**1990**). A descriptive atmospheric transport climatology for Mauna Loa Observatory, using clustered trajectories. Journal of Geophysical Research, pp. 13651-13667.

Harris, J.M. (**1992**): An Analysis of 5-day Midtropospheric Flow Patterns for the South Pole: 1985-1989. Tellus, 44B, p 409-421

Harris, J.M. and Kahl, J.D. (**1994**): Analysis of 10-day Isentropic Flow Patterns for Barrow, Alaska: 1985-1992. Journal of Geophysical Research, Vol 99, p 25,845-25,855

INTAS (**2000**) Assessment of Potential Risk of Environmental Radioactive Contamination in Northern Europe from Terrestrial Nuclear Units in North-West Russia. Research Report, INTAS Project 96-1802, , 125 p., November 2000

Ishikawa H. (**1991**): Development of regionally Extended/ Worldwide Version of System for Prediction of Environmental Emergency Dose Information: WSPEEDI, (I) – Application of Mass-Consistent Wind Field Model to Synoptic Wind Fields. Journal of Nuclear Science and Technology, Vol 28, #6, pp. 535-546

Ishikawa H., M. Chino (**1991**): Development of regionally Extended/ Worldwide Version of System for Prediction of Environmental Emergency Dose Information: WSPEEDI, (II) – Long-Range Transport Model and Its Application to Dispersion of Cesium-137 from Chernobyl. Journal of Nuclear Science and Technology, Vol 28, #7, pp. 542-655

Ishikawa H. (**1994**): Development of regionally Extended/ Worldwide Version of System for Prediction of Environmental Emergency Dose Information: WSPEEDI, (III) – Revised numerical models, Integrated Software Environment and Verification. Journal of Nuclear Science and Technology, Vol 31, #9, pp. 969-978

Jaffe, D., Mahura, A., Andres R. (**1997a**): Atmospheric Transport Pathways to Alaska from Potential Radionuclide Sites in the Former Soviet Union. Research Report, UAF-ADEC Project 96-001, 71 pp.

Jaffe, D.A., Mahura A., Kelley, J., Atkins J., Novelli P.C., Merrill J. (**1997b**) Impact of Asian Emissions on the Remote North Pacific Atmosphere: Interpretation of CO Data from Shemya, Guam, Midway and Mauna Loa. Journal of Geophysical Research, Vol. 23, pp.28627-28636

Jaffe, D., Mahura, A., Andres, R., Baklanov, A., Thaning, L., Bergman, R., & Morozov, S. (**1998**). Atmospheric Transport from the Kola Nuclear Power Plant. Pilot Study Research Report, UAF-FOA-BECN Joint Project, 61 p.

Kahl J.D. (**1996**). On the prediction of trajectory model error. Atmospheric Environment, Vol 30, pp. 2945-2957.

Laverov N., V. Novikov, F. Parker (**1997a**): First Soviet Nuclear Complex and its Environmental Impacts. IIASA Research Report, XP-97-028

Laverov N., V. Novikov, F. Parker (**1997b**): Environmental Impacts of First Soviet Nuclear Complex, IIASA Research Report, XP-97-029

Mahura, A., Jaffe D., Andres, R., Dasher, D., Merrill, J. (**1997a)**: Atmospheric Transport Pathways to Alaska from Potential Radionuclide Sites in the Former Soviet Union. Proceedings of American Nuclear Society Sixth Topical Meeting on Emergency Preparedness and Response, San Francisco, California, April 1997, Vol 1, p 173-174,

Mahura, A., Jaffe D., Andres, R., Dasher, D., Merrill, J.(**1997b)**: Atmospheric Transport Pathways from the Kola Nuclear Power Plant. Extended abstracts of International Symposium on Environmental Pollution of the Arctic and The Third International Conference on Environmental Radioactivity in the Arctic, Tromso, Norway, June 1-5, 1997, Vol 2, p 52-54

Mahura A., D.Jaffe & R.Andres (**1999**): Air Flow Patterns and Precipitation Probability Fields for the Kola NPP. Abstracts of the International Conference "Nuclear Risks, Environmental and Development Cooperation in the North of Europe", Apatity, Murmansk region, Russia, 19-23 June 1999, pp. 87-93

Mahura A., D.A. Jaffe, R.J. Andres, J. T. Merrill (**1999**): Atmospheric transport pathways from the Bilibino nuclear power plant to Alaska. Atmosppheric Environment, Vol 33, Iss 30, pp.5115-5122

Merrill, J., Bleck, R. and Avila, L. (**1985)**: Modeling Atmospheric Transport to the Marshall Islands. Journal of Geophysical Research, Vol 90, p 12,927-12,936

Merrill, J., Bleck, R. and Boudra, D.B. (**1986)**: Techniques of Lagrangian Trajectory Analysis in Isentropic Coordinates. Monthly Weather Review, Vol 114, p 571-581

Merrill, J. (**1994**): Isentropic Airflow Probability Analysis. Journal of Geophysical Research, Vol 99, pp 25881-25889

Miller, J.M. (**1981**): A Five-Year Climatology of Back Trajectories from the Mauna Loa Observatory, Hawaii. Atmospheric Environment, Vol 15, Iss 9, pp 1553-1558

Moody, J.L. (**1986**): The Influence of Meteorology on Precipitation Chemistry at Selected Sites in the Eastern United States. Ph.D. thesis, University of Michigan, Ann Arbor, pp 1-176

Moody, J.L. and Gallow, J.N. (**1988**): Quantifying the Relationship Between Atmospheric Transport and the Chemical Composition of Precipitation on Bermuda. Tellus, 40B, p 463-479

Moody, J.L., Oltmans, S.J., Hiram Levy II, Merrill, J.T. (**1994**): Transport Climatology of Tropospheric Ozone: Bermuda, 1988-1991. Journal of Geophysical Research, Vol 100, pp 7,179-7,194

Nilsen, T. & Bohmer, N. **(1994).** Sources to Radioactive Contamination in Murmansk and Arkhangel'sk Couties. Bellona Report, Vol 1, 162 p.

Nilsen, Th., Kudrik, I. & Nikitin, A. (**1996**). The Russian Northern Fleet. Source of Radioactive Contamination.Bellona Report, Vol 2, 168 p.

Novikov V. (**1997**): Nuclear Inheritance of the Cold War Challenges Nuclear Power. IIASA Research Report, XP-97-030

Nuclear Wastes in the Arctic (**1995**): An Analysis of Arctic and Other Regional Impacts From Soviet Nuclear Contamination. Research Report OTA-ENV-632

OCB (**2000**) Assessment of Potential Risk for Kola's Population from Radiological Impact of Accident on Spent Nuclear Fuel Facilities Research Report, OCB-RW Project 98-03-26, 101 p., September 2000

Parker F.L., K.L. Compton, V. Novikov (**1999a**): Comparative Impacts of Contamination of the Clinch and Techa Rivers. IIASA Research Report, XP-99-003

Parker F.L.., R. Waters, K.L. Compton, V. Novikov (**1999b**): Impact of the Release of Radioactive Materials from Krasnoyarsk-26 to the Yenisei River, IIASA Research Report, XP-99-006

Parker F. L., A.I. Rybalchenko, V. Velichkin, K.L. Compton, V. Novikov, A. Pek, V. Malkovsky, B. Sigaev (**1999c**): Analysis of Long Term Consequences of Deep Well Injection of Liquid Radioactive Waste at the Mining and Chemical Combine, Krasnoyarsk Krai: I. Normal Scenario, XJ-99-017, IIASA Research Report

Parker F., A.I. Rybalchenko, V. Velichkin, K.L. Compton, V. Novikov, A. Pek, V. Malkovsky, B. Sigaev (**2000**): Analysis of Long Term Consequences of Deep Well Injection of Liquid Radioactive Waste at the Mining and Chemical Combine Krasnoyarsk Krai: II. Hypothetical Scenarios, IIASA Research Report, XJ-00-003

Poirot R.L., P.R. Wishinski (**1984**): Visibility, sulfate and air mass history associated with the summertime aerosol in northern Vermont. Atmospheric Environment, 20, 1457-1469

Randel, William (**1992**) Global Atmospheric Circulation Statistics, 1000-1mb; NCAR Technical Note TN-366+STR, 256 pp

Romanova V, M. Takano, F.Parker (**2001**): Atmospheric Transport of Radioactive Nuclides from Russia to Neighbouring Countries. IIASA Interim Report.

Romesburg, C.H. (**1984**): Cluster Analysis for Researchers. Lifetime Learning, Belmont, California, 334p

SAS/GRAPH Software: Introduction, Version 6, First Edition, **1990**

SAS Language and Procedures: Introduction, Version 6, First Edition, **1991**

SAS/STAT User's Guide, Version 6, Fourth Edition, Vol 1 and Vol 2, **1990**

SAS Technical Report P-229, SAS/STAT Software: Changes and Enhancements. Release 6.07, **1992**

Saltbones J., A.Foss, J.Bartnicki (**2000**): Threat to Norway from potential accidents at the Kola nuclear power plant. Climatological trajectory analysis and episode studies. Atmospheric Environment, Vol 34, Iss 3, pp. 407-41

Segerstahl B., A. Akleyev, V. Novikov (**1997**): The Long Shadow of Soviet Plutonium Production. IIASA Research Report, XJ-97-071

Stohl A. (**1998**): Computation, accuracy and applications of trajectories - A review and bibliography. Atmospheric Environment, Vol 32, Iss 6, pp. 947-966

Shaw, G.E. (**1988**): Chemical Air Mass Systems in Alaska. Atmospheric Environment, Vol 22, p 2,239-2,248

Takano M., V.Romanova, H.Yamazawa, Y.Sivintsev, K.Compton, V.Novikov, F.Parker (**2001**): Reactivity Accident of Nuclear Submarine near Vladivostok. Journal of Nuclear Science and Technology, Vol 38, N2, pp. 143-157.

Trenberth, Kevin & Olson, Jerry (**1988)**: Evaluation of NMC Global Analyses: 1979-1987; NCAR Technical Note TN-299+STR, 82 pp

Waters R.D., K.L. Compton, V. Novikov, F. Parker (**1999**): Releases of Radionuclides to Surface Waters at Krasnoyarsk-26 and Tomsk-7. IIASA Research Report, RR-99-003

APPENDIX A: Figures

Seasonal Atmospheric Transport Pathways for the Kamchatka and Vladivostok NRSs

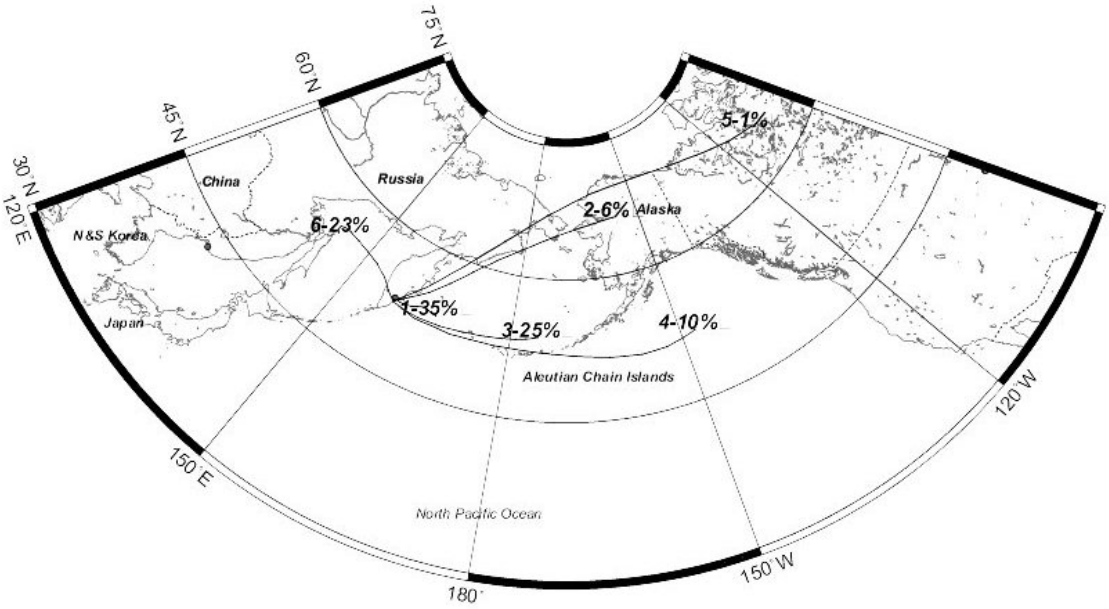

Figure A1. Atmospheric transport pathways from the Kamchatka NRS during spring

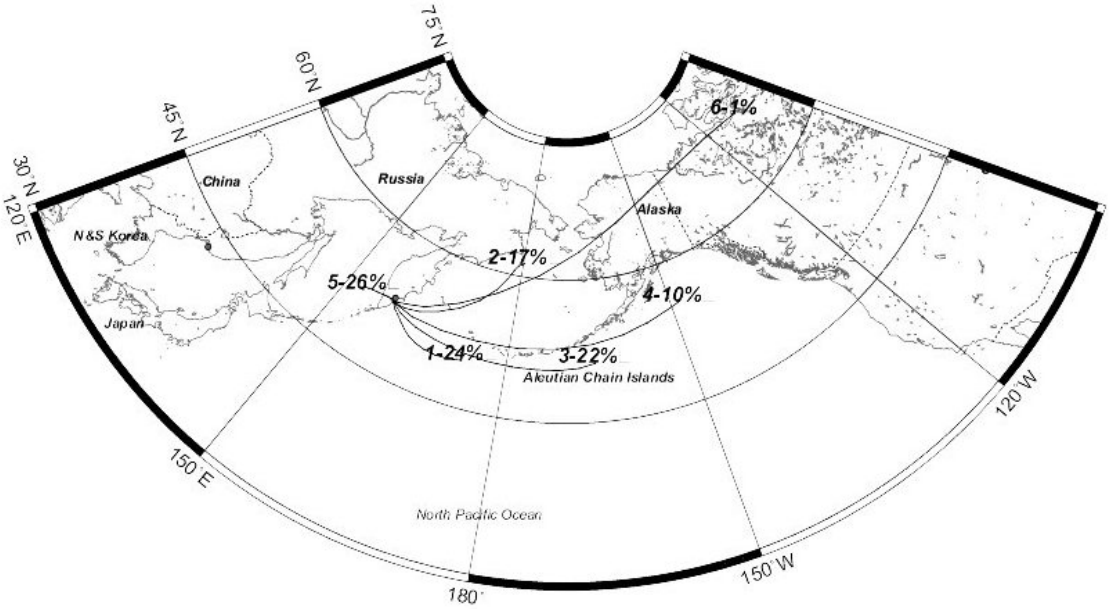

Figure A2. Atmospheric transport pathways from the Kamchatka NRS during summer

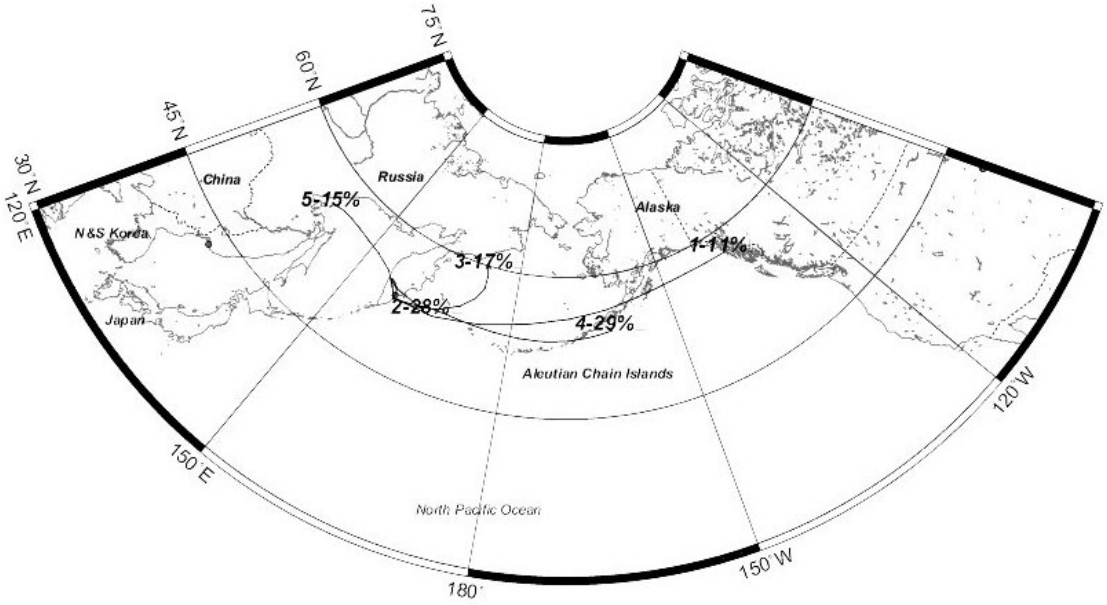

Figure A3. Atmospheric transport pathways from the Kamchatka NRS during fall

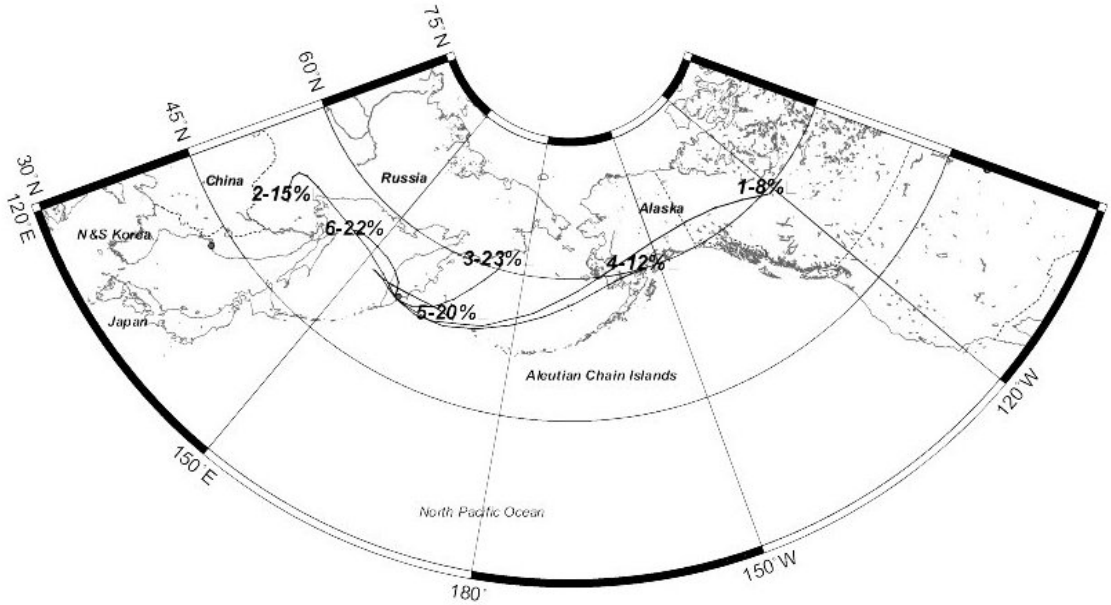

Figure A4. Atmospheric transport pathways from the Kamchatka NRS during winter

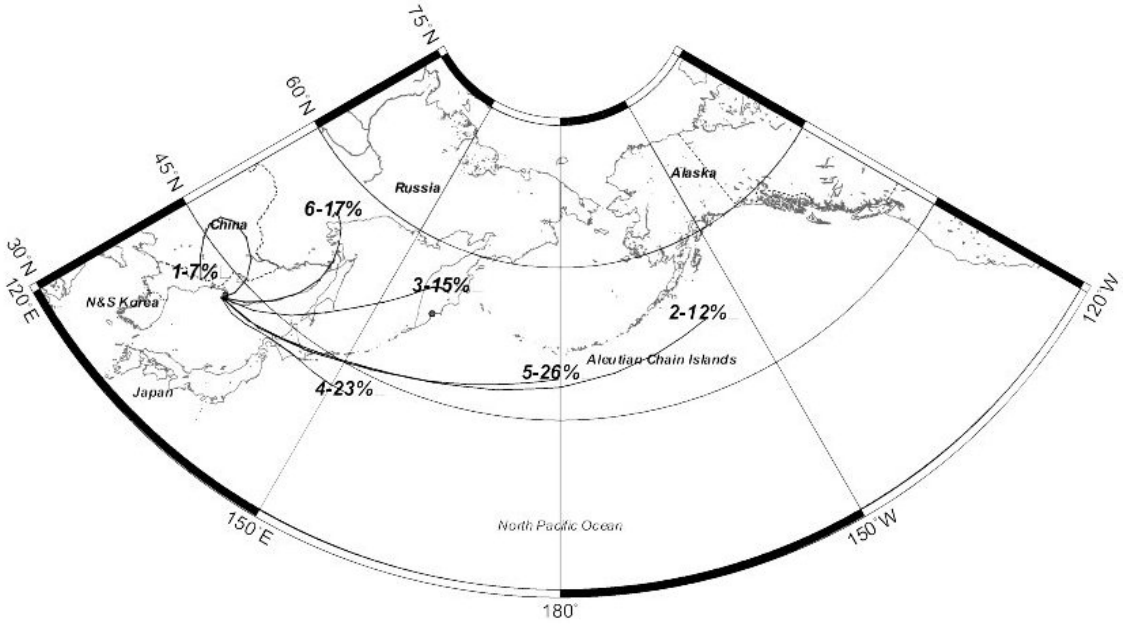

Figure A5. Atmospheric transport pathways from the Vladivostok NRS during spring

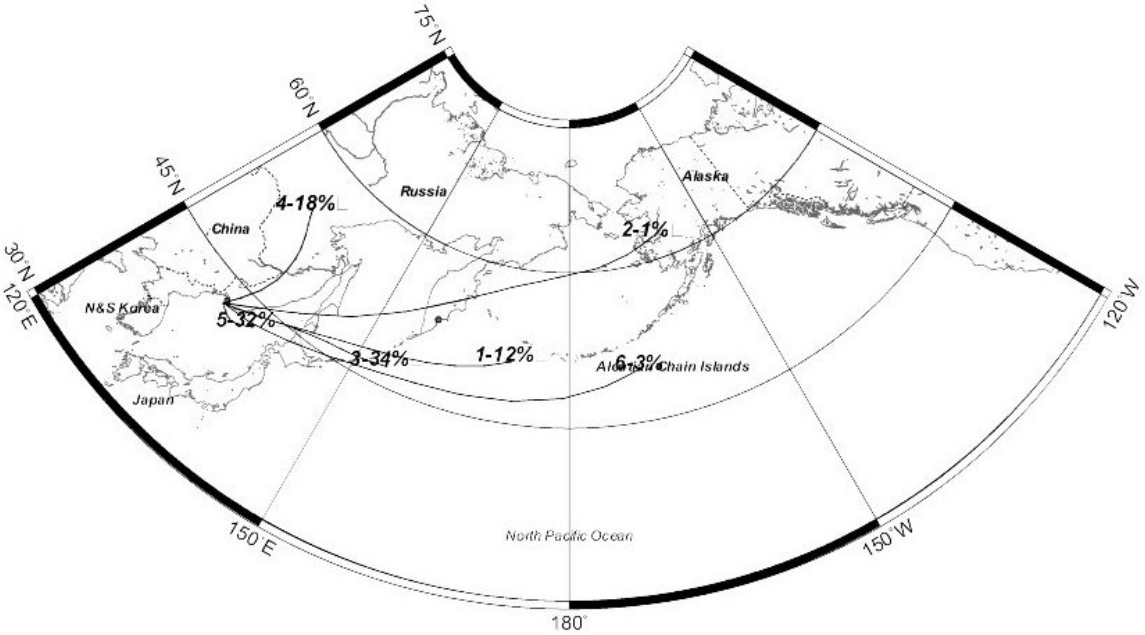

Figure A6. Atmospheric transport pathways from the Vladivostok NRS during summer

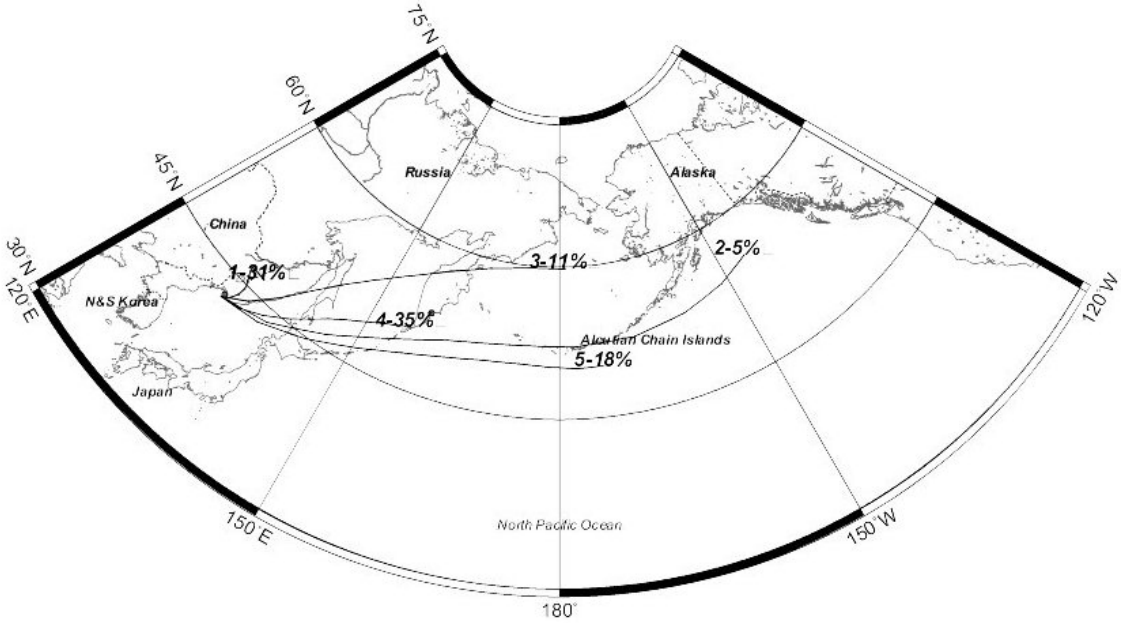

Figure A7. Atmospheric transport pathways from the Vladivostok NRS during fall

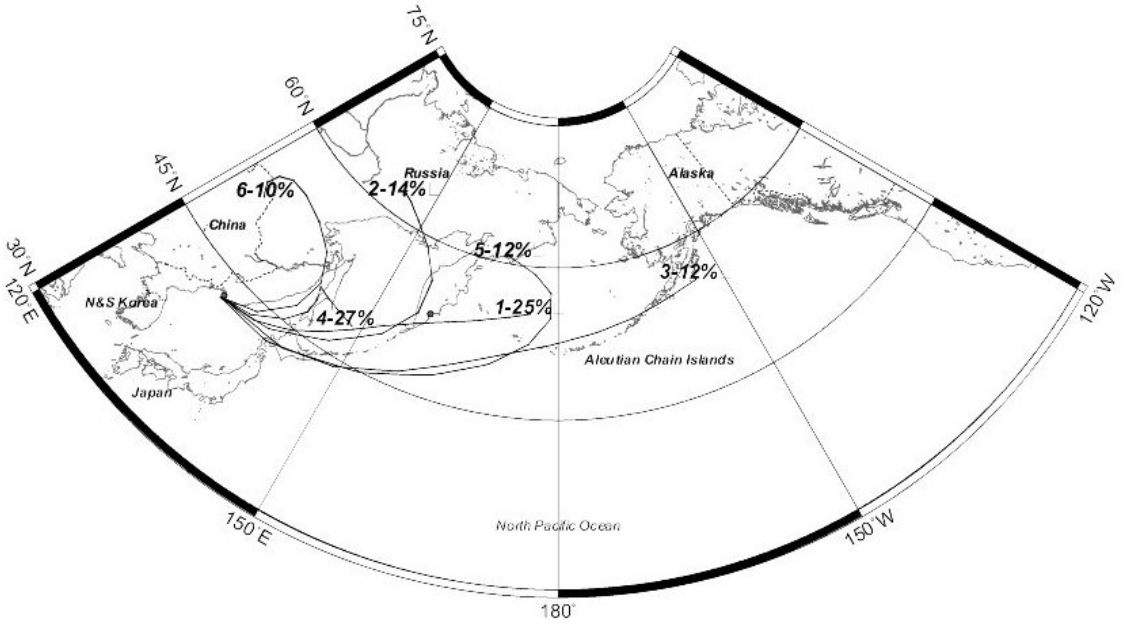

Figure A8. Atmospheric transport pathways from the Vladivostok NRS during winter.

APPENDIX B: Figures

Seasonal Airflow Probability Fields within the Boundary Layer for the Kamchatka and Vladivostok NRSs

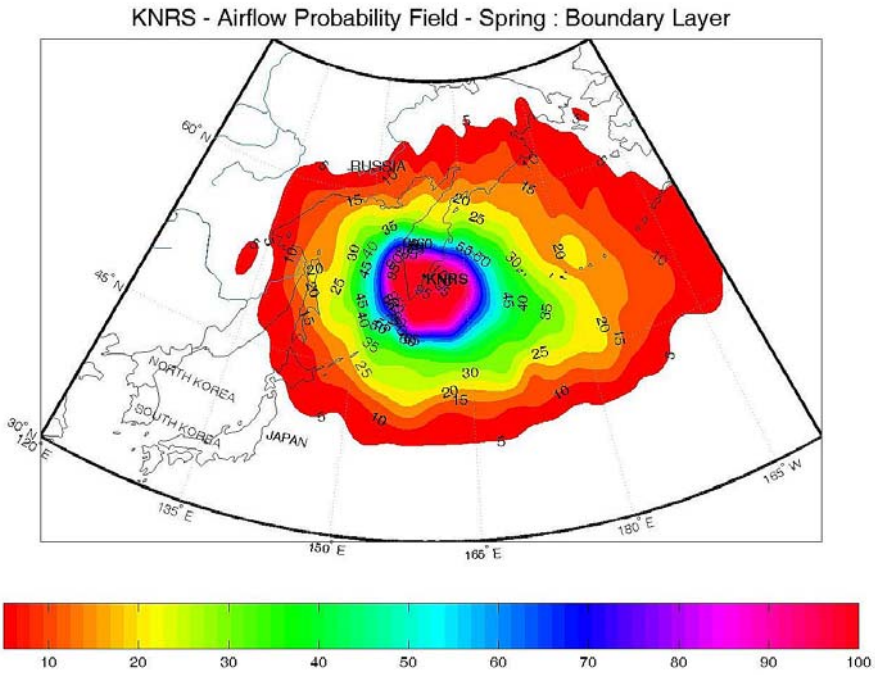

Figure B1. KNRS Spring airflow probability field within the boundary layer

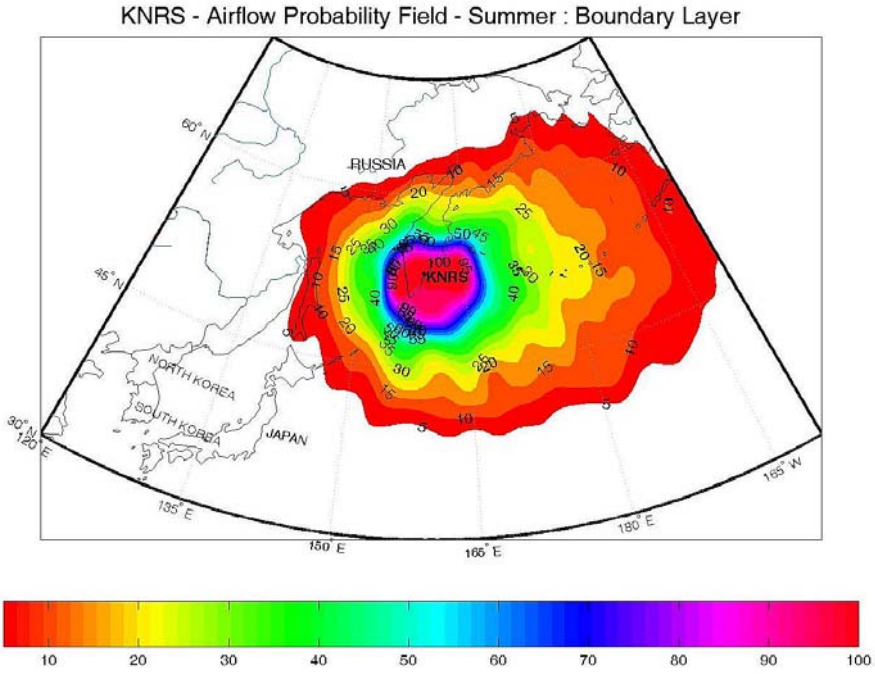

Figure B2. KNRS Summer airflow probability field within the boundary layer

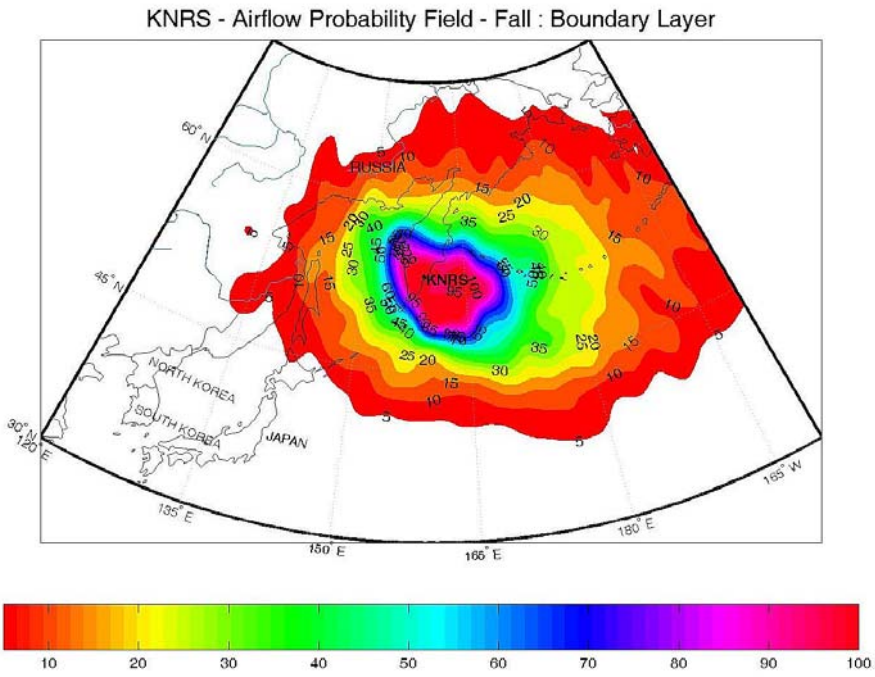

Figure B3. KNRS Fall airflow probability field within the boundary layer

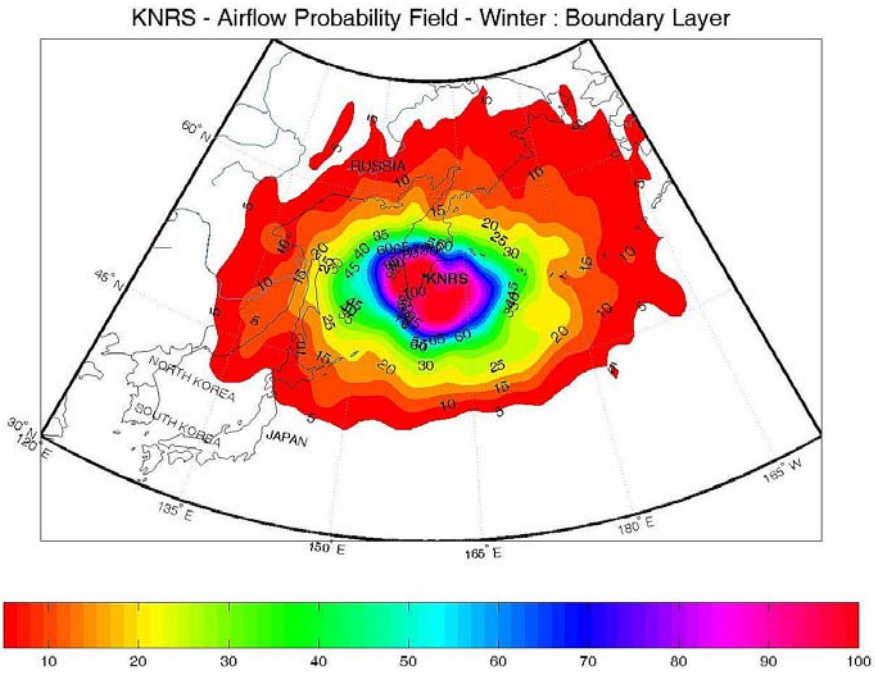

Figure B4. KNRS Winter airflow probability field within the boundary layer

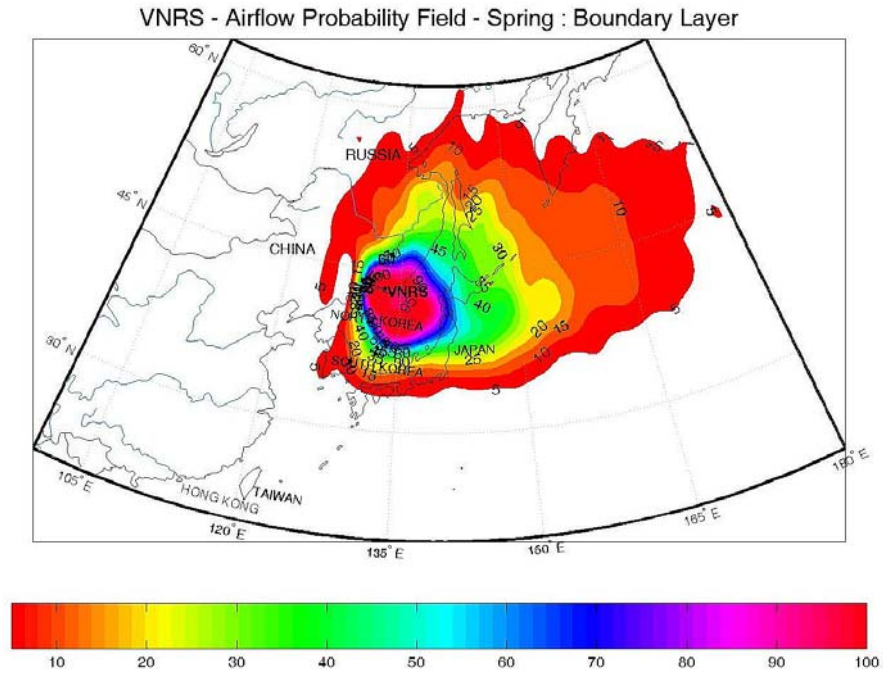

Figure B5. VNRS Spring airflow probability field within the boundary layer

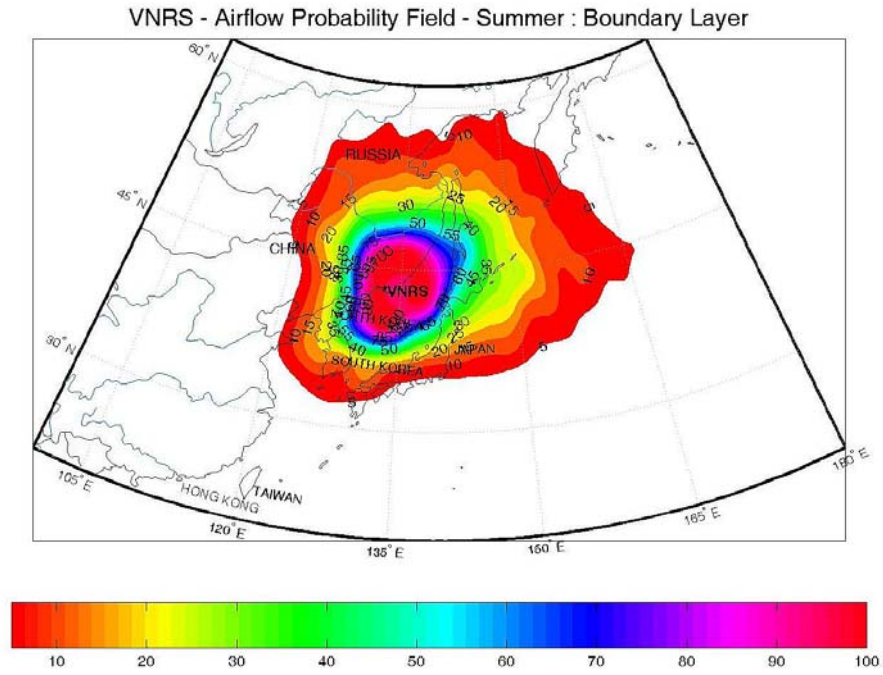

Figure B6. VNRS Summer airflow probability field within the boundary layer

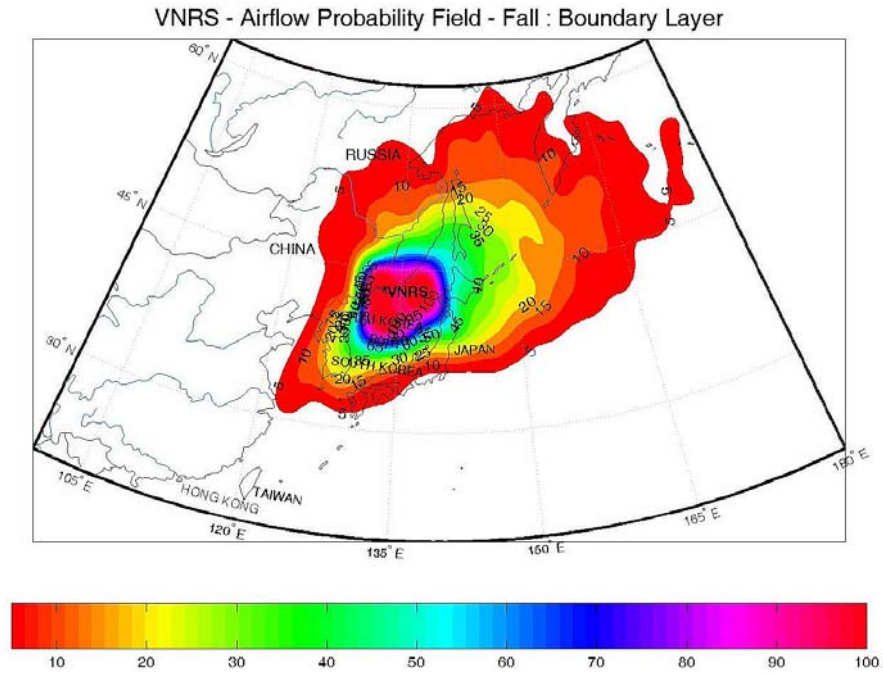

Figure B7. VNRS Fall airflow probability field within the boundary layer

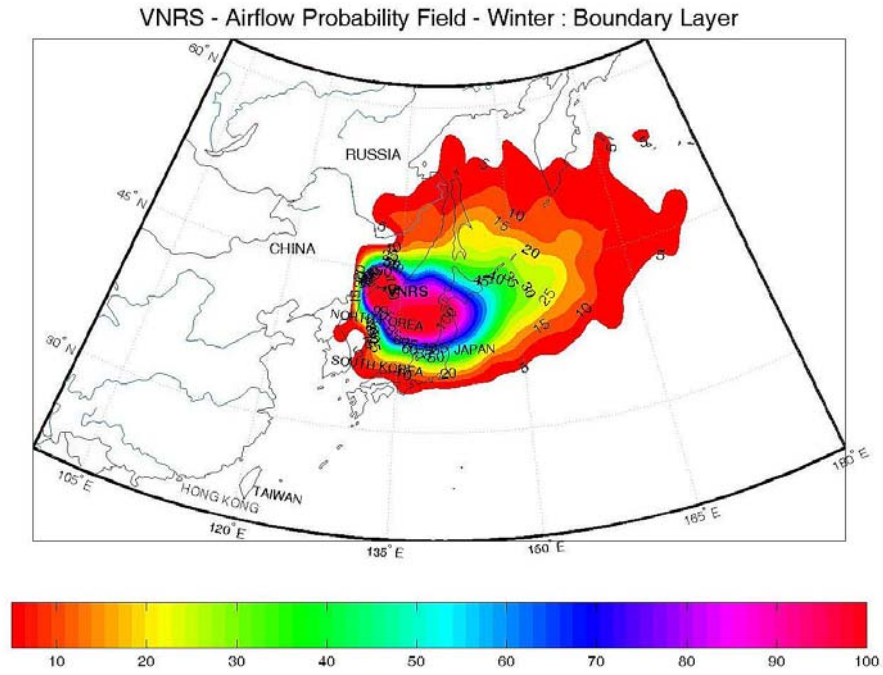

Figure B8. VNRS Winter airflow probability field within the boundary layer

APPENDIX C: Figures

Seasonal Fast Transport Probability Fields within the Boundary Layer for the Kamchatka and Vladivostok NRSs

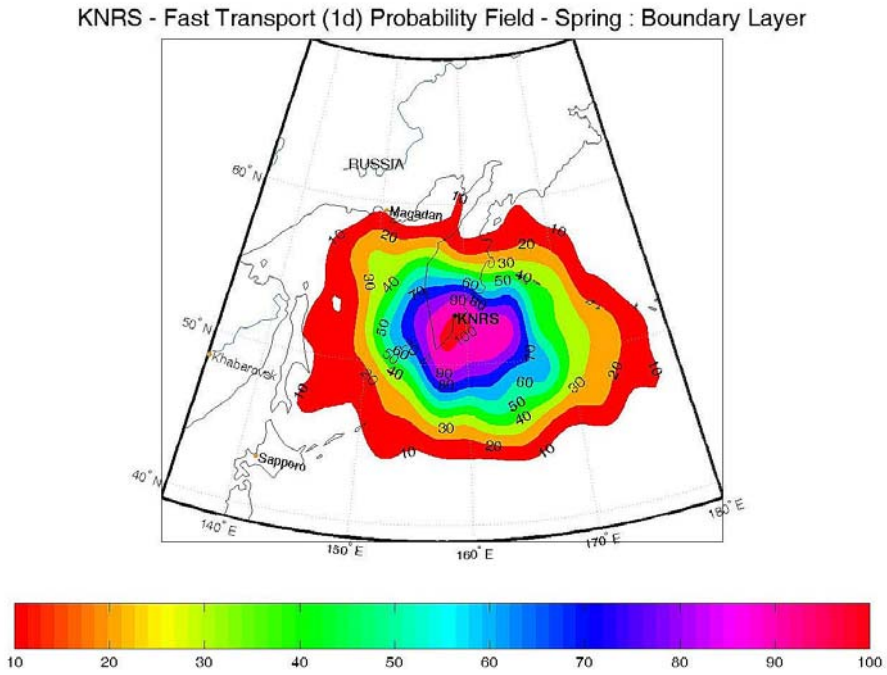

Figure C1. KNRS Spring fast transport probability field within boundary layer

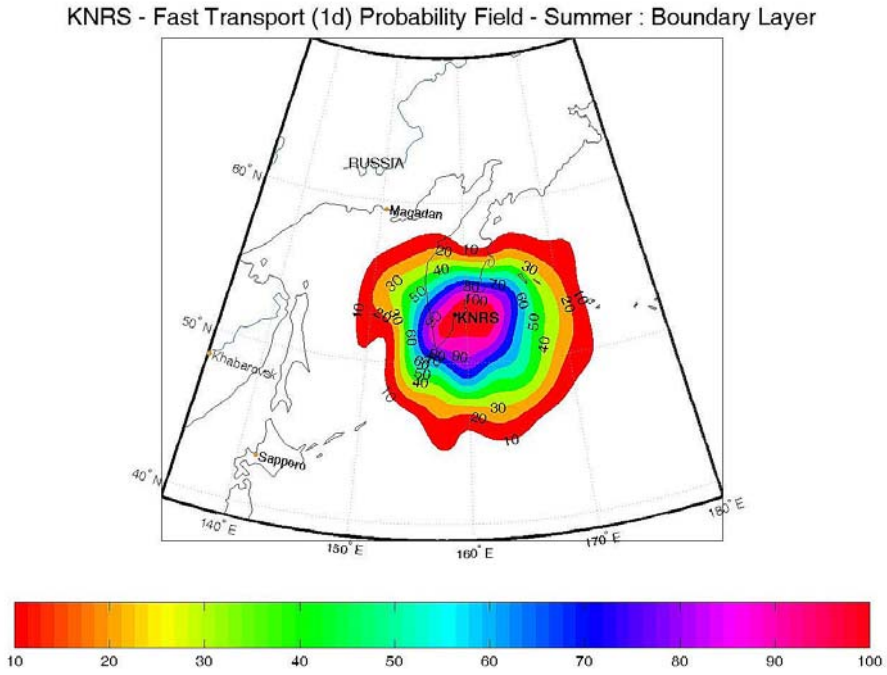

Figure C2. KNRS Summer fast transport probability field within the boundary layer

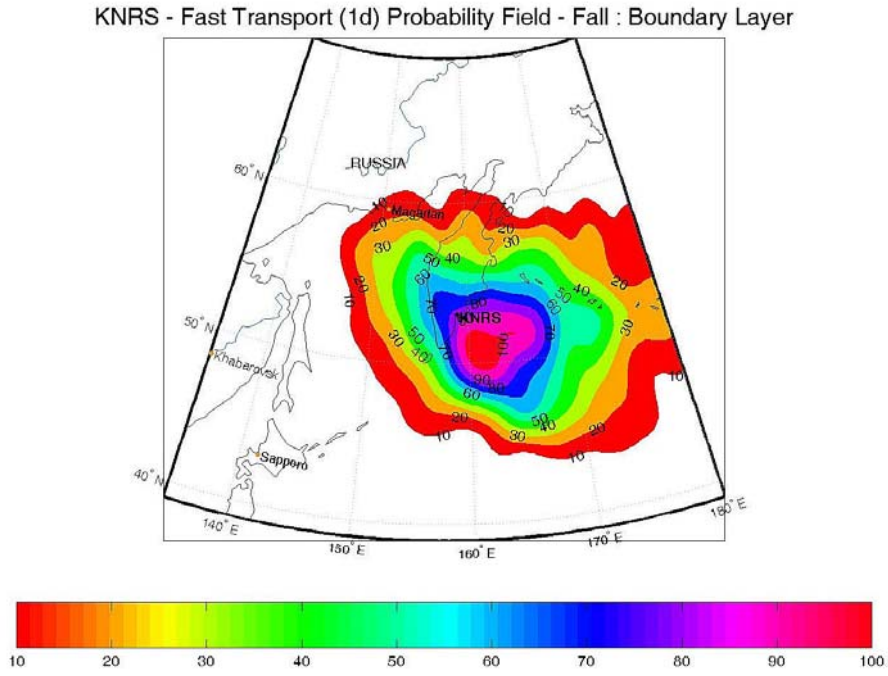

Figure C3. KNRS Fall fast transport probability field within the boundary layer

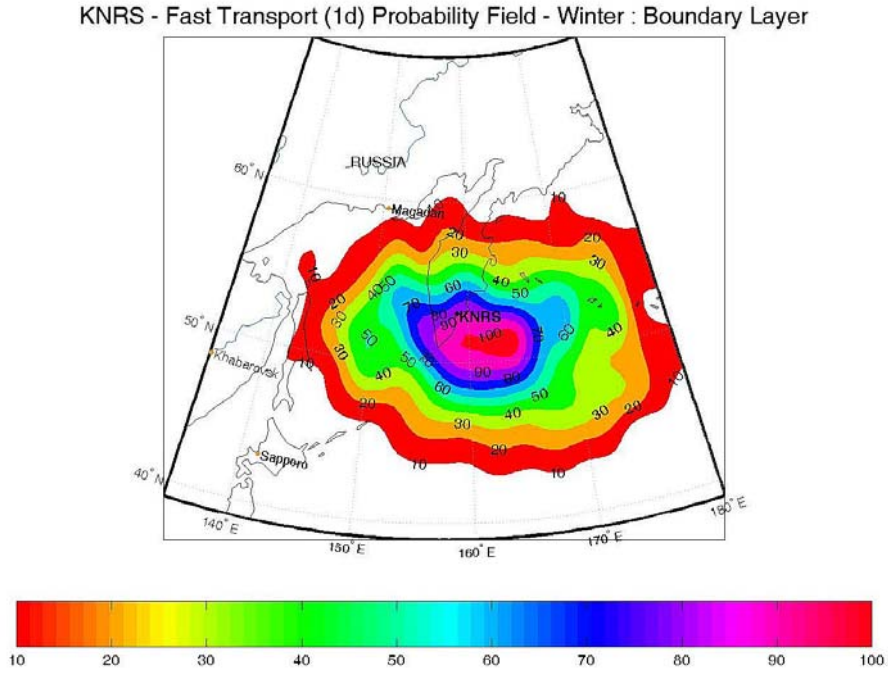

Figure C4. KNRS Winter fast transport probability field within the boundary layer

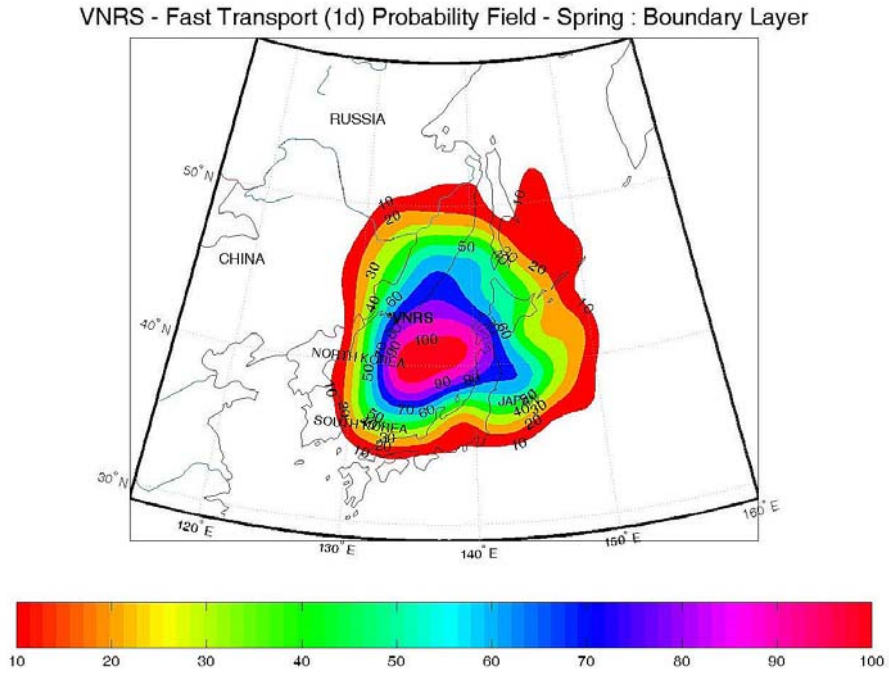

Figure C5. VNRS Spring fast transport probability field within the boundary layer

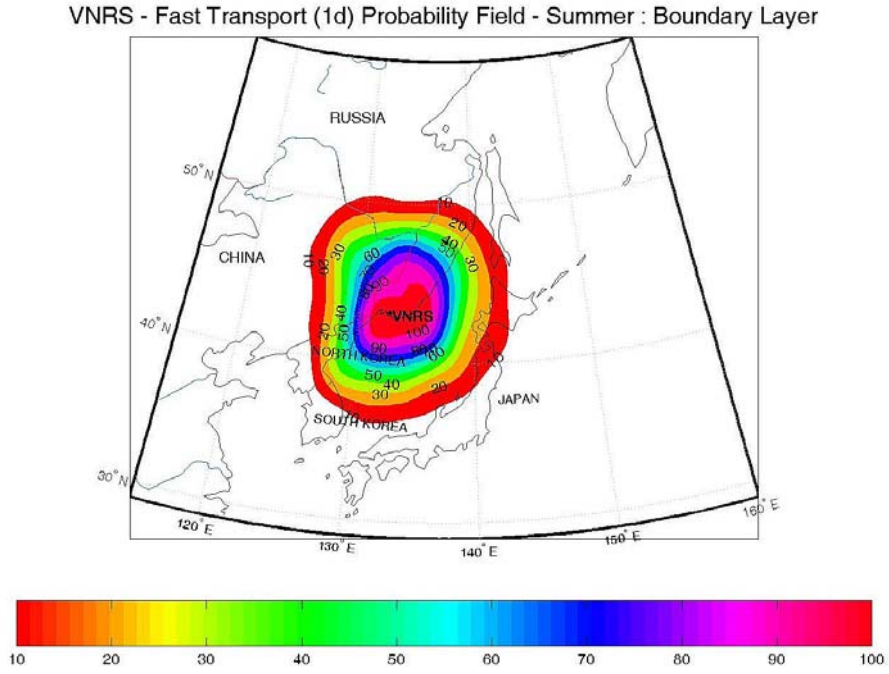

Figure C6. VNRS Summer fast transport probability field within the boundary layer

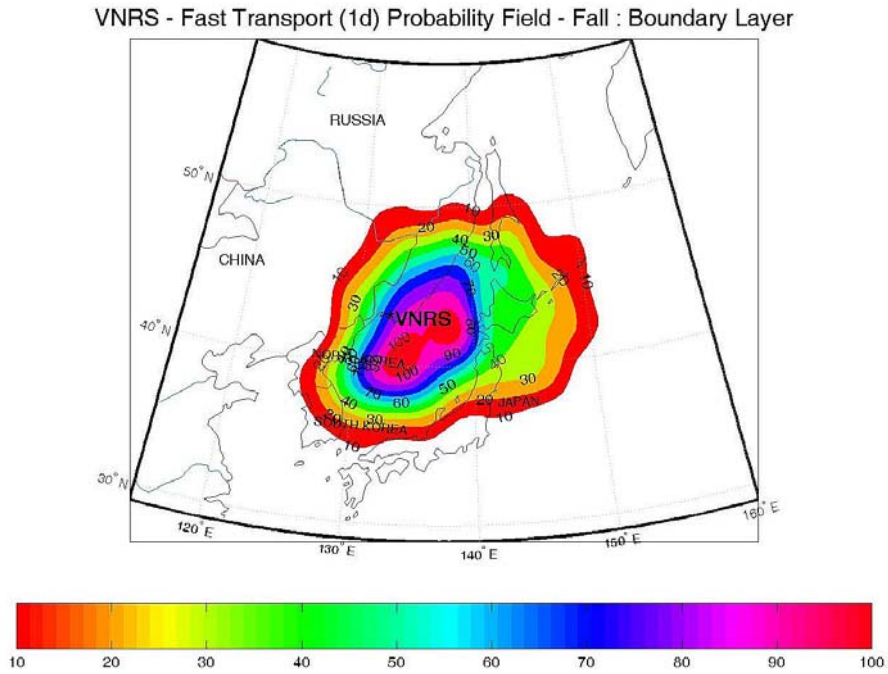

Figure C7. VNRS Fall fast transport probability field within the boundary layer

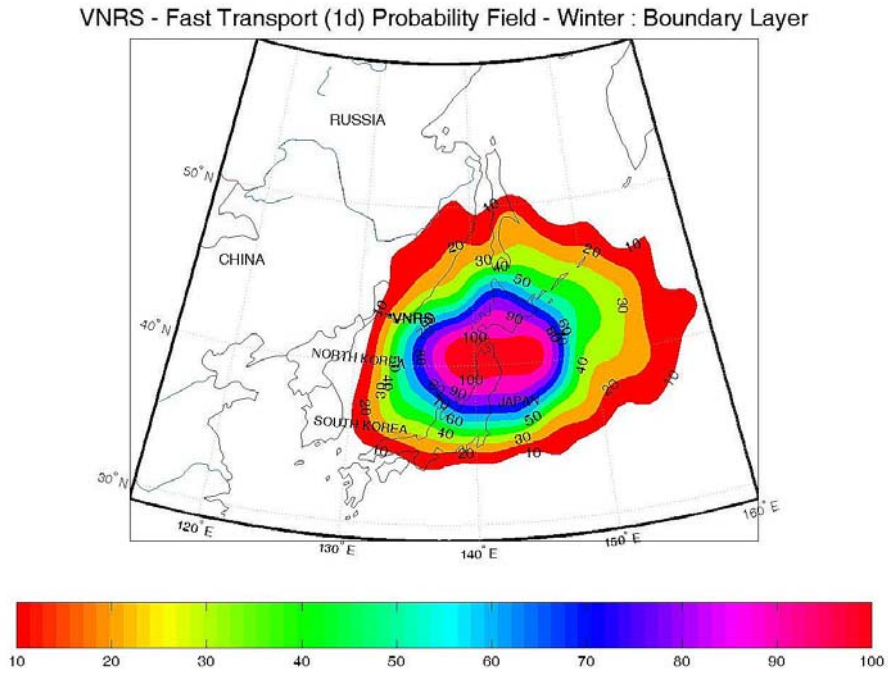

Figure C8. VNRS Winter fast transport probability field within the boundary layer

APPENDIX D: Tables

Data for Typical Transport Time Fields for the Kamchatka and Vladivostok NRSs

Table D1: Date for the Typical Transport Time from the Kamchaka NRS (Spring)

Table D1. Data for the Typical Transport Time from the Kamchatka NRS (Spring)																									
Term			0.5 day					1.0 day					1.5 day					2.0 day					2.5 day		
	Trajectory Statistics and Geographical Coordinates for the Absolute Maximum Cell (AMC)																								
Sector (deg)	#	%	SS	Lat	Long	#	%	SS	Lat	Long	#	%	SS	Lat	Long	#	%	SS	Lat	Long	#	%	SS	Lat	Long
0-10.	33	0.5	-	54.0	158.6	48	0.7	--	56.0	158.8	46	0.8	--	56.0	158.8	44	0.8	--	56.0	158.8	27	0.6	-	58.0	158.9
10- 20.	37	0.6	-	54.0	158.8	48	0.7	--	54.0	158.8	39	0.7	-	57.8	159.8	53	1.0	--	55.9	159.3	42	0.9	--	59.8	160.3
20- 30.	51	0.8	--	53.9	158.9	41	0.6	-	53.9	158.9	50	0.8	--	53.9	158.9	44	0.8	--	57.5	160.6	48	1.0	--	63.0	163.2
30- 40.	55	0.8	--	53.8	159.1	54	0.8	--	53.8	159.1	66	1.1	--	55.5	160.2	70	1.3	--	57.1	161.4	86	1.8	>50	58.7	162.5
40- 50.	72	1.1	--	53.7	159.2	85	1.3	--	53.7	159.2	86	1.5	>50	55.1	160.6	89	1.7	>50	58.0	163.5	88	1.8	>50	59.4	164.9
50- 60.	103	1.5	>50	53.6	159.3	115	1.8	>50	53.6	159.3	133	2.2	>75	57.0	164.2	144	2.7	>75	55.9	162.6	118	2.4	>75	61.6	170.8
60- 70.	127	1.9	>50	54.3	161.2	170	2.6	>75	56.8	166.7	195	3.3	OK	55.1	163.0	221	4.1	OK	56.0	164.8	239	4.9	OK	59.3	172.1
70- 80.	197	3.0	OK	53.3	159.5	272	4.2	OK	54.3	163.3	311	5.2	OK	54.3	163.3	285	5.3	OK	55.3	167.2	276	5.7	OK	55.9	169.1
80- 90.	240	3.6	OK	53.3	161.5	359	5.5	OK	53.4	163.5	426	7.2	OK	53.6	165.5	458	8.5	OK	54.1	171.5	404	8.3	OK	54.8	179.4
90-100.	441	6.6	OK	52.7	161.5	532	8.2	OK	52.6	163.5	511	8.6	OK	52.4	165.5	510	9.5	OK	51.5	175.4	514	10.6	OK	51.5	175.4
100-110.	432	6.5	OK	52.2	161.4	496	7.6	OK	51.7	163.3	514	8.7	OK	50.7	167.2	430	8.0	OK	49.1	173.0	434	8.9	OK	48.6	174.9
110-120.	487	7.3	OK	52.6	159.4	449	6.9	OK	50.9	163.0	333	5.6	OK	48.4	168.5	316	5.9	OK	45.8	173.9	264	5.4	OK	46.7	172.1
120-130.	376	5.6	OK	52.4	159.3	289	4.4	OK	51.3	161.0	222	3.7	OK	47.8	165.9	202	3.8	OK	45.6	169.2	186	3.8	OK	46.7	167.5
130-140.	270	4.0	OK	52.3	159.2	246	3.8	OK	49.5	162.0	238	4.0	OK	45.2	166.3	151	2.8	OK	48.1	163.5	116	2.4	>75	45.2	166.3
140-150.	226	3.4	OK	52.2	159.1	200	3.1	OK	48.9	161.4	157	2.6	>75	47.3	162.5	136	2.5	>75	48.9	161.4	105	2.2	>75	47.3	162.5
150-160.	197	3.0	OK	52.1	158.9	161	2.5	>75	48.5	160.6	110	1.9	>50	46.7	161.5	100	1.9	>50	44.9	162.3	99	2.0	>50	43.0	163.2
160-170.	189	2.8	OK	52.0	158.8	140	2.2	>75	50.1	159.3	102	1.7	>50	50.1	159.3	104	1.9	>50	48.2	159.8	67	1.4	--	46.2	160.3
170-180.	167	2.5	>75	52.0	158.6	108	1.7	>50	50.0	158.8	98	1.7	>50	48.0	158.9	86	1.6	>50	48.0	158.9	92	1.9	>50	46.0	159.1
180-190.	165	2.5	>75	52.0	158.4	149	2.3	>75	50.0	158.2	123	2.1	>50	50.0	158.2	96	1.8	>50	46.0	157.9	91	1.9	>50	44.0	157.7
190-200.	149	2.2	>75	52.0	158.2	141	2.2	>75	50.1	157.7	105	1.8	>50	50.1	157.7	102	1.9	>50	46.2	156.7	94	1.9	>50	46.2	156.7
200-210.	149	2.2	>75	52.1	158.1	126	1.9	>50	50.3	157.2	130	2.2	>75	50.3	157.2	95	1.8	>50	48.5	156.4	85	1.8	>50	50.3	157.2
210-220.	153	2.3	>75	52.2	157.9	144	2.2	>75	50.5	156.8	112	1.9	>50	50.5	156.8	126	2.4	>75	47.3	154.5	91	1.9	>50	47.3	154.5
220-230.	173	2.6	>75	52.3	157.8	140	2.2	>75	50.9	156.4	156	2.6	>75	49.5	155.0	126	2.4	>75	49.5	155.0	91	1.9	>50	46.6	152.1
230-240.	195	2.9	OK	52.4	157.7	160	2.5	>75	51.3	156.0	181	3.0	OK	51.3	156.0	127	2.4	>75	49.0	152.8	99	2.0	>50	49.0	152.8
240-250.	234	3.5	OK	52.6	157.6	212	3.3	OK	50.9	154.0	163	2.7	>75	50.9	154.0	130	2.4	>75	50.9	154.0	106	2.2	>75	48.4	148.5
250-260.	324	4.9	OK	52.7	157.5	267	4.1	OK	51.7	153.7	184	3.1	OK	50.7	149.8	171	3.2	OK	51.2	151.7	119	2.4	>75	49.6	145.9
260-270.	317	4.7	OK	52.9	157.5	261	4.0	OK	52.6	153.5	221	3.7	OK	52.7	155.5	161	3.0	OK	51.5	141.6	155	3.2	OK	51.5	141.6
270-280.	250	3.7	OK	53.3	155.5	208	3.2	OK	53.3	155.5	213	3.6	OK	54.3	143.6	174	3.3	OK	54.3	143.6	147	3.0	OK	54.0	147.5
280-290.	201	3.0	OK	53.3	157.5	250	3.8	OK	53.8	155.6	202	3.4	OK	55.9	147.9	154	2.9	OK	56.9	144.0	143	2.9	OK	56.4	145.9
290-300.	201	3.0	OK	53.4	157.6	202	3.1	OK	54.3	155.8	165	2.8	>75	55.1	154.0	158	3.0	OK	56.0	152.2	123	2.5	>75	56.8	150.3
300-310.	130	2.0	>50	53.6	157.7	129	2.0	>50	55.9	154.4	100	1.7	>50	54.7	156.0	88	1.6	>50	54.7	156.0	90	1.9	>50	57.0	152.8
310-320.	96	1.4	>50	53.7	157.8	93	1.4	>50	53.7	157.8	59	1.0	--	58.0	153.6	45	0.8	--	55.1	156.4	57	1.2	--	56.5	155.0
320-330.	67	1.0	--	53.8	157.9	49	0.8	--	53.8	157.9	56	0.9	--	55.5	156.8	39	0.7	--	55.5	156.8	40	0.8	--	62.0	152.2
330-340.	63	0.9	--	53.9	158.1	54	0.8	--	53.9	158.1	46	0.8	--	53.9	158.1	43	0.8	--	55.7	157.2	40	0.8	--	59.3	155.5
340-350.	56	0.8	--	54.0	158.2	55	0.9	--	54.0	158.2	46	0.8	--	54.0	158.2	39	0.7	--	57.8	157.2	42	0.9	--	57.8	157.2
350-360.	58	0.9	--	54.0	158.4	49	0.8	--	56.0	158.2	46	0.8	--	56.0	158.2	45	0.8	--	58.0	158.1	50	1.0	--	58.0	158.1

Table D2: Date for the Typical Transport Time from the Kamchaka NRS (Summer)

Table D2. Data for the Typical Transport Time from the Kamchatka NRS (Summer)																									
Term			0.5 day					1.0 day					1.5 day					2.0 day					2.5 day		
	Trajectory Statistics and Geographical Coordinates for the Absolute Maximum Cell (AMC)																								
Sector (deg)	#	%	SS	Lat	Long	#	%	SS	Lat	Long	#	%	SS	Lat	Long	#	%	SS	Lat	Long	#	%	SS	Lat	Long
0-10.	33	0.5	-	54.0	158.6	34	0.5	-	54.0	158.6	37	0.6	-	54.0	158.6	50	0.8	--	56.0	158.8	49	0.9	--	58.0	158.9
10- 20.	54	0.8	--	54.0	158.8	53	0.8	--	54.0	158.8	62	1.0	--	54.0	158.8	38	0.6	-	55.9	159.3	55	1.0	--	57.8	159.8
20- 30.	53	0.8	--	53.9	158.9	63	1.0	--	53.9	158.9	56	0.9	--	53.9	158.9	65	1.1	--	57.5	160.6	54	0.9	--	57.5	160.6
30- 40.	46	0.7	--	53.8	159.1	64	1.0	--	53.8	159.1	65	1.1	--	53.8	159.1	86	1.5	>50	55.5	160.2	77	1.3	--	58.7	162.5
40- 50.	79	1.2	--	53.7	159.2	86	1.4	--	53.7	159.2	93	1.5	>50	53.7	159.2	92	1.6	>50	58.0	163.5	109	1.9	>50	60.8	166.3
50- 60.	107	1.7	>50	53.6	159.3	127	2.0	>50	53.6	159.3	154	2.5	>75	54.7	161.0	164	2.8	>75	55.9	162.6	139	2.4	>75	57.0	164.2
60- 70.	150	2.3	>75	53.4	159.4	235	3.8	OK	55.1	163.0	301	4.9	OK	55.1	163.0	311	5.2	OK	55.1	163.0	323	5.6	OK	56.0	164.8
70- 80.	259	4.1	OK	53.3	159.5	420	6.7	OK	54.3	163.3	490	8.0	OK	54.3	163.3	485	8.2	OK	54.3	163.3	489	8.5	OK	56.9	173.0
80- 90.	318	5.0	OK	53.1	159.5	486	7.8	OK	53.3	161.5	460	7.5	OK	54.0	169.5	507	8.5	OK	54.5	175.4	562	9.8	OK	54.7	177.4
90-100.	470	7.4	OK	52.9	159.5	486	7.8	OK	52.7	161.5	542	8.9	OK	52.0	169.5	612	10.3	OK	51.5	175.4	647	11.3	OK	51.2	179.4
100-110.	473	7.4	OK	52.7	159.5	471	7.5	OK	52.2	161.4	499	8.2	OK	51.7	163.3	501	8.4	OK	50.2	169.1	505	8.8	OK	47.6	178.8
110-120.	456	7.1	OK	52.6	159.4	419	6.7	OK	51.7	161.2	386	6.3	OK	48.4	168.5	339	5.7	OK	46.7	172.1	296	5.2	OK	46.7	172.1
120-130.	407	6.4	OK	52.4	159.3	314	5.0	OK	52.4	159.3	266	4.4	OK	49.0	164.2	245	4.1	OK	49.0	164.2	211	3.7	OK	45.6	169.2
130-140.	310	4.9	OK	52.3	159.2	256	4.1	OK	52.3	159.2	215	3.5	OK	52.3	159.2	184	3.1	OK	49.5	162.0	164	2.9	OK	43.8	167.7
140-150.	266	4.2	OK	52.2	159.1	216	3.4	OK	52.2	159.1	227	3.7	OK	48.9	161.4	168	2.8	OK	45.6	163.7	149	2.6	>75	48.9	161.4
150-160.	222	3.5	OK	52.1	158.9	173	2.8	>75	52.1	158.9	125	2.1	>50	50.3	159.8	111	1.9	>50	44.9	162.3	114	2.0	>50	48.5	160.6
160-170.	201	3.1	OK	52.0	158.8	151	2.4	>75	52.0	158.8	113	1.9	>50	50.1	159.3	90	1.5	>50	48.2	159.8	95	1.7	>50	48.2	159.8
170-180.	145	2.3	>75	52.0	158.6	120	1.9	>50	52.0	158.6	102	1.7	>50	50.0	158.8	95	1.6	>50	48.0	158.9	69	1.2	--	48.0	158.9
180-190.	219	3.4	OK	52.0	158.4	140	2.2	>75	52.0	158.4	104	1.7	>50	52.0	158.4	101	1.7	>50	46.0	157.9	75	1.3	--	46.0	157.9
190-200.	154	2.4	>75	52.0	158.2	125	2.0	>50	52.0	158.2	103	1.7	>50	50.1	157.7	117	2.0	>50	50.1	157.7	96	1.7	>50	48.2	157.2
200-210.	161	2.5	>75	52.1	158.1	103	1.6	>50	50.3	157.2	110	1.8	>50	48.5	156.4	108	1.8	>50	48.5	156.4	107	1.9	>50	52.1	158.1
210-220.	159	2.5	>75	52.2	157.9	129	2.1	>50	50.5	156.8	124	2.0	>50	50.5	156.8	100	1.7	>50	48.9	155.6	96	1.7	>50	47.3	154.5
220-230.	159	2.5	>75	52.3	157.8	132	2.1	>75	50.9	156.4	112	1.8	>50	50.9	156.4	90	1.5	>50	49.5	155.0	90	1.6	>50	48.1	153.6
230-240.	150	2.3	>75	52.4	157.7	125	2.0	>50	52.4	157.7	109	1.8	>50	51.3	156.0	106	1.8	>50	51.3	156.0	107	1.9	>50	49.0	152.8
240-250.	184	2.9	OK	52.6	157.6	167	2.7	>75	51.7	155.8	132	2.2	>75	51.7	155.8	133	2.2	>75	50.9	154.0	112	2.0	>50	50.0	152.2
250-260.	160	2.5	>75	52.7	157.5	150	2.4	>75	52.7	157.5	171	2.8	OK	52.7	157.5	160	2.7	>75	52.2	155.6	164	2.9	OK	51.2	151.7
260-270.	189	3.0	OK	52.9	157.5	156	2.5	>75	52.9	157.5	157	2.6	>75	52.6	153.5	171	2.9	OK	52.4	151.5	134	2.3	>75	52.2	149.5
270-280.	156	2.4	>75	53.1	157.5	176	2.8	OK	53.3	155.5	176	2.9	OK	53.4	153.5	137	2.3	>75	53.8	149.5	138	2.4	>75	53.6	151.5
280-290.	146	2.3	>75	53.3	157.5	162	2.6	>75	53.8	155.6	155	2.5	>75	54.3	153.7	161	2.7	>75	54.8	151.7	140	2.4	>75	54.8	151.7
290-300.	132	2.1	>50	53.4	157.6	116	1.9	>50	54.3	155.8	106	1.7	>50	54.3	155.8	104	1.8	>50	55.1	154.0	101	1.8	>50	53.4	157.6
300-310.	92	1.4	>50	53.6	157.7	106	1.7	>50	53.6	157.7	89	1.5	>50	54.7	156.0	50	0.8	--	54.7	156.0	55	1.0	--	55.9	154.4
310-320.	73	1.1	--	53.7	157.8	92	1.5	>50	53.7	157.8	60	1.0	--	55.1	156.4	61	1.0	--	55.1	156.4	47	0.8	--	56.5	155.0
320-330.	60	0.9	--	53.8	157.9	70	1.1	--	53.8	157.9	52	0.9	--	55.5	156.8	52	0.9	--	57.1	155.6	36	0.6	-	55.5	156.8
330-340.	41	0.6	-	53.9	158.1	50	0.8	--	53.9	158.1	50	0.8	--	53.9	158.1	42	0.7	--	55.7	157.2	47	0.8	--	57.5	156.4
340-350.	55	0.9	--	54.0	158.2	53	0.8	--	54.0	158.2	56	0.9	--	55.9	157.7	44	0.7	--	54.0	158.2	43	0.8	--	57.8	157.2
350-360.	58	0.9	--	54.0	158.4	49	0.8	--	54.0	158.4	50	0.8	--	56.0	158.2	64	1.1	--	56.0	158.2	58	1.0	--	56.0	158.2

Table D3. Data for the Typical Transport Time from the Kamchatka NRS (Fall)

Term			0.5 day					1.0 day					1.5 day					2.0 day					2.5 day		
	Trajectory Statistics and Geographical Coordinates for the Absolute Maximum Cell (AMC)																								
Sector (deg)	#	%	SS	Lat	Long	#	%	SS	Lat	Long	#	%	SS	Lat	Long	#	%	SS	Lat	Long	#	%	SS	Lat	Long
0-10.	35	0.6	-	54.0	158.6	54	0.9	--	54.0	158.6	50	1.0	--	56.0	158.8	51	1.1	--	56.0	158.8	41	1.0	--	58.0	158.9
10- 20.	43	0.7	-	54.0	158.8	50	0.9	--	55.9	159.3	55	1.1	--	54.0	158.8	50	1.1	--	55.9	159.3	36	0.8	--	55.9	159.3
20- 30.	41	0.7	-	53.9	158.9	45	0.8	--	53.9	158.9	58	1.1	--	57.5	160.6	56	1.2	--	59.3	161.5	55	1.3	--	61.2	162.3
30- 40.	58	0.9	--	53.8	159.1	70	1.2	--	53.8	159.1	81	1.6	>50	57.1	161.4	71	1.5	>50	58.7	162.5	78	1.8	>50	63.7	166.0
40- 50.	62	1.0	--	55.1	160.6	64	1.1	--	55.1	160.6	74	1.4	>50	58.0	163.5	90	1.9	>50	55.1	160.6	88	2.1	>50	55.1	160.6
50- 60.	85	1.4	--	53.6	159.3	110	1.9	>50	57.0	164.2	131	2.5	>75	55.9	162.6	131	2.8	>75	57.0	164.2	103	2.4	>75	57.0	164.2
60- 70.	174	2.8	OK	53.4	159.4	212	3.6	OK	56.0	164.8	221	4.2	OK	56.0	164.8	193	4.1	OK	61.0	175.7	172	4.0	OK	58.5	170.3
70- 80.	272	4.4	OK	54.3	163.3	392	6.7	OK	55.3	167.2	382	7.3	OK	56.4	171.1	349	7.4	OK	56.4	171.1	308	7.2	OK	59.0	180.7
80- 90.	430	6.9	OK	53.3	161.5	518	8.8	OK	53.6	165.5	513	9.8	OK	54.1	171.5	553	11.7	OK	54.5	175.4	553	12.9	OK	55.2	183.4
90-100.	648	10.4	OK	52.7	161.5	709	12.0	OK	51.9	171.5	657	12.5	OK	52.2	167.5	566	11.9	OK	51.7	173.4	483	11.3	OK	51.7	173.4
100-110.	645	10.4	OK	52.2	161.4	529	9.0	OK	51.7	163.3	425	8.1	OK	50.2	169.1	385	8.1	OK	49.6	171.1	399	9.3	OK	48.6	174.9
110-120.	522	8.4	OK	51.7	161.2	440	7.5	OK	50.0	164.8	367	7.0	OK	45.8	173.9	316	6.7	OK	46.7	172.1	257	6.0	OK	48.4	168.5
120-130.	439	7.1	OK	52.4	159.3	365	6.2	OK	49.0	164.2	270	5.2	OK	47.8	165.9	227	4.8	OK	45.6	169.2	163	3.8	OK	46.7	167.5
130-140.	334	5.4	OK	52.3	159.2	279	4.7	OK	49.5	162.0	172	3.3	OK	46.6	164.9	102	2.2	>75	43.8	167.7	99	2.3	>75	48.1	163.5
140-150.	253	4.1	OK	52.2	159.1	156	2.6	>75	52.2	159.1	108	2.1	>50	48.9	161.4	92	1.9	>50	47.3	162.5	57	1.3	--	48.9	161.4
150-160.	162	2.6	>75	52.1	158.9	120	2.0	>50	50.3	159.8	86	1.6	>50	50.3	159.8	64	1.4	--	50.3	159.8	51	1.2	--	48.5	160.6
160-170.	128	2.1	>50	52.0	158.8	79	1.3	--	52.0	158.8	61	1.2	--	48.2	159.8	48	1.0	--	50.1	159.3	53	1.2	--	48.2	159.8
170-180.	80	1.3	--	52.0	158.6	62	1.1	--	50.0	158.8	56	1.1	--	52.0	158.6	52	1.1	--	48.0	158.9	28	0.7	-	46.0	159.1
180-190.	107	1.7	>50	52.0	158.4	69	1.2	--	50.0	158.2	65	1.2	--	48.0	158.1	49	1.0	--	46.0	157.9	36	0.8	--	42.0	157.5
190-200.	69	1.1	--	52.0	158.2	63	1.1	--	52.0	158.2	68	1.3	--	46.2	156.7	50	1.1	--	44.3	156.2	42	1.0	--	46.2	156.7
200-210.	73	1.2	--	52.1	158.1	60	1.0	--	50.3	157.2	55	1.1	--	46.7	155.5	53	1.1	--	50.3	157.2	50	1.2	--	48.5	156.4
210-220.	77	1.2	--	52.2	157.9	57	1.0	--	52.2	157.9	51	1.0	--	50.5	156.8	41	0.9	--	47.3	154.5	44	1.0	--	44.0	152.2
220-230.	73	1.2	--	52.3	157.8	57	1.0	--	52.3	157.8	49	0.9	--	50.9	156.4	51	1.1	--	45.2	150.7	47	1.1	--	50.9	156.4
230-240.	81	1.3	--	52.4	157.7	63	1.1	--	50.1	154.4	59	1.1	--	52.4	157.7	79	1.7	>50	50.1	154.4	56	1.3	--	50.1	154.4
240-250.	94	1.5	>50	51.7	155.8	70	1.2	--	52.6	157.6	68	1.3	--	50.9	154.0	56	1.2	--	50.0	152.2	68	1.6	>50	48.4	148.5
250-260.	124	2.0	>50	52.7	157.5	104	1.8	>50	51.7	153.7	92	1.8	>50	51.2	151.7	83	1.8	>50	49.1	144.0	101	2.4	>75	50.7	149.8
260-270.	174	2.8	OK	52.9	157.5	140	2.4	>75	52.7	155.5	145	2.8	>75	52.2	149.5	128	2.7	>75	51.9	145.6	126	2.9	OK	51.7	143.6
270-280.	150	2.4	>75	53.3	155.5	148	2.5	>75	53.3	155.5	140	2.7	>75	53.6	151.5	142	3.0	OK	54.0	147.5	114	2.7	>75	53.8	149.5
280-290.	149	2.4	>75	53.3	157.5	166	2.8	OK	55.3	149.8	144	2.8	>75	55.3	149.8	120	2.5	>75	55.3	149.8	112	2.6	>75	55.9	147.9
290-300.	125	2.0	>50	53.4	157.6	156	2.6	>75	55.1	154.0	128	2.4	>75	56.0	152.2	119	2.5	>75	55.1	154.0	118	2.8	>75	56.8	150.3
300-310.	110	1.8	>50	54.7	156.0	131	2.2	>75	57.0	152.8	134	2.6	>75	55.9	154.4	117	2.5	>75	58.2	151.1	86	2.0	>50	57.0	152.8
310-320.	116	1.9	>50	55.1	156.4	100	1.7	>50	53.7	157.8	74	1.4	>50	58.0	153.6	69	1.5	>50	55.1	156.4	53	1.2	--	56.5	155.0
320-330.	91	1.5	>50	53.8	157.9	99	1.7	>50	53.8	157.9	51	1.0	--	55.5	156.8	44	0.9	--	55.5	156.8	52	1.2	--	60.4	153.3
330-340.	83	1.3	--	53.9	158.1	66	1.1	--	53.9	158.1	42	0.8	--	55.7	157.2	46	1.0	--	59.3	155.5	55	1.3	--	59.3	155.5
340-350.	43	0.7	-	54.0	158.2	46	0.8	--	54.0	158.2	56	1.1	--	54.0	158.2	50	1.1	--	55.9	157.7	48	1.1	--	55.9	157.7
350-360.	73	1.2	--	54.0	158.4	49	0.8	--	56.0	158.2	54	1.0	--	56.0	158.2	46	1.0	--	56.0	158.2	56	1.3	--	58.0	158.1

Table D3. Date for the typical transport time from the Kamchatka NRS (Fall)

Table D4. Data for the typical transport time from the Kamchatka NRS (Winter)

Term			0.5 day					1.0 day					1.5 day					2.0 day					2.5 day		
	Trajectory Statistics and Geographical Coordinates for the Absolute Maximum Cell (AMC)																								
Sector (deg)	#	%	SS	Lat	Long	#	%	SS	Lat	Long	#	%	SS	Lat	Long	#	%	SS	Lat	Long	#	%	SS	Lat	Long
0-10.	22	0.3	-	54.0	158.6	48	0.8	--	56.0	158.8	43	0.8	--	54.0	158.6	58	1.4	--	56.0	158.8	26	0.7	--	71.9	160.2
10- 20.	27	0.4	-	54.0	158.8	38	0.6	-	55.9	159.3	52	1.0	--	54.0	158.8	39	0.9	--	67.5	162.4	44	1.2	--	55.9	159.3
20- 30.	35	0.5	-	53.9	158.9	48	0.8	--	59.3	161.5	62	1.2	--	55.7	159.8	52	1.2	--	69.4	162.9	44	1.2	--	63.0	163.2
30- 40.	38	0.6	-	53.8	159.1	66	1.0	--	55.5	160.2	74	1.4	>50	57.1	161.4	58	1.4	--	55.7	159.8	63	1.8	>50	58.7	162.5
40- 50.	63	0.9	--	53.7	159.2	72	1.1	--	56.5	162.0	93	1.8	>50	55.1	160.6	79	1.9	>50	63.7	166.0	85	2.4	>75	60.8	166.3
50- 60.	73	1.1	--	53.6	159.3	90	1.4	>50	54.7	161.0	100	1.9	>50	57.0	164.2	135	3.2	OK	62.2	167.7	119	3.3	OK	61.6	170.8
60- 70.	112	1.6	>50	54.3	161.2	167	2.6	>75	56.0	164.8	160	3.1	OK	56.8	166.7	166	3.9	OK	60.5	169.2	135	3.7	OK	65.3	184.8
70- 80.	231	3.4	OK	53.8	161.4	294	4.6	OK	54.3	163.3	291	5.6	OK	58.4	178.8	238	5.6	OK	64.4	183.0	277	7.7	OK	58.4	178.8
80- 90.	346	5.1	OK	53.3	161.5	485	7.5	OK	54.0	169.5	394	7.6	OK	54.7	177.4	338	7.9	OK	60.0	184.6	286	7.9	OK	54.3	173.4
90-100.	654	9.6	OK	52.6	163.5	593	9.2	OK	52.2	167.5	456	8.8	OK	51.2	179.4	384	9.0	OK	54.7	177.4	321	8.9	OK	50.3	189.4
100-110.	612	9.0	OK	52.2	161.4	567	8.8	OK	51.7	163.3	393	7.6	OK	48.1	176.9	295	6.9	OK	52.2	167.5	204	5.7	OK	48.6	174.9
110-120.	491	7.2	OK	52.6	159.4	444	6.9	OK	50.9	163.0	297	5.7	OK	47.5	170.3	199	4.7	OK	45.5	186.5	145	4.0	OK	45.8	173.9
120-130.	402	5.9	OK	52.4	159.3	348	5.4	OK	51.3	161.0	197	3.8	OK	45.6	169.2	113	2.6	>75	45.8	173.9	71	2.0	>50	49.0	164.2
130-140.	316	4.6	OK	52.3	159.2	233	3.6	OK	48.1	163.5	153	3.0	OK	46.6	164.9	93	2.2	>75	45.6	169.2	50	1.4	--	46.6	164.9
140-150.	214	3.1	OK	52.2	159.1	177	2.8	>75	50.5	160.2	127	2.5	>75	45.6	163.7	60	1.4	>50	45.2	166.3	56	1.6	>50	47.3	162.5
150-160.	200	2.9	OK	52.1	158.9	160	2.5	>75	52.1	158.9	73	1.4	>50	48.5	160.6	62	1.5	>50	48.9	161.4	50	1.4	--	44.9	162.3
160-170.	163	2.4	>75	52.0	158.8	129	2.0	>50	50.1	159.3	88	1.7	>50	48.2	159.8	51	1.2	--	46.7	161.5	47	1.3	--	48.2	159.8
170-180.	116	1.7	>50	52.0	158.6	97	1.5	>50	50.0	158.8	71	1.4	--	50.0	158.8	58	1.4	--	50.1	159.3	41	1.1	--	46.0	159.1
180-190.	175	2.6	>75	52.0	158.4	108	1.7	>50	52.0	158.4	71	1.4	--	52.0	158.4	58	1.4	--	48.0	158.9	50	1.4	--	48.0	158.1
190-200.	108	1.6	>50	52.0	158.2	112	1.7	>50	50.1	157.7	79	1.5	>50	48.2	157.2	77	1.8	>50	48.0	158.1	26	0.7	--	46.2	156.7
200-210.	113	1.7	>50	52.1	158.1	104	1.6	>50	50.3	157.2	78	1.5	>50	48.5	156.4	54	1.3	--	46.2	156.7	42	1.2	--	48.5	156.4
210-220.	116	1.7	>50	52.2	157.9	99	1.5	>50	52.2	157.9	80	1.5	>50	47.3	154.5	68	1.6	>50	48.5	156.4	60	1.7	>50	45.6	153.3
220-230.	151	2.2	>75	52.3	157.8	117	1.8	>50	52.3	157.8	104	2.0	>50	50.9	156.4	107	2.5	>75	45.6	153.3	75	2.1	>50	45.2	150.7
230-240.	191	2.8	OK	52.4	157.7	157	2.4	>75	51.3	156.0	154	3.0	OK	47.8	151.1	110	2.6	>75	46.6	152.1	87	2.4	>75	49.0	152.8
240-250.	241	3.5	OK	52.6	157.6	217	3.4	OK	50.0	152.2	192	3.7	OK	49.2	150.3	118	2.8	>75	44.4	146.2	141	3.9	OK	47.5	146.7
250-260.	281	4.1	OK	52.2	155.6	225	3.5	OK	51.2	151.7	196	3.8	OK	51.2	151.7	192	4.5	OK	47.5	146.7	181	5.0	OK	47.1	136.3
260-270.	334	4.9	OK	52.7	155.5	292	4.5	OK	52.2	149.5	241	4.6	OK	51.9	145.6	240	5.6	OK	50.7	149.8	182	5.0	OK	52.0	147.5
270-280.	297	4.4	OK	53.3	155.5	243	3.8	OK	53.4	153.5	231	4.5	OK	53.6	151.5	185	4.3	OK	52.0	147.5	164	4.6	OK	53.6	151.5
280-290.	228	3.3	OK	53.3	157.5	218	3.4	OK	54.3	153.7	162	3.1	OK	54.3	153.7	138	3.2	OK	53.8	149.5	123	3.4	OK	55.3	149.8
290-300.	120	1.8	>50	53.4	157.6	147	2.3	>75	54.3	155.8	137	2.6	>75	55.1	154.0	125	2.9	OK	54.8	151.7	92	2.6	>75	55.1	154.0
300-310.	107	1.6	>50	53.6	157.7	113	1.8	>50	53.6	157.7	91	1.8	>50	57.0	152.8	71	1.7	>50	57.7	148.5	98	2.7	>75	59.3	149.5
310-320.	68	1.0	--	53.7	157.8	61	1.0	--	53.7	157.8	60	1.2	--	55.1	156.4	61	1.4	>50	55.9	154.4	51	1.4	>50	55.1	156.4
320-330.	50	0.7	--	53.8	157.9	49	0.8	--	55.5	156.8	37	0.7	--	57.1	155.6	54	1.3	--	55.1	156.4	60	1.7	>50	66.9	148.7
330-340.	57	0.8	--	53.9	158.1	35	0.5	-	53.9	158.1	39	0.8	--	53.9	158.1	44	1.0	--	58.7	154.5	37	1.0	--	59.3	155.5
340-350.	27	0.4	-	54.0	158.2	46	0.7	--	55.9	157.7	46	0.9	--	59.8	156.7	44	1.0	--	55.7	157.2	37	1.0	--	59.8	156.7
350-360.	49	0.7	--	54.0	158.4	43	0.7	-	54.0	158.4	68	1.3	--	54.0	158.4	55	1.3	--	55.9	157.7	38	1.1	--	66.0	157.4

Table D5. Data for the typical transport time from the Vladivostok NRS (Spring)

Term			0.5 day					1.0 day					1.5 day					2.0 day					2.5 day		
	Trajectory Statistics and Geographical Coordinates for the Absolute Maximum Cell (AMC)																								
Sector (deg)	#	%	SS	Lat	Long	#	%	SS	Lat	Long	#	%	SS	Lat	Long	#	%	SS	Lat	Long	#	%	SS	Lat	Long
0-10.	42	0.8	--	44.0	132.6	47	1.0	--	44.0	132.6	41	1.1	--	50.0	133.1	34	1.1	--	50.0	133.1	32	1.1	--	57.9	133.8
10- 20.	54	1.1	--	44.0	132.8	51	1.1	--	45.9	133.3	49	1.3	--	49.8	134.3	55	1.7	>50	49.8	134.3	43	1.5	>50	45.9	133.3
20- 30.	69	1.4	--	43.9	132.9	73	1.6	>50	45.7	133.8	69	1.8	>50	49.3	135.5	80	2.5	>75	53.0	137.2	79	2.8	=OK	49.3	135.5
30- 40.	85	1.7	>50	43.8	133.1	107	2.3	>75	45.5	134.2	124	3.3	=OK	50.4	137.7	109	3.5	=OK	53.7	140.0	101	3.6	=OK	53.7	140.0
40- 50.	129	2.5	>75	43.7	133.2	135	2.9	=OK	46.5	136.0	134	3.6	=OK	48.0	137.5	136	4.3	=OK	49.4	138.9	127	4.5	=OK	53.6	143.1
50- 60.	152	3.0	=OK	43.6	133.3	190	4.0	=OK	45.9	136.6	182	4.8	=OK	48.2	139.9	190	6.0	=OK	48.2	139.9	172	6.1	=OK	51.6	144.8
60- 70.	217	4.2	=OK	43.4	133.4	296	6.3	=OK	46.0	138.8	310	8.3	=OK	46.8	140.7	282	8.9	=OK	48.5	144.3	243	8.6	=OK	51.0	149.7
70- 80.	278	5.4	=OK	43.3	133.5	310	6.6	=OK	44.3	137.3	319	8.5	=OK	44.8	139.3	337	10.7	=OK	45.9	143.1	372	13.2	=OK	46.9	147.0
80- 90.	301	5.9	=OK	43.1	133.5	364	7.7	=OK	43.8	141.5	372	9.9	=OK	43.6	139.5	408	12.9	=OK	44.0	143.5	458	16.3	=OK	45.7	163.4
90-100.	448	8.8	=OK	42.7	135.5	481	10.2	=OK	42.6	137.5	502	13.4	=OK	42.0	143.5	460	14.6	=OK	41.3	151.4	373	13.2	=OK	41.3	151.4
100-110.	510	10.0	=OK	42.2	135.4	532	11.3	=OK	41.2	139.3	399	10.6	=OK	41.2	139.3	274	8.7	=OK	39.1	147.0	200	7.1	=OK	39.6	145.1
110-120.	497	9.7	=OK	41.7	135.2	407	8.6	=OK	40.9	137.0	296	7.9	=OK	38.4	142.5	156	4.9	=OK	37.5	144.3	113	4.0	=OK	38.4	142.5
120-130.	410	8.0	=OK	41.3	135.0	318	6.7	=OK	41.3	135.0	151	4.0	=OK	40.1	136.6	90	2.9	=OK	41.3	135.0	65	2.3	>75	39.0	138.2
130-140.	332	6.5	=OK	42.3	133.2	204	4.3	=OK	40.9	134.6	99	2.6	>75	39.5	136.0	38	1.2	--	39.5	136.0	39	1.4	--	39.5	136.0
140-150.	280	5.5	=OK	42.2	133.1	163	3.5	=OK	40.5	134.2	71	1.9	>50	40.5	134.2	35	1.1	--	40.5	134.2	21	0.7	--	40.5	134.2
150-160.	223	4.4	=OK	42.1	132.9	155	3.3	=OK	40.3	133.8	67	1.8	>50	38.5	134.6	36	1.1	--	40.3	133.8	21	0.7	--	33.0	137.2
160-170.	204	4.0	=OK	42.0	132.8	127	2.7	>75	38.2	133.8	69	1.8	>50	38.2	133.8	33	1.1	--	42.0	132.8	12	0.4	-	42.0	132.8
170-180.	144	2.8	=OK	42.0	132.6	107	2.3	>75	40.0	132.8	61	1.6	>50	40.0	132.8	19	0.6	-	40.0	132.8	19	0.7	-	38.0	132.9
180-190.	141	2.8	>75	42.0	132.4	106	2.3	>75	40.0	132.2	51	1.4	--	40.0	132.2	35	1.1	--	38.0	132.1	11	0.4	-	40.0	132.2
190-200.	86	1.7	>50	42.0	132.2	82	1.7	>50	40.1	131.7	47	1.3	--	42.0	132.2	30	1.0	--	36.2	130.7	32	1.1	--	38.2	131.2
200-210.	77	1.5	>50	42.1	132.1	52	1.1	--	42.1	132.1	36	1.0	--	40.3	131.2	33	1.1	--	40.3	131.2	14	0.5	-	34.9	128.7
210-220.	50	1.0	--	42.2	131.9	40	0.9	--	42.2	131.9	20	0.5	-	42.2	131.9	21	0.7	-	38.9	129.6	21	0.7	--	35.6	127.3
220-230.	42	0.8	--	42.3	131.8	38	0.8	--	42.3	131.8	26	0.7	-	42.3	131.8	14	0.4	-	36.6	126.1	10	0.4	-	39.5	129.0
230-240.	26	0.5	-	42.4	131.7	28	0.6	-	42.4	131.7	18	0.5	-	36.7	123.5	13	0.4	-	39.0	126.8	4	0.1	-	33.3	118.6
240-250.	32	0.6	-	42.6	131.6	21	0.4	-	41.7	129.8	12	0.3	-	42.6	131.6	7	0.2	-	37.5	120.7	9	0.3	-	39.2	124.3
250-260.	24	0.5	-	42.7	131.5	12	0.3	-	41.2	125.7	19	0.5	-	41.2	125.7	13	0.4	-	42.2	129.6	11	0.4	-	41.7	127.7
260-270.	21	0.4	-	42.9	131.5	28	0.6	-	42.9	131.5	15	0.4	-	42.9	131.5	16	0.5	-	42.2	123.5	11	0.4	-	42.7	129.5
270-280.	15	0.3	-	43.1	131.5	11	0.2	-	43.6	125.5	9	0.2	-	43.4	127.5	12	0.4	-	43.6	125.5	13	0.5	-	43.4	127.5
280-290.	25	0.5	-	43.3	131.5	21	0.4	-	43.8	129.6	11	0.3	-	44.8	125.7	12	0.4	-	44.8	125.7	13	0.5	-	44.8	125.7
290-300.	29	0.6	-	43.4	131.6	19	0.4	-	43.4	131.6	12	0.3	-	45.1	128.0	13	0.4	-	44.3	129.8	21	0.7	--	46.0	126.2
300-310.	18	0.4	-	43.6	131.7	22	0.5	-	44.7	130.0	17	0.5	-	47.0	126.8	16	0.5	-	48.2	125.1	15	0.5	-	45.9	128.4
310-320.	22	0.4	-	43.7	131.8	18	0.4	-	45.1	130.4	19	0.5	-	46.5	129.0	22	0.7	--	48.0	127.6	21	0.7	--	46.5	129.0
320-330.	23	0.5	-	43.8	131.9	25	0.5	-	43.8	131.9	31	0.8	--	47.1	129.6	20	0.6	-	45.5	130.8	23	0.8	--	48.7	128.5
330-340.	29	0.6	-	43.9	132.1	36	0.8	--	43.9	132.1	24	0.6	-	43.9	132.1	25	0.8	--	54.8	127.0	31	1.1	--	49.3	129.5
340-350.	31	0.6	-	44.0	132.2	45	1.0	--	44.0	132.2	32	0.9	--	49.8	130.7	39	1.2	--	49.8	130.7	30	1.1	--	51.7	130.2
350-360.	55	1.1	--	44.0	132.4	50	1.1	--	44.0	132.4	45	1.2	--	48.0	132.1	43	1.4	--	50.0	131.9	39	1.4	--	54.0	131.5

Table D6. Data for the typical transport time from the Vladivostok NRS (Summer)

Term	0.5 day					1.0 day					1.5 day					2.0 day					2.5 day				
	Trajectory Statistics and Geographical Coordinates for the Absolute Maximum Cell (AMC)																								
Sector (deg)	#	%	SS	Lat	Long	#	%	SS	Lat	Long	#	%	SS	Lat	Long	#	%	SS	Lat	Long	#	%	SS	Lat	Long
0-10.	114	2.0	>50	44.0	132.6	114	2.1	>75	44.0	132.6	93	2.0	>50	46.0	132.8	87	2.1	>50	48.0	132.9	76	2.0	>50	46.0	132.8
10- 20.	139	2.4	>75	44.0	132.8	139	2.6	>75	44.0	132.8	109	2.3	>75	45.9	133.3	85	2.0	>50	45.9	133.3	67	1.7	>50	47.8	133.8
20- 30.	161	2.8	=OK	43.9	132.9	171	3.2	=OK	43.9	132.9	128	2.7	>75	45.7	133.8	104	2.5	>75	49.3	135.5	94	2.4	>75	47.5	134.6
30- 40.	198	3.4	=OK	43.8	133.1	181	3.3	=OK	43.8	133.1	151	3.2	=OK	47.1	135.4	145	3.4	=OK	47.1	135.4	122	3.2	=OK	47.1	135.4
40- 50.	207	3.6	=OK	43.7	133.2	249	4.6	=OK	43.7	133.2	228	4.8	=OK	46.5	136.0	198	4.7	=OK	46.5	136.0	189	4.9	=OK	46.5	136.0
50- 60.	232	4.0	=OK	43.6	133.3	291	5.4	=OK	44.7	135.0	301	6.4	=OK	44.7	135.0	283	6.7	=OK	47.0	138.2	253	6.5	=OK	49.3	141.5
60- 70.	276	4.8	=OK	43.4	133.4	286	5.3	=OK	44.3	135.2	335	7.1	=OK	45.1	137.0	326	7.7	=OK	46.8	140.7	324	8.4	=OK	47.7	142.5
70- 80.	278	4.8	=OK	43.3	133.5	339	6.3	=OK	43.8	135.4	310	6.6	=OK	43.8	135.4	343	8.1	=OK	45.3	141.2	371	9.6	=OK	44.8	139.3
80- 90.	199	3.5	=OK	43.1	133.5	254	4.7	=OK	43.1	133.5	285	6.0	=OK	43.6	139.5	291	6.9	=OK	43.4	137.5	312	8.1	=OK	43.4	137.5
90-100.	303	5.3	=OK	42.9	133.5	269	5.0	=OK	42.7	135.5	267	5.7	=OK	42.6	137.5	271	6.4	=OK	42.7	135.5	271	7.0	=OK	42.6	137.5
100-110.	239	4.1	=OK	42.7	133.5	241	4.5	=OK	42.7	133.5	217	4.6	=OK	42.2	135.4	208	4.9	=OK	42.2	135.4	201	5.2	=OK	42.2	135.4
110-120.	216	3.7	=OK	42.6	133.4	196	3.6	=OK	42.6	133.4	177	3.8	=OK	42.6	133.4	140	3.3	=OK	41.7	135.2	125	3.2	=OK	41.7	135.2
120-130.	188	3.3	=OK	42.4	133.3	143	2.6	>75	42.4	133.3	106	2.3	>75	42.4	133.3	97	2.3	>75	42.4	133.3	94	2.4	>75	41.3	135.0
130-140.	172	3.0	=OK	42.3	133.2	113	2.1	>75	40.9	134.6	81	1.7	>50	42.3	133.2	79	1.9	>50	42.3	133.2	55	1.4	>50	42.3	133.2
140-150.	160	2.8	>75	42.2	133.1	118	2.2	>75	42.2	133.1	90	1.9	>50	42.2	133.1	62	1.5	>50	40.5	134.2	55	1.4	>50	40.5	134.2
150-160.	134	2.3	>75	42.1	132.9	93	1.7	>50	42.1	132.9	85	1.8	>50	42.1	132.9	70	1.7	>50	42.1	132.9	46	1.2	--	40.3	133.8
160-170.	144	2.5	>75	42.0	132.8	97	1.8	>50	42.0	132.8	64	1.4	--	42.0	132.8	61	1.4	>50	42.0	132.8	42	1.1	--	42.0	132.8
170-180.	94	1.6	>50	42.0	132.6	88	1.6	>50	42.0	132.6	57	1.2	--	42.0	132.6	50	1.2	--	42.0	132.6	39	1.0	--	38.0	132.9
180-190.	158	2.7	>75	42.0	132.4	101	1.9	>50	42.0	132.4	92	2.0	>50	38.0	132.1	66	1.6	>50	42.0	132.4	50	1.3	--	42.0	132.4
190-200.	128	2.2	>75	42.0	132.2	101	1.9	>50	42.0	132.2	86	1.8	>50	42.0	132.2	65	1.5	>50	42.0	132.2	58	1.5	>50	42.0	132.2
200-210.	140	2.4	>75	42.1	132.1	106	2.0	>50	40.3	131.2	70	1.5	>50	42.1	132.1	72	1.7	>50	40.3	131.2	37	1.0	--	38.5	130.4
210-220.	161	2.8	=OK	42.2	131.9	137	2.5	>75	40.5	130.8	88	1.9	>50	40.5	130.8	54	1.3	--	42.2	131.9	72	1.9	>50	40.5	130.8
220-230.	150	2.6	>75	42.3	131.8	112	2.1	>50	42.3	131.8	117	2.5	>75	40.9	130.4	90	2.1	>75	39.5	129.0	77	2.0	>50	36.6	126.1
230-240.	138	2.4	>75	42.4	131.7	112	2.1	>50	42.4	131.7	90	1.9	>50	41.3	130.0	90	2.1	>75	40.1	128.4	92	2.4	>75	39.0	126.8
240-250.	115	2.0	>50	42.6	131.6	88	1.6	>50	42.6	131.6	71	1.5	>50	41.7	129.8	64	1.5	>50	41.7	129.8	49	1.3	--	40.9	128.0
250-260.	112	1.9	>50	42.7	131.5	79	1.5	>50	42.2	129.6	58	1.2	--	42.2	129.6	54	1.3	--	41.7	127.7	34	0.9	--	41.7	127.7
260-270.	136	2.4	>75	42.9	131.5	90	1.7	>50	42.9	131.5	69	1.5	>50	42.6	127.5	44	1.0	--	42.7	129.5	38	1.0	--	42.6	127.5
270-280.	113	2.0	>50	43.1	131.5	72	1.3	--	43.3	129.5	61	1.3	--	43.3	129.5	56	1.3	--	43.3	129.5	39	1.0	--	43.3	129.5
280-290.	96	1.7	>50	43.3	131.5	80	1.5	>50	43.8	129.6	71	1.5	>50	43.8	129.6	54	1.3	--	44.3	127.7	49	1.3	--	44.3	127.7
290-300.	121	2.1	>75	43.4	131.6	133	2.5	>75	44.3	129.8	77	1.6	>50	45.1	128.0	83	2.0	>50	46.8	124.3	84	2.2	>75	45.1	128.0
300-310.	127	2.2	>75	43.6	131.7	135	2.5	>75	45.9	128.4	137	2.9	=OK	44.7	130.0	81	1.9	>50	48.2	125.1	75	1.9	>50	44.7	130.0
310-320.	118	2.1	>50	43.7	131.8	127	2.4	>75	45.1	130.4	100	2.1	>75	46.5	129.0	97	2.3	>75	46.5	129.0	71	1.8	>50	48.0	127.6
320-330.	127	2.2	>75	43.8	131.9	139	2.6	>75	45.5	130.8	119	2.5	>75	47.1	129.6	98	2.3	>75	47.1	129.6	93	2.4	>75	47.1	129.6
330-340.	117	2.0	>50	43.9	132.1	150	2.8	>75	45.7	131.2	107	2.3	>75	45.7	131.2	87	2.1	>50	47.5	130.4	67	1.7	>50	45.7	131.2
340-350.	117	2.0	>50	44.0	132.2	135	2.5	>75	44.0	132.2	112	2.4	>75	45.9	131.7	78	1.9	>50	45.9	131.7	66	1.7	>50	49.8	130.7
350-360.	141	2.4	>75	44.0	132.4	133	2.5	>75	44.0	132.4	107	2.3	>75	46.0	132.2	93	2.2	>75	46.0	132.2	89	2.3	>75	48.0	132.1

Table D7. Data for the typical transport time from the Vladivostok NRS (Fall)

Term			0.5 day					1.0 day					1.5 day					2.0 day					2.5 day		
	Trajectory Statistics and Geographical Coordinates for the Absolute Maximum Cell (AMC)																								
Sector (deg)	#	%	SS	Lat	Long	#	%	SS	Lat	Long	#	%	SS	Lat	Long	#	%	SS	Lat	Long	#	%	SS	Lat	Long
0-10.	29	0.6	-	44.0	132.6	48	1.1	--	44.0	132.6	50	1.4	--	46.0	132.8	36	1.1	--	46.0	132.8	46	1.6	>50	50.0	133.1
10- 20.	46	0.9	--	44.0	132.8	42	1.0	--	44.0	132.8	57	1.6	>50	45.9	133.3	52	1.6	>50	49.8	134.3	46	1.6	>50	45.9	133.3
20- 30.	58	1.1	--	43.9	132.9	72	1.7	>50	43.9	132.9	59	1.6	>50	45.7	133.8	69	2.1	>75	53.0	137.2	55	1.9	>50	51.2	136.3
30- 40.	84	1.7	>50	43.8	133.1	87	2.0	>50	45.5	134.2	96	2.6	>75	45.5	134.2	91	2.8	=OK	45.5	134.2	91	3.1	=OK	48.7	136.5
40- 50.	121	2.4	>75	43.7	133.2	136	3.1	=OK	46.5	136.0	142	3.9	=OK	46.5	136.0	155	4.8	=OK	46.5	136.0	155	5.3	=OK	48.0	137.5
50- 60.	149	2.9	=OK	43.6	133.3	202	4.6	=OK	45.9	136.6	212	5.8	=OK	48.2	139.9	216	6.7	=OK	49.3	141.5	231	7.9	=OK	49.3	141.5
60- 70.	200	3.9	=OK	43.4	133.4	313	7.2	=OK	45.1	137.0	318	8.7	=OK	48.5	144.3	310	9.6	=OK	47.7	142.5	312	10.6	=OK	50.2	147.9
70- 80.	318	6.2	=OK	43.3	133.5	372	8.5	=OK	45.3	141.2	408	11.2	=OK	45.9	143.1	414	12.8	=OK	46.9	147.0	376	12.8	=OK	51.0	162.4
80- 90.	372	7.3	=OK	43.3	135.5	417	9.6	=OK	44.0	143.5	371	10.2	=OK	44.3	147.4	378	11.7	=OK	44.3	147.4	350	11.9	=OK	45.5	161.4
90-100.	507	9.9	=OK	42.7	135.5	422	9.7	=OK	42.6	137.5	316	8.7	=OK	42.0	143.5	224	6.9	=OK	41.5	149.4	240	8.2	=OK	41.7	147.4
100-110.	477	9.3	=OK	42.7	133.5	356	8.2	=OK	41.7	137.3	258	7.1	=OK	41.2	139.3	174	5.4	=OK	40.2	143.1	136	4.6	=OK	41.2	139.3
110-120.	443	8.7	=OK	42.6	133.4	240	5.5	=OK	41.7	135.2	153	4.2	=OK	40.0	138.8	114	3.5	=OK	39.2	140.7	82	2.8	=OK	40.9	137.0
120-130.	308	6.0	=OK	42.4	133.3	179	4.1	=OK	41.3	135.0	94	2.6	>75	42.4	133.3	71	2.2	>75	42.4	133.3	41	1.4	>50	42.4	133.3
130-140.	255	5.0	=OK	42.3	133.2	122	2.8	=OK	40.9	134.6	63	1.7	>50	42.3	133.2	44	1.4	--	40.9	134.6	35	1.2	--	40.9	134.6
140-150.	229	4.5	=OK	42.2	133.1	128	2.9	=OK	40.5	134.2	57	1.6	>50	42.2	133.1	46	1.4	>50	40.5	134.2	27	0.9	--	38.9	135.4
150-160.	203	4.0	=OK	42.1	132.9	112	2.6	>75	40.3	133.8	61	1.7	>50	40.3	133.8	37	1.2	--	40.3	133.8	29	1.0	--	42.1	132.9
160-170.	173	3.4	=OK	42.0	132.8	123	2.8	=OK	42.0	132.8	58	1.6	>50	40.1	133.3	46	1.4	>50	42.0	132.8	34	1.2	--	42.0	132.8
170-180.	141	2.8	>75	42.0	132.6	91	2.1	>75	40.0	132.8	64	1.8	>50	40.0	132.8	45	1.4	>50	42.0	132.6	36	1.2	--	40.0	132.8
180-190.	161	3.2	=OK	42.0	132.4	110	2.5	>75	42.0	132.4	91	2.5	>75	40.0	132.2	59	1.8	>50	40.0	132.2	41	1.4	>50	40.0	132.2
190-200.	116	2.3	>75	42.0	132.2	103	2.4	>75	40.1	131.7	81	2.2	>75	38.2	131.2	61	1.9	>50	38.2	131.2	60	2.1	>50	38.2	131.2
200-210.	91	1.8	>50	42.1	132.1	97	2.2	>75	40.3	131.2	88	2.4	>75	38.5	130.4	91	2.8	=OK	38.5	130.4	59	2.0	>50	36.7	129.5
210-220.	91	1.8	>50	42.2	131.9	85	2.0	>50	40.5	130.8	85	2.3	>75	37.3	128.5	67	2.1	>50	37.3	128.5	66	2.3	>75	38.9	129.6
220-230.	83	1.6	>50	42.3	131.8	65	1.5	>50	40.9	130.4	65	1.8	>50	39.5	129.0	62	1.9	>50	40.9	130.4	47	1.6	>50	35.2	124.7
230-240.	68	1.3	--	42.4	131.7	68	1.6	>50	40.1	128.4	46	1.3	--	40.1	128.4	46	1.4	>50	39.0	126.8	49	1.7	>50	39.0	126.8
240-250.	46	0.9	--	42.6	131.6	48	1.1	--	42.6	131.6	29	0.8	--	40.9	128.0	30	0.9	--	40.9	128.0	26	0.9	--	41.7	129.8
250-260.	34	0.7	-	42.7	131.5	19	0.4	-	42.7	131.5	21	0.6	-	42.2	129.6	21	0.7	-	41.7	127.7	13	0.4	-	39.1	118.0
260-270.	47	0.9	--	42.9	131.5	24	0.6	-	42.9	131.5	18	0.5	-	42.9	131.5	9	0.3	-	42.6	127.5	20	0.7	-	42.9	131.5
270-280.	22	0.4	-	43.1	131.5	31	0.7	--	43.1	131.5	27	0.7	--	43.3	129.5	12	0.4	-	43.3	129.5	14	0.5	-	44.0	121.5
280-290.	26	0.5	-	43.3	131.5	27	0.6	-	43.3	131.5	21	0.6	-	43.8	129.6	23	0.7	--	44.3	127.7	16	0.6	-	45.3	123.8
290-300.	19	0.4	-	43.4	131.6	15	0.3	-	43.4	131.6	22	0.6	-	44.3	129.8	27	0.8	--	46.0	126.2	18	0.6	-	45.1	128.0
300-310.	25	0.5	-	43.6	131.7	28	0.6	-	43.6	131.7	30	0.8	--	43.6	131.7	23	0.7	--	47.0	126.8	20	0.7	-	48.2	125.1
310-320.	22	0.4	-	43.7	131.8	33	0.8	--	43.7	131.8	34	0.9	--	45.1	130.4	33	1.0	--	55.0	120.5	18	0.6	-	55.0	120.5
320-330.	30	0.6	-	43.8	131.9	33	0.8	--	43.8	131.9	41	1.1	--	43.8	131.9	15	0.5	-	47.1	129.6	34	1.2	--	60.2	120.5
330-340.	27	0.5	-	43.9	132.1	37	0.9	--	43.9	132.1	15	0.4	-	43.9	132.1	39	1.2	--	54.8	127.0	27	0.9	--	49.3	129.5
340-350.	29	0.6	-	45.9	131.7	37	0.9	--	45.9	131.7	33	0.9	--	47.8	131.2	44	1.4	--	45.9	131.7	37	1.3	--	47.8	131.2
350-360.	55	1.1	--	44.0	132.4	43	1.0	--	46.0	132.2	54	1.5	>50	46.0	132.2	46	1.4	>50	46.0	132.2	46	1.6	>50	52.0	131.7

Table D8. Data for the typical transport time from the Vladivostok NRS (Winter)

Term			0.5 day					1.0 day					1.5 day					2.0 day					2.5 day		
	Trajectory Statistics and Geographical Coordinates for the Absolute Maximum Cell (AMC)																								
Sector (deg)	#	%	SS	Lat	Long	#	%	SS	Lat	Long	#	%	SS	Lat	Long	#	%	SS	Lat	Long	#	%	SS	Lat	Long
0-10.	14	0.2	-	44.0	132.6	11	0.2	-	46.0	132.8	20	0.6	-	50.0	133.1	28	1.3	--	48.0	132.9	19	1.1	--	56.0	133.6
10- 20.	11	0.2	-	44.0	132.8	17	0.3	-	45.9	133.3	32	1.0	--	47.8	133.8	22	1.0	--	57.5	136.4	30	1.8	>50	63.3	138.0
20- 30.	17	0.3	-	43.9	132.9	23	0.4	-	47.5	134.6	27	0.8	--	47.5	134.6	28	1.3	--	49.3	135.5	41	2.4	>75	53.0	137.2
30- 40.	32	0.5	-	43.8	133.1	43	0.8	--	47.1	135.4	53	1.7	>50	47.1	135.4	51	2.4	>75	53.7	140.0	59	3.5	OK	55.3	141.1
40- 50.	50	0.7	--	43.7	133.2	61	1.1	--	48.0	137.5	64	2.0	>50	48.0	137.5	71	3.3	OK	52.2	141.7	64	3.8	OK	56.4	145.9
50- 60.	77	1.1	--	43.6	133.3	105	1.9	>50	47.0	138.2	112	3.5	OK	49.3	141.5	122	5.7	OK	49.3	141.5	105	6.2	OK	55.0	149.7
60- 70.	161	2.4	>75	44.3	135.2	202	3.6	OK	46.8	140.7	210	6.6	OK	48.5	144.3	211	9.8	OK	48.5	144.3	170	10.1	OK	49.3	146.1
70- 80.	294	4.4	OK	43.8	135.4	379	6.8	OK	45.9	143.1	398	12.5	OK	46.9	147.0	332	15.4	OK	49.0	154.7	341	20.2	OK	48.4	152.8
80- 90.	535	7.9	OK	43.3	135.5	748	13.4	OK	43.6	139.5	663	20.7	OK	44.3	147.4	547	25.4	OK	44.3	147.4	433	25.7	OK	46.1	167.4
90-100.	1039	15.4	OK	42.6	137.5	1045	18.7	OK	42.0	143.5	644	20.2	OK	41.9	145.5	374	17.4	OK	41.5	149.4	195	11.6	OK	41.0	155.4
100-110.	1182	17.6	OK	41.7	137.3	954	17.1	OK	40.2	143.1	392	12.3	OK	40.2	143.1	149	6.9	OK	40.2	143.1	51	3.0	OK	39.6	145.1
110-120.	974	14.5	OK	41.7	135.2	647	11.6	OK	39.2	140.7	173	5.4	OK	38.4	142.5	41	1.9	>50	39.2	140.7	15	0.9	--	36.7	146.1
120-130.	741	11.0	OK	41.3	135.0	435	7.8	OK	39.0	138.2	109	3.4	OK	37.8	139.9	14	0.7	-	42.4	133.3	13	0.8	--	39.0	138.2
130-140.	533	7.9	OK	40.9	134.6	250	4.5	OK	39.5	136.0	53	1.7	>50	38.1	137.5	18	0.8	--	40.9	134.6	5	0.3	-	39.5	136.0
140-150.	332	4.9	OK	40.5	134.2	185	3.3	OK	37.3	136.5	39	1.2	--	38.9	135.4	10	0.5	-	40.5	134.2	4	0.2	-	35.6	137.7
150-160.	256	3.8	OK	42.1	132.9	133	2.4	>75	40.3	133.8	32	1.0	--	40.3	133.8	7	0.3	-	33.0	137.2	3	0.2	-	40.3	133.8
160-170.	167	2.5	>75	42.0	132.8	95	1.7	>50	38.2	133.8	20	0.6	-	40.1	133.3	8	0.4	-	40.1	133.3	5	0.3	-	38.2	133.8
170-180.	96	1.4	>50	42.0	132.6	67	1.2	--	40.0	132.8	25	0.8	--	40.0	132.8	6	0.3	-	40.0	132.8	4	0.2	-	40.0	132.8
180-190.	77	1.1	--	40.0	132.2	48	0.9	--	38.0	132.1	26	0.8	--	38.0	132.1	2	0.1	-	40.0	132.2	3	0.2	-	38.0	132.1
190-200.	41	0.6	-	42.0	132.2	38	0.7	-	38.2	131.2	12	0.4	-	34.3	130.2	3	0.1	-	42.0	132.2	4	0.2	-	42.0	132.2
200-210.	16	0.2	-	42.1	132.1	21	0.4	-	38.5	130.4	8	0.3	-	36.7	129.5	4	0.2	-	38.5	130.4	5	0.3	-	36.7	129.5
210-220.	9	0.1	-	42.2	131.9	13	0.2	-	37.3	128.5	12	0.4	-	42.2	131.9	5	0.2	-	38.9	129.6	7	0.4	-	38.9	129.6
220-230.	13	0.2	-	42.3	131.8	11	0.2	-	39.5	129.0	7	0.2	-	40.9	130.4	6	0.3	-	38.1	127.6	7	0.4	-	39.5	129.0
230-240.	10	0.2	-	41.3	130.0	5	0.1	-	39.0	126.8	3	0.1	-	39.0	126.8	11	0.5	-	41.3	130.0	6	0.4	-	40.1	128.4
240-250.	4	0.1	-	42.6	131.6	4	0.1	-	42.6	131.6	7	0.2	-	40.9	128.0	0	0.0	-	16.4	75.4	2	0.1	-	40.0	126.2
250-260.	8	0.1	-	42.7	131.5	4	0.1	-	42.7	131.5	0	0.0	-	26.7	71.6	0	0.0	-	20.6	84.5	0	0.0	-	26.7	71.6
260-270.	4	0.1	-	42.9	131.5	5	0.1	-	42.9	131.5	5	0.2	-	29.3	81.3	5	0.2	-	24.8	93.5	1	0.1	-	29.3	81.3
270-280.	4	0.1	-	43.1	131.5	6	0.1	-	43.3	129.5	6	0.2	-	31.9	91.0	7	0.3	-	29.1	102.6	4	0.2	-	31.9	91.0
280-290.	4	0.1	-	43.3	131.5	1	0.0	-	43.3	131.5	3	0.1	-	34.5	100.6	3	0.1	-	33.3	111.7	9	0.5	-	34.5	100.6
290-300.	3	0.0	-	43.4	131.6	1	0.0	-	43.4	131.6	0	0.0	-	37.1	110.3	3	0.1	-	37.5	120.7	4	0.2	-	37.1	110.3
300-310.	2	0.0	-	43.6	131.7	6	0.1	-	45.9	128.4	2	0.1	-	39.6	119.9	3	0.1	-	41.7	129.8	5	0.3	-	39.6	119.9
310-320.	6	0.1	-	43.7	131.8	3	0.1	-	45.1	130.4	5	0.2	-	42.2	129.6	14	0.7	-	40.0	126.2	8	0.5	-	42.2	129.6
320-330.	3	0.0	-	43.8	131.9	4	0.1	-	43.8	131.9	8	0.3	-	41.2	125.7	2	0.1	-	35.8	117.1	9	0.5	-	41.2	125.7
330-340.	6	0.1	-	43.9	132.1	6	0.1	-	43.9	132.1	8	0.3	-	38.6	116.1	10	0.5	-	31.6	108.0	11	0.7	-	38.6	116.1
340-350.	7	0.1	-	44.0	132.2	10	0.2	-	44.0	132.2	8	0.3	-	36.0	106.4	14	0.7	-	27.4	99.0	20	1.2	--	36.0	106.4
350-360.	8	0.1	-	44.0	132.4	10	0.2	-	46.0	132.2	10	0.3	-	33.4	96.8	23	1.1	--	23.2	89.9	25	1.5	>50	33.4	96.8

Table D9. Data for the typical transport time from the Kamchatka NRS (Year)

Term			0.5 day					1.0 day					1.5 day					2.0 day					2.5 day		
	Trajectory Statistics and Geographical Coordinates for the Absolute Maximum Cell (AMC)																								
Sector (deg)	#	%	SS	Lat	Long	#	%	SS	Lat	Long	#	%	SS	Lat	Long	#	%	SS	Lat	Long	#	%	SS	Lat	Long
0-10.	123	0.5	-	54.0	158.6	184	0.7	--	54.0	158.6	176	0.8	--	56.0	158.8	203	1.0	--	56.0	158.8	143	0.8	--	58.0	158.9
10- 20.	161	0.6	-	54.0	158.8	189	0.8	--	55.9	159.3	208	0.9	--	54.0	158.8	180	0.9	--	55.9	159.3	177	1.0	--	57.8	159.8
20- 30.	180	0.7	-	53.9	158.9	197	0.8	--	53.9	158.9	226	1.0	--	53.9	158.9	217	1.1	--	57.5	160.6	201	1.1	--	55.7	159.8
30- 40.	197	0.8	--	53.8	159.1	254	1.0	--	53.8	159.1	286	1.3	--	53.8	159.1	285	1.4	>50	58.7	162.5	304	1.6	>50	58.7	162.5
40- 50.	276	1.1	--	53.7	159.2	307	1.2	--	53.7	159.2	346	1.5	>50	55.1	160.6	350	1.7	>50	58.0	163.5	370	2.0	>50	58.0	163.5
50- 60.	368	1.4	>50	53.6	159.3	442	1.8	>50	53.6	159.3	518	2.3	>75	55.9	162.6	574	2.8	OK	57.0	164.2	479	2.6	>75	57.0	164.2
60- 70.	563	2.2	>75	53.4	159.4	784	3.1	OK	55.1	163.0	877	3.9	OK	55.1	163.0	891	4.4	OK	55.1	163.0	869	4.7	OK	56.0	164.8
70- 80.	959	3.7	OK	53.3	159.5	1378	5.5	OK	54.3	163.3	1474	6.6	OK	54.8	165.3	1357	6.7	OK	54.3	163.3	1350	7.3	OK	57.9	176.9
80- 90.	1334	5.1	OK	53.3	161.5	1848	7.4	OK	53.3	161.5	1793	8.0	OK	54.0	169.5	1856	9.1	OK	54.1	171.5	1805	9.8	OK	54.7	177.4
90-100.	2213	8.5	OK	52.7	161.5	2320	9.2	OK	52.4	165.5	2166	9.6	OK	52.2	167.5	2072	10.2	OK	51.5	175.4	1965	10.6	OK	51.7	173.4
100-110.	2162	8.3	OK	52.7	159.5	2063	8.2	OK	51.7	163.3	1831	8.1	OK	51.2	165.3	1611	7.9	OK	50.2	169.1	1542	8.3	OK	48.6	174.9
110-120.	1956	7.5	OK	52.6	159.4	1752	7.0	OK	50.9	163.0	1383	6.2	OK	48.4	168.5	1170	5.8	OK	46.7	172.1	962	5.2	OK	46.7	172.1
120-130.	1624	6.2	OK	52.4	159.3	1316	5.2	OK	51.3	161.0	955	4.3	OK	47.8	165.9	787	3.9	OK	45.6	169.2	631	3.4	OK	46.7	167.5
130-140.	1230	4.7	OK	52.3	159.2	1014	4.0	OK	49.5	162.0	778	3.5	OK	46.6	164.9	530	2.6	>75	48.1	163.5	429	2.3	>75	48.1	163.5
140-150.	959	3.7	OK	52.2	159.1	749	3.0	OK	52.2	159.1	619	2.8	>75	48.9	161.4	456	2.2	>75	48.9	161.4	367	2.0	>50	47.3	162.5
150-160.	781	3.0	OK	52.1	158.9	614	2.4	>75	52.1	158.9	394	1.8	>50	50.3	159.8	337	1.7	>50	46.7	161.5	314	1.7	>50	48.5	160.6
160-170.	681	2.6	>75	52.0	158.8	499	2.0	>50	52.0	158.8	364	1.6	>50	50.1	159.3	293	1.4	>50	48.2	159.8	262	1.4	>50	48.2	159.8
170-180.	508	1.9	>50	52.0	158.6	387	1.5	>50	50.0	158.8	327	1.5	>50	50.0	158.8	291	1.4	>50	48.0	158.9	230	1.2	--	46.0	159.1
180-190.	666	2.6	>75	52.0	158.4	466	1.9	>50	52.0	158.4	363	1.6	>50	48.0	158.1	304	1.5	>50	46.0	157.9	252	1.4	--	48.0	158.1
190-200.	480	1.8	>50	52.0	158.2	441	1.8	>50	52.0	158.2	355	1.6	>50	50.1	157.7	346	1.7	>50	46.2	156.7	258	1.4	>50	46.2	156.7
200-210.	496	1.9	>50	52.1	158.1	393	1.6	>50	50.3	157.2	373	1.7	>50	48.5	156.4	310	1.5	>50	48.5	156.4	284	1.5	>50	48.5	156.4
210-220.	505	1.9	>50	52.2	157.9	429	1.7	>50	52.2	157.9	367	1.6	>50	50.5	156.8	335	1.7	>50	50.5	156.8	291	1.6	>50	47.3	154.5
220-230.	556	2.1	>75	52.3	157.8	446	1.8	>50	50.9	156.4	421	1.9	>50	50.9	156.4	374	1.8	>50	49.5	155.0	303	1.6	>50	46.6	152.1
230-240.	617	2.4	>75	52.4	157.7	505	2.0	>50	52.4	157.7	503	2.2	>75	51.3	156.0	422	2.1	>50	50.1	154.4	349	1.9	>50	49.0	152.8
240-250.	753	2.9	OK	52.6	157.6	666	2.7	>75	51.7	155.8	555	2.5	>75	51.7	155.8	437	2.2	>75	50.9	154.0	427	2.3	>75	50.0	152.2
250-260.	889	3.4	OK	52.7	157.5	746	3.0	OK	52.2	155.6	643	2.9	OK	52.2	155.6	606	3.0	OK	50.7	149.8	565	3.1	OK	51.2	151.7
260-270.	1014	3.9	OK	52.9	157.5	849	3.4	OK	52.6	153.5	764	3.4	OK	52.2	149.5	700	3.4	OK	52.0	147.5	597	3.2	OK	52.0	147.5
270-280.	853	3.3	OK	53.1	157.5	775	3.1	OK	53.3	155.5	760	3.4	OK	53.6	151.5	638	3.1	OK	53.8	149.5	563	3.0	OK	53.6	151.5
280-290.	724	2.8	>75	53.3	157.5	796	3.2	OK	53.8	155.6	663	3.0	OK	54.3	153.7	573	2.8	OK	54.8	151.7	518	2.8	OK	55.3	149.8
290-300.	578	2.2	>75	53.4	157.6	621	2.5	>75	54.3	155.8	536	2.4	>75	56.0	152.2	506	2.5	>75	55.1	154.0	434	2.3	>75	56.8	150.3
300-310.	439	1.7	>50	53.6	157.7	479	1.9	>50	53.6	157.7	414	1.8	>50	54.7	156.0	326	1.6	>50	58.2	151.1	329	1.8	>50	55.9	154.4
310-320.	353	1.4	--	53.7	157.8	346	1.4	--	53.7	157.8	253	1.1	--	55.1	156.4	236	1.2	--	55.1	156.4	208	1.1	--	56.5	155.0
320-330.	268	1.0	--	53.8	157.9	267	1.1	--	53.8	157.9	196	0.9	--	55.5	156.8	189	0.9	--	55.5	156.8	188	1.0	--	55.5	156.8
330-340.	244	0.9	--	53.9	158.1	205	0.8	--	53.9	158.1	177	0.8	--	53.9	158.1	175	0.9	--	55.7	157.2	179	1.0	--	57.5	156.4
340-350.	181	0.7	-	54.0	158.2	200	0.8	--	54.0	158.2	204	0.9	--	54.0	158.2	177	0.9	--	55.9	157.7	170	0.9	--	57.8	157.2
350-360.	238	0.9	--	54.0	158.4	190	0.8	--	54.0	158.4	218	1.0	--	56.0	158.2	210	1.0	--	56.0	158.2	202	1.1	--	58.0	158.1

Table D10. Data for the Typical Transport Time from the Vladivostok NRS (Year)

Term	0.5 day					1.0 day					1.5 day					2.0 day					2.5 day				
Trajectory Statistics and Geographical Coordinates for the Absolute Maximum Cell (AMC)																									
Sector (deg)	#	%	SS	Lat	Long	#	%	SS	Lat	Long	#	%	SS	Lat	Long	#	%	SS	Lat	Long	#	%	SS	Lat	Long
0-10.	199	0.9	--	44.0	132.6	220	1.1	--	44.0	132.6	204	1.3	--	46.0	132.8	185	1.5	>50	48.0	132.9	173	1.5	>50	48.0	132.9
10-20.	250	1.1	--	44.0	132.8	249	1.2	--	44.0	132.8	247	1.6	>50	45.9	133.3	214	1.7	>50	49.8	134.3	186	1.6	>50	45.9	133.3
20-30.	305	1.3	--	43.9	132.9	339	1.7	>50	43.9	132.9	283	1.9	>50	47.5	134.6	281	2.2	>75	49.3	135.5	269	2.4	>75	51.2	136.3
30-40.	399	1.8	>50	43.8	133.1	418	2.1	>50	45.5	134.2	424	2.8	>75	48.7	136.5	396	3.1	=OK	47.1	135.4	373	3.3	=OK	48.7	136.5
40-50.	507	2.2	>75	43.7	133.2	581	2.9	=OK	43.7	133.2	568	3.7	=OK	46.5	136.0	560	4.4	=OK	46.5	136.0	535	4.7	=OK	48.0	137.5
50-60.	610	2.7	>75	43.6	133.3	788	3.9	=OK	44.7	135.0	807	5.3	=OK	48.2	139.9	811	6.4	=OK	49.3	141.5	761	6.7	=OK	49.3	141.5
60-70.	854	3.8	=OK	43.4	133.4	1097	5.5	=OK	44.3	135.2	1173	7.7	=OK	46.8	140.7	1129	8.8	=OK	46.8	140.7	1049	9.3	=OK	47.7	142.5
70-80.	1168	5.1	=OK	43.3	133.5	1400	7.0	=OK	44.3	137.3	1435	9.4	=OK	45.9	143.1	1426	11.2	=OK	46.9	147.0	1460	12.9	=OK	45.3	141.2
80-90.	1407	6.2	=OK	43.3	135.5	1783	8.9	=OK	43.6	139.5	1691	11.1	=OK	43.6	139.5	1624	12.7	=OK	44.3	147.4	1553	13.7	=OK	44.3	147.4
90-100.	2297	10.1	=OK	42.7	135.5	2217	11.0	=OK	42.6	137.5	1729	11.3	=OK	42.0	143.5	1329	10.4	=OK	41.7	147.4	1079	9.5	=OK	41.7	147.4
100-110.	2408	10.6	=OK	42.2	135.4	2083	10.4	=OK	40.7	141.2	1266	8.3	=OK	40.7	141.2	805	6.3	=OK	40.2	143.1	588	5.2	=OK	39.6	145.1
110-120.	2130	9.4	=OK	41.7	135.2	1490	7.4	=OK	40.9	137.0	799	5.2	=OK	40.0	138.8	451	3.5	=OK	39.2	140.7	335	3.0	=OK	39.2	140.7
120-130.	1647	7.3	=OK	42.4	133.3	1075	5.4	=OK	41.3	135.0	460	3.0	=OK	40.1	136.6	272	2.1	>75	41.3	135.0	213	1.9	>50	41.3	135.0
130-140.	1292	5.7	=OK	42.3	133.2	689	3.4	=OK	40.9	134.6	296	1.9	>50	42.3	133.2	179	1.4	>50	40.9	134.6	134	1.2	--	42.3	133.2
140-150.	1001	4.4	=OK	42.2	133.1	594	3.0	=OK	40.5	134.2	257	1.7	>50	40.5	134.2	153	1.2	--	40.5	134.2	107	1.0	--	40.5	134.2
150-160.	816	3.6	=OK	42.1	132.9	493	2.5	>75	40.3	133.8	245	1.6	>50	42.1	132.9	150	1.2	--	40.3	133.8	99	0.9	--	40.3	133.8
160-170.	688	3.0	=OK	42.0	132.8	442	2.2	>75	42.0	132.8	211	1.4	--	40.1	133.3	148	1.2	--	42.0	132.8	93	0.8	--	42.0	132.8
170-180.	475	2.1	>75	42.0	132.6	353	1.8	>50	40.0	132.8	207	1.4	--	40.0	132.8	120	0.9	--	42.0	132.6	98	0.9	--	40.0	132.8
180-190.	537	2.4	>75	42.0	132.4	365	1.8	>50	40.0	132.2	260	1.7	>50	40.0	132.2	162	1.3	--	42.0	132.4	105	0.9	--	40.0	132.2
190-200.	371	1.6	>50	42.0	132.2	324	1.6	>50	40.1	131.7	226	1.5	>50	42.0	132.2	159	1.3	--	42.0	132.2	154	1.4	--	38.2	131.2
200-210.	324	1.4	>50	42.1	132.1	276	1.4	--	40.3	131.2	202	1.3	--	40.3	131.2	200	1.6	>50	38.5	130.4	115	1.0	--	40.3	131.2
210-220.	311	1.4	--	42.2	131.9	275	1.4	--	40.5	130.8	205	1.3	--	40.5	130.8	147	1.2	--	38.9	129.6	166	1.5	>50	37.3	128.5
220-230.	288	1.3	--	42.3	131.8	226	1.1	--	40.9	130.4	215	1.4	>50	39.5	129.0	172	1.4	--	39.5	129.0	141	1.3	--	36.6	126.1
230-240.	242	1.1	--	42.4	131.7	213	1.1	--	41.3	130.0	157	1.0	--	40.1	128.4	160	1.3	--	40.1	128.4	151	1.3	--	39.0	126.8
240-250.	197	0.9	--	42.6	131.6	161	0.8	--	42.6	131.6	119	0.8	--	41.7	129.8	101	0.8	--	41.7	129.8	86	0.8	--	40.0	126.2
250-260.	178	0.8	--	42.7	131.5	114	0.6	-	42.7	131.5	98	0.6	-	42.2	129.6	88	0.7	-	41.7	127.7	58	0.5	-	41.7	127.7
260-270.	208	0.9	--	42.9	131.5	147	0.7	--	42.9	131.5	107	0.7	--	42.9	131.5	74	0.6	-	42.7	129.5	70	0.6	-	42.7	129.5
270-280.	154	0.7	-	43.1	131.5	120	0.6	-	43.1	131.5	103	0.7	-	43.3	129.5	87	0.7	-	43.3	129.5	70	0.6	-	43.3	129.5
280-290.	151	0.7	-	43.3	131.5	129	0.6	-	43.8	129.6	106	0.7	-	43.8	129.6	92	0.7	--	44.3	127.7	87	0.8	--	43.8	129.6
290-300.	172	0.8	--	43.4	131.6	168	0.8	--	43.4	131.6	111	0.7	--	45.1	128.0	126	1.0	--	46.0	126.2	127	1.1	--	45.1	128.0
300-310.	172	0.8	--	43.6	131.7	191	1.0	--	43.6	131.7	186	1.2	--	44.7	130.0	123	1.0	--	44.7	130.0	115	1.0	--	45.9	128.4
310-320.	168	0.7	--	43.7	131.8	181	0.9	--	45.1	130.4	158	1.0	--	46.5	129.0	166	1.3	--	46.5	129.0	118	1.0	--	48.0	127.6
320-330.	183	0.8	--	43.8	131.9	201	1.0	--	43.8	131.9	199	1.3	--	47.1	129.6	135	1.1	--	47.1	129.6	159	1.4	>50	47.1	129.6
330-340.	179	0.8	--	43.9	132.1	229	1.1	--	43.9	132.1	154	1.0	--	45.7	131.2	161	1.3	--	47.5	130.4	136	1.2	--	49.3	129.5
340-350.	184	0.8	--	44.0	132.2	227	1.1	--	44.0	132.2	185	1.2	--	45.9	131.7	175	1.4	--	45.9	131.7	153	1.4	--	49.8	130.7
350-360.	259	1.1	--	44.0	132.4	236	1.2	--	44.0	132.4	216	1.4	>50	46.0	132.2	205	1.6	>50	50.0	131.9	199	1.8	>50	54.0	131.5

Table D10. Data for the typical transport time from the Vladivostok NRS (Year)

APPENDIX E:Software Visualization Tools

Trajectory visualization was done using NCAR Graphics (developed by University Corporation for Atmospheric Research Foundation, http://ngwww.ucar.edu/) and General Mapping Tools, GMT (developed by P.Wessel & W.Smith, http://gmt.soest.hawaii.edu/) software. We performed cluster analysis of trajectories using SAS software (developed by SAS Institute Inc., http://www.sas.com/) and programs for analysis were written in SAS language. Probabilistic fields were constructed using MATLAB software (developed by MathWorks Inc., http://www.mathworks.com/), which includes the geographical mapping toolbox. The isentropic trajectory model was modified using FORTRAN-77 and 90 languages. Some blocks for model and statistical data analysis were developed in FORTRAN, SAS, MATLAB, and C++.

Visualization of the probabilistic fields for airflow and fast transport we combined for both NRSs – Vladivostok and Kamchatka - into a software application. This application can be executed from the MATLAB command line (by typing the command “farecs” and pressing the “Enter” key). It will create a menu which contains several buttons, two of which are airflow and another two – fast transport fields for the nuclear risk sites. Select a button to visualize a probabilistic field and press it. Each shown probabilistic field is presented using isolines, given with an interval of 5-10%, on the background of the geographical maps. To run this application User should follow menu items shown below.

The “*ColorMap”-menu provides a variety of color background pallettes for isolines: jet, bone, copper, cool, gray, hsv, hot, pink, spring, summer, and winter. The “* Resolution”-menu has three options allowing the choice of the interpolation of the original data into various grids. It has resolutions of 2.5° x 2.5°, 1.25° x 1.25°, and 0.625° x 0.625° degrees latitude vs. longitude. The “* GridDomain”-menu also has three options. It gives three areas of research interest, which are limited by chosen boundaries. These boundaries are slightly different for each NRS, but all of them show regional, FARECS study, and large scale domains.

The probabilistic fields are presented by the “*Season” and “*Month”-menus. The first menu includes probabilistic fields calculated for the boundary layer during summer, fall, winter, and spring, as well as a year. The second menu consists of monthly probabilistic fields. Each time, when User chooses an option in the “*Season” and “*Month”-menus, application will be running and re-drawing a probabilistic field.

The visualization Matlab-oriented software tool had been saved at the RAD FARECS CD. It also includes monthly and seasonal variations of the airflow and fast transport patterns for both sites for the FARECS and regional domain scales.